

Electronic Thesis and Dissertation Repository

---

11-22-2013 12:00 AM

## Study on Fine Powder Coating with Modified Additive

Dangchen Xue, *The University of Western Ontario*

Supervisor: Dr. Jesse Zhu, *The University of Western Ontario*

A thesis submitted in partial fulfillment of the requirements for the Master of Engineering  
Science degree in Chemical and Biochemical Engineering

© Dangchen Xue 2013

Follow this and additional works at: <https://ir.lib.uwo.ca/etd>

 Part of the [Other Chemical Engineering Commons](#)

---

### Recommended Citation

Xue, Dangchen, "Study on Fine Powder Coating with Modified Additive" (2013). *Electronic Thesis and Dissertation Repository*. 1720.

<https://ir.lib.uwo.ca/etd/1720>

This Dissertation/Thesis is brought to you for free and open access by Scholarship@Western. It has been accepted for inclusion in Electronic Thesis and Dissertation Repository by an authorized administrator of Scholarship@Western. For more information, please contact [wlsadmin@uwo.ca](mailto:wlsadmin@uwo.ca).

# STUDY ON FINE POWDER COATING WITH MODIFIED ADDITIVE

(Thesis format: Monograph)

by

Dangchen Xue

Graduate Program in Engineering Science

Chemical and Biochemical Engineering

A thesis submitted in partial fulfillment  
of the requirements for the degree of  
Master of Engineering Science

The School of Graduate and Postdoctoral Studies  
The University of Western Ontario  
London, Ontario, Canada

© Dangchen Xue 2013

## Abstract

Powder coating is a dry coating technology competing with conventional liquid coatings and offers many benefits such as the elimination of volatile organic compounds, high efficiency of material usage and improved coating durability. However, the rough and thick film surface restricts its wide application. The fine powder coating, which can solve the film quality issues, also has its own limitation: the powder is too cohesive to handle. Although, nanoparticle flow additives can significantly improve the flowability of fine powders, it leads to another obstacle at the same time. Since the inorganic nano additives are not fully compatible with the organic fine powder coating materials during the curing process, the agglomerates formed by nanoparticles can result in film defects such as seeds and pinholes, as well as the reduction of gloss.

A technology of encapsulating polymer resins on the surface of nano silica additive is used for this work. By modifying the surface of the inorganic additives, the compatibility issues are expected to be solved while the effect of additive on flowabilities remains.

The modified additives were prepared by encapsulating commercial nano silica additives with 2 organic materials, polyester or hybrid, in 4 different Resin-to-Encapsulated Additive ratios (R-EA ratios) and evaluated by TEM. The additives were incorporated into fine coating powders in 4 different additive loading ratios (LOAs). All of the 40 samples were tested by flow property measurements to obtain their angle of repose (for semi-static flow property) and avalanche angle (for dynamic flow property). The results show that with a suitable R-EA ratio and additive loading ratio, the powder sample performs better with improved semi-static and dynamic flow properties. And the optimum R-EA ratios and LOAs were suggested for specific applications.

For each powder samples, three panels were sprayed with an electrostatic method and all of the 120 coated panels were evaluated by measuring gloss and the number of seeds on the film surface. Some panels were evaluated by a roughness profiler. The results show that coating films from the samples with modified additives have higher gloss, lower roughness and less seeds on the surface.

## Keywords

Fine powder coating, flow additive, encapsulation of nanoparticle, flow properties, film qualities

## Acknowledgments

To begin with, I would like to express my utmost gratitude and sincere appreciation to my supervisors Dr. Jesse Zhu and Dr. Hui Zhang, for offering me this wonderful opportunity to pursue my Master program in Canada, and giving me this great chance to step into a totally new field to me, powder coating. I would like to thank them to their continuous support, invaluable guidance and immense encouragement through all the steps of my study, research work, as well as writing this thesis. I would like to thank Dr. Hui Zhang for his invaluable inspiration and patient guidance all along my study and research. His immense knowledge, extraordinary creativity, and professional experience did provide me great help to overcome obstacles one by one. Without his supports and assistance, it is impossible for me to finish my program ahead of time.

A green hand like me did learn much in these one and a half years. The specific knowledge I gained, and more importantly, how to study and how to be a man, really means a lot in my future work and life.

Furthermore, special appreciations are to my colleague, Danni Bao, who taught me every single technical and research issue from the very beginning with great patience and kindness. Owing to her selfless help, I can quickly grasp the experimental skills and progress the research smoothly.

To all my friends and group mates; Tang Li, Jing Fu, Qingliang Yang, Jiangshan Liu, Shan Gao, Yijun Dong, Chengxiu Wang, Long Sang, Yong Liu, Bhuiyan Mohammad, Rezwana Yeasmin, thanks very much for your help and support. Many thanks go to Zhi Zhang for his aid and support.

At last, my deepest gratitude will go to all of my family members. My grandfather, who passed away when I was thousands of miles far away from him, my grandmother and parents, also my girlfriend Lu Lu-they love me, trust me and keep supporting me without any hesitate. When I was in straits and wanted to give up, it was you that warmed me and strengthened me.

# Table of Contents

Abstract .....	II
Acknowledgments.....	IV
Table of Contents .....	V
List of Tables .....	IX
List of Figures.....	X
List of Abbreviations, Symbols and Nomenclature .....	XV
Chapter 1 .....	1
1 Introduction .....	1
1.1 Introduction to Fine powder Coating and its Limitations .....	1
1.2 Objectives .....	4
1.3 Thesis Structure .....	4
1.4 Contributions.....	5
Chapter 2.....	6
2 Background and Literature Review .....	6
2.1 Powder Coating Technology.....	6
2.2 Fine Powder Coating Technology .....	8
2.3 Flow Additives for Fine Powder Coating .....	11
2.4 Surface Modification of Nano-Additives.....	15
2.5 Summary and concluding remarks.....	16
Chapter 3.....	18
3 Experimental Methods .....	18
3.1 Experimental Procedures .....	19
3.1.1 Modification of Nano-size Additives.....	19

3.1.2	Preparation of Coating Powder Samples .....	24
3.1.3	Spraying and Curing of Panel Samples .....	30
3.2	Measurement Techniques .....	32
3.2.1	Measurement of Particle Size .....	32
3.2.2	Characterization for Flow Properties- Angle of Repose and Avalanche Angle.....	32
3.2.3	Evaluation of Film Qualities-Thickness, Gloss, Number of Seeds and Roughness .....	35
Chapter 4	.....	39
4	Flow Characterization of Fine Powders with Modified Additives .....	39
4.1	Introduction.....	39
4.2	Effect of Resin-to-Encapsulated Additive Ratio on Flow Properties of Fine Powders.....	40
4.2.1	Semi-Static Flow Characterization .....	40
4.2.2	Dynamic Flow Characterization .....	44
4.3	Effect of Loading Ratio of Additive on Flow Properties of Fine Powders .....	51
4.3.1	Semi-static Flow Characterization.....	52
4.3.2	Dynamic Flow Characterization .....	54
4.4	Chapter Summary .....	58
Chapter 5	.....	60
5	Film Quality Characterization of Fine Powders with Modified Additives .....	60
5.1	Introduction.....	60
5.2	Effect of Resin-to-Additive Ratio on Film Qualities of Fine Powders.....	62
5.2.1	Gloss .....	62
5.2.2	Roughness.....	64
5.2.3	Number of Seeds.....	67

5.3 Effect of Additive Loading Ratio on Film Qualities of Fine Powders .....	70
5.3.1 Gloss .....	70
5.3.2 Roughness .....	70
5.3.3 Number of Seeds.....	73
5.4 Summary.....	75
Chapter 6.....	76
6 Conclusions and Recommendations .....	76
6.1 Conclusions.....	76
6.1.1 Flow Characteristic of Coating Powder.....	76
6.1.2 Film Characteristic of Coating Film .....	77
6.2 Recommendations.....	78
References.....	79
Appendices.....	84
A1 Particle size .....	84
A2 Semi-static flow property.....	85
A3.1 Original Data.....	85
A3.2 Error Analysis .....	86
A3 Dynamic flow property .....	88
A3.1 Original Data.....	88
A3.2 Error Analysis .....	89
A4 Film qualities.....	91
A4.1 Thickness .....	91
A4.2 Film Gloss .....	97
A4.3 Roughness .....	102
A4.4 Number of Seeds.....	103



Curriculum Vitae ..... 108

## List of Tables

Table 2.1 Classification of flow properties by angle of repose .....	11
Table 3.1 List of materials used in this work.....	18
Table 3.2 Mass ratios of encapsulating resin to nano-size silica additive .....	20
Table 3.3 List of additives prepared .....	24
Table 3.4 Operation conditions of ACM .....	26
Table 3.5 List of all powder samples prepared.....	29
Table 4.1 Optimum conditons for best flow properies of fine powder.....	59
Table A.1 Particle size of polyester and hybrid coating powder samples .....	84
Table A.2 Angle of repose of polyester powder samples .....	85
Table A.3 Angle of repose of hybrid powder samples .....	86
Table A.4 Avalanche angle of polyester powder samples.....	88
Table A.5 Avalanche angle of hybrid powder samples .....	89
Table A.6 Thickness of polyester coated panel samples .....	91
Table A.7 Thickness of hybrid coated panel samples.....	94
Table A.8 Film gloss of polyester coated panel samples.....	97
Table A.9 Film gloss of hybrid coated panel samples .....	99
Table A.10 Roughness of panel samples .....	102
Table A.11 Number of seeds of polyester coated panel samples .....	103
Table A.12 Number of seeds of hybrid coated panel samples.....	104

## List of Figures

Figure 1.1 Geldart's Powder Classification .....	2
Figure 2.1 Schematic diagram of powder coating process .....	7
Figure 2.2 Schematic of film formation in powder coating.....	7
Figure 2.3 Film thickness of (a) coarse powder film and (b) fine powder film.....	9
Figure 2.4 Surface profiles of panels (a) coarse powder (b) fine powder.....	9
Figure 2.5 Schematic of plugging and channeling.....	10
Figure 2.6 Possible mechanism of flow additive .....	12
Figure 2.7 Schematic diagram of cohesion forces between (a) host particles uncoated with additive (b) host particles coated with additive .....	13
Figure 2.8 Train of thought in powder coating technology .....	17
Figure 3.1 Four stages for encapsulation of additive.....	19
Figure 3.2 Schematic of dissolving.....	20
Figure 3.3 Schematic of jet mill of additive clumps.....	21
Figure 3.4 Schematic of Jet Mill.....	22
Figure 3.5 Schematic of collector .....	23
Figure 3.6 Air Classifying Mill (ACM).....	25
Figure 3.7 Schematic of Air Classifying Mill.....	26
Figure 3.8 Ultrasonic-Vibration Sifter.....	27
Figure 3.9 Schematic of mixing.....	28

Figure 3.10 Schematic of panel spraying.....	31
Figure 3.11 Schematic of AOR Measurement.....	33
Figure 3.12 Schematic of AVA Measurement.....	34
Figure 3.13 Schematic of Avalanche Angle .....	35
Figure 3.14 Coating Thickness Gauge.....	36
Figure 3.15 Schematic of thickness measurement.....	36
Figure 3.16 Schematic of gloss measurement.....	37
Figure 3.17 Schematic of roughness measurement.....	38
Figure 4.1 Effects of R-EA ratio on AOR-PE (Additives were encapsulated with PE. Encapsulated additives were incorporated into PE powder).....	42
Figure 4.2 Effects of R-EA ratio on AOR-HB (Additives were encapsulated with HB. Encapsulated additives were incorporated into HB powder).....	43
Figure 4.3 Effects of R-EA ratio on AVA-PE (Additives were encapsulated with PE. Encapsulated additives were incorporated into PE powder).....	45
Figure 4.4 Effects of R-EA ratio on AVA-HB (Additives were encapsulated with HB. Encapsulated additives were incorporated into HB powder).....	46
Figure 4.5 TEM image of control additive (180k magnificant).....	47
Figure 4.6 Schematic of “Chain” effect of additive.....	48
Figure 4.7 TEM images of encapsulated additives (a) additive encapsulated with PE with R-EA ratio of 10% (b) additive encapsulated with PE with R-EA ratio of 20% (c) additive encapsulated with HB with R-EA ratio of 10% (d) additive encapsulated with HB with R-EA ratio of 20% (180k magnification).....	49

Figure 4.8 SEM images of powder loaded with modified additive with LOA of 0.3% (a) PE powder with control additive (b) PE powder with additive in R-EA ratio of 10% (c) PE powder with additive in R-EA ratio of 20% (d) HB powder with control additive (e) HB powder with additive in R-EA ratio of 10% (f) HB powder with additive in R-EA ratio of 20% (10k magnification).....	50
Figure 4.9 Schematic of suitable and excessive encapsulation on additive.....	51
Figure 4.10 Effects of LOA on AOR-PE (Additives were encapsulated with PE. Encapsulated additives were incorporated into PE powder).....	53
Figure 4.11 Effects of LOA on AOR-HB (Additives were encapsulated with HB. Encapsulated additives were incorporated into HB powder).....	54
Figure 4.12 Effects of LOA on AVA-PE (Additives were encapsulated with PE. Encapsulated additives were incorporated into PE powder).....	56
Figure 4.13 Effects of LOA on AVA-HB (Additives were encapsulated with HB. Encapsulated additives were incorporated into HB powder).....	56
Figure 4.14 Schematic of contacts of particles under different LOA .....	57
Figure 4.15 SEM images of powder loaded with modified additive with R-EA ratio of 10% (a) PE powder with LOA of 0.3% (b) PE powder with LOA of 0.8% (c) HB powder with LOA of 0.3% (d) HB powder with LOA of 0.8% (10k magnification).....	58
Figure 5.1 Schematic of seeds on film surface .....	61
Figure 5.2 Effects of R-EA ratio on gloss-PE (Additives were encapsulated with PE. Encapsulated additives were incorporated into PE powder).....	63
Figure 5.3 Effects of R-EA ratio on gloss-HB (Additives were encapsulated with HB. Encapsulated additives were incorporated into HB powder).....	63
Figure 5.4 Effects of net silica to powder coating ratio on gloss.....	64

Figure 5.5 Cured film surface characterized by roughness (Ra) and waviness (Rz) .....	65
Figure 5.6 Effects of R-EA ratio on roughness-PE (Additives were encapsulated with PE. Encapsulated additives were incorporated into PE powder).....	66
Figure 5.7 Effects of R-EA ratio on roughness-HB (Additives were encapsulated with HB. Encapsulated additives were incorporated into HB powder).....	66
Figure 5.8 Effects of R-EA ratio on number of seeds-PE (Additives were encapsulated with PE. Encapsulated additives were incorporated into PE powder).....	67
Figure 5.9 Effects of R-EA ratio on number of seeds-HB (Additives were encapsulated with HB. Encapsulated additives were incorporated into HB powder) .....	68
Figure 5.10 Effects of LOA on gloss-PE (Additives were encapsulated with PE. Encapsulated additives were incorporated into PE powder).....	71
Figure 5.11 Effects of LOA on gloss-HB (Additives were encapsulated with HB. Encapsulated additives were incorporated into HB powder).....	71
Figure 5.12 Effects of LOA on roughness-PE (Additives were encapsulated with PE. Encapsulated additives were incorporated into PE powder).....	72
Figure 5.13 Effects of LOA on roughness-HB (Additives were encapsulated with HB. Encapsulated additives were incorporated into HB powder).....	72
Figure 5.14 Effects of LOA on number of seeds-PE (Additives were encapsulated with PE. Encapsulated additives were incorporated into PE powder).....	73
Figure 5.15 Effects of LOA on number of seeds-HB (Additives were encapsulated with HB. Encapsulated additives were incorporated into HB powder) .....	74
Figure A.1 Error analysis of AOR for polyester samples (Additives were encapsulated with PE. Encapsulated additives were incorporated into PE powder).....	87

FigureA.2 Error analysis of AOR for hybrid samples (Additives were encapsulated with HB. Encapsulated additives were incorporated into HB powder) ..... 87

Figure A.3 Error analysis of AVA for polyester samples (Additives were encapsulated with PE. Encapsulated additives were incorporated into PE powder)..... 90

Figure A.4 Error analysis of AVA for hybrid samples (Additives were encapsulated with HB. Encapsulated additives were incorporated into HB powder) ..... 90

FigureA.5 Error analysis of gloss for polyester samples (Additives were encapsulated with PE. Encapsulated additives were incorporated into PE powder)..... 101

Figure A.6 Error analysis of gloss for hybrid samples (Additives were encapsulated with HB. Encapsulated additives were incorporated into HB powder) ..... 101

Figure A.7 Error analysis for number of seeds for polyester samples (Additives were encapsulated with PE. Encapsulated additives were incorporated into PE powder) ..... 107

Figure A.8 Error analysis for number of seeds for hybrid samples (Additives were encapsulated with HB. Encapsulated additives were incorporated into HB powder) .... 107

# List of Abbreviations, Symbols and Nomenclature

## **Abbreviations**

ACM	Air Classifying Mill
AOR	Angle of Repose
AVA	Avalanche Angle
ESA	Effective Surface Area
HB	Hybrid
LOA	Loading Ratio of Additive
PE	Polyester
PSD	Particle Size Distribution
PTRC	Particle Technology Research Centre
R-EA	Resin-to-Encapsulated Additive
SAC	Surface Area Coverage
SGPS	Scholl of Graduate and Postdoctoral Studies
UWO	University of Western Ontario



## Symbols and Nomenclature

$A$	The Hamaker coefficient
$d$	Diameter of guest particle
$D$	Diameter of host particle
$D_{10}$	Particle diameter at which 10% of particles by volume are smaller or equal to
$D_{50}$	Particle diameter at which 50% of particles by volume are smaller or equal to
$D_{90}$	Particle diameter at which 90% of particles by volume are smaller or equal to
$h_0$	The atomic scale separation distance between the two particles
$P_{coated}$	The force needed to pull the two particles coated with additive apart
$P_{uncoated}$	The force needed to pull the two particles without additive apart

## Chapter 1

### 1 Introduction

#### 1.1 Introduction to Fine powder Coating and its Limitations

Powder coating is a dry coating process in which powdered paint is coated directly onto targets without any organic solvent involved. Associated with environmental aspects, the first development of powder coating was introduced early in the 1950s (Misev 1991). During the powder coating process, paint ingredients, like resin, pigment and some other necessary filler, are first mixed and extruded into solid composite chips, instead of using a solvent to keep ingredients in a liquid suspension form. These chips are then ground into dry powder and then ready for spraying. During the powder coating application process, the coating powder is transported to the substrate via electro-static spray. After being heated, the powder melts and transforms to a continuous film.

Due to its many advantages over traditional liquid coating, such as no harmful volatile organic compounds (VOCs) are emitted into the atmosphere and the powder can be recycled, this environmental friendly and economic efficient powder coating technology has gained much popularity (Kittle and Rushman 1997; Lucari 2003). After sixty years of development, powder coating is a mature technology which has been applied in many applications like in automobile and pharmaceutical industry (Gribble 2003; Mullarney et al. 2011).

However, powder coating technology still suffers in several aspects and its application is limited. Because of the large particle size powders are being used, with the median particle diameter larger than 30 microns, issues like relatively poor aesthetic quality and excessive film thickness are inevitable. To overcome this limitation, finer powders are employed. By reducing the particle size, the surface quality and film thickness are expected to be improved.

However, the application of fine powders has to conquer another obstacle. The fine powders, which belong to Group C powder based on Geldart's Powder Classification

(Geldart 1973) as shown in Figure 1.1, are not as easily fluidized as coarse powders. Under this classification, powders are divided into four Groups: A (Aeratable), B (Bubble-ready), C (Cohesive), and D (Different or Dense), depending on the mean diameter and density difference from gas. Hence, fine powders with size under 25 to 30 microns are referred to as Cohesive. Just as its name implies, Group C powders are normally extremely cohesive, easily to form agglomerates and clumps when subjected to fluidization and intermittency or choking when transported, making them difficult to handle (Zhu 2003). The major cause contributing to this difficulty in fluidizing is recognized as the large interparticle forces resulting from van der Waal's Forces when particles come adequately close to one another (Hamaker 1937; Visser 1989).

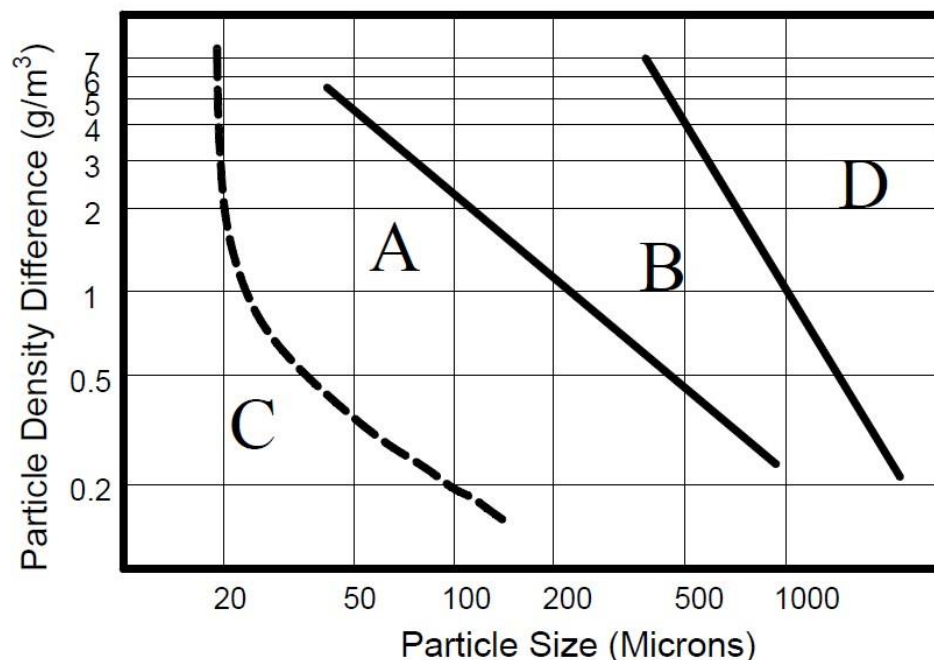


**Figure 1.1 Geldart's Powder Classification  
(Geldart 1973)**

Therefore, to fulfill the increasing needs of fine powder coating, the research on flow additives has been conducted by many researchers (Frank and Pettit 1993; Zhu and Zhang 2004; Ishida et al. 2013). Among them, an ultrafine powder coating technology was developed in 2005 (Zhu and Zhang 2005), in which ultrafine powder with average particle sizes between 10 and 20 microns has been successfully applied by adding much smaller nanoparticles as the flow additive. These nanoparticles work to reduce their

interparticle forces by increasing the distance between the host particles and thus improve the flow properties of fine powders. With this innovative technology, the surface roughness of powder coatings is reduced by 80 to 90 percent and the thickness is comparable to liquid coatings (Zhu and Zhang 2005).

However, all of the nano additives used nowadays are inorganic materials, for example silica, aluminium oxide and titanium dioxide. The coating powders, on the other hand, mainly consist of organic materials like polyester and epoxy resins. This difference in material results in poor compatibility between coating powders and flow additive. During the curing process, additives/agglomerates with poor wettability are apt to flow “up” to the surface of the coating film due to the difference in surface tension, which leads to the reduction of gloss and the appearance of film defects like “fish eyes” and seeds.

Using organic nano additives seems to be a good solution, but it is extremely expensive to manufacture the organic nano particles. In addition, previous works done by our group have tried to use a couple of organic nano particles as flow additives, but the results showed that those additives cannot increase the flowability of fine powders effectively. Therefore, to replace inorganic additive with organic materials may not be achievable.

Under such circumstances, another idea is inspired by the encapsulation technology. To make the flow additive more compatible with coating powders, organic material, best being the same material as the coating powder, is coated onto the inorganic nano particles. With a suitable encapsulation level, the film qualities of coating film are expected to be significantly improved while keeping the flow properties of fine powder at the same or a better level.

## 1.2 Objectives

Corresponding to the limitations of fine powder coating, several efforts have been made by the Particle Technology Research Center (PTRC) in recent years and the idea of encapsulating nano additives has been shown to be promising. To give an overall and detailed evaluation of this encapsulation technology, the present study follows the whole process of powder coating application used in the industry and aims to attain the objectives as following:

- To improve the compatibility of inorganic additive to organic fine powders by modifying the nano-size silica additive with organic resin using encapsulation technology;
- To evaluate the semi-static and dynamic flow abilities of fine powders with modified additive, and to optimize the encapsulation level and additive loading ratio in terms of flow properties;
- To study the film qualities of final surface of fine powders with encapsulated additive, which are affected by resin bases, encapsulation levels and additive loading ratios;
- To determine the optimum encapsulation ratio on the silica additive and additive loading ratio by combining the considerations of flow properties and film qualities.

## 1.3 Thesis Structure

This thesis consists of six chapters and follows the “monograph” format as outlined in the Master’s Programs of *General Thesis Regulations* by the school of Graduated and Postgraduate of Studies (SGPS) in the University of Western Ontario (UWO). The thesis structure is provided below.

**Chapter 1** provides a general introduction of fine powder coating and its limitations. Research objectives, thesis structure and major contributions of this work are stated simultaneously.

**Chapter 2** presents the detailed background of fine powder coating technology, flow additive for fine powder coating and modification methods for nanoparticles by reviewing the literature papers.

**Chapter 3** summarizes the experimental methods that were used in the processes of additive encapsulation, powder sample preparation and coating panel spraying. Measurement techniques and testing equipment of flow characterization and film quality evaluation are also detailed in this chapter.

**Chapter 4** evaluates the effects of Resin-to-Encapsulated Additive (R-EA) ratio in additive modification and loading ratio of additive (LOA) in powder samples on the semi-static and dynamic flow properties. Forty samples with two resin bases, four R-EA ratios and four LOA were prepared and characterized with Angle of Repose and Avalanche Angle. In this chapter, optimum value of R-EA ratio and LOA were found for different resin bases and characterization states.

**Chapter 5** focuses on the effects of R-EA ratio and LOA on the film qualities of final coating surface. One hundred and twenty panels, three panels for each powder sample, were sprayed using electrostatic spraying method and evaluated by measuring the gloss, roughness and number of seeds. The results were compared by two resin bases, four R-EA ratios and four LOA and optimum values for specific situations were chosen.

**Chapter 6** summarizes the general conclusions got from Chapter 4 and 5, and compromise between the flow properties and film qualities are suggested to make for specific applications. In addition, recommendations for future work are also listed.

## 1.4 Contributions

A technology of encapsulating resins on nano silica is used to modify the flow additive for ultrafine powder coating. With suitable encapsulation level and additive loading ratio, modified silica additive is proved to be effective to improve the flow properties and promote film qualities of coating surface at the same time.

## Chapter 2

### 2 Background and Literature Review

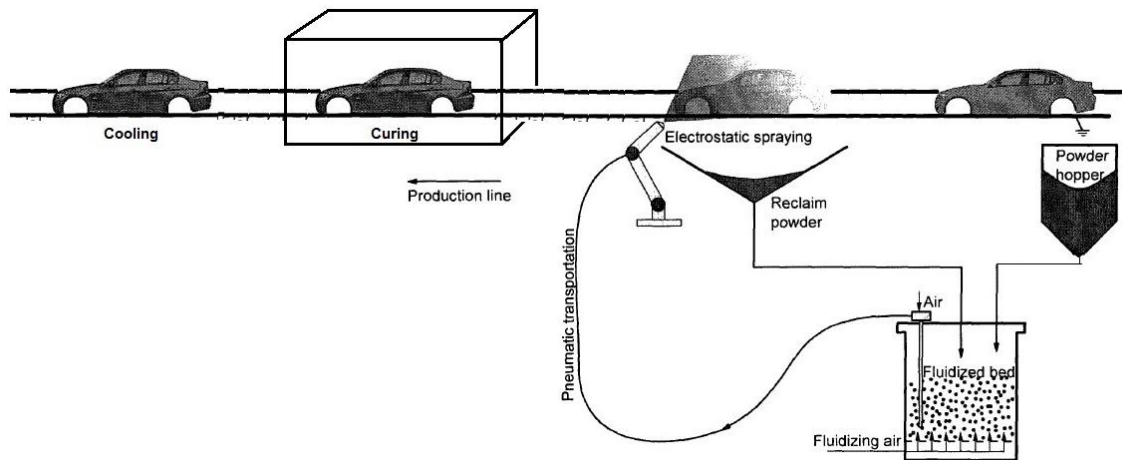
#### 2.1 Powder Coating Technology

Powder coating is a method for decorative and protective coatings using dry powders, which is different from traditional liquid coatings. Conventionally, paint, which may include various resins or binders, pigments and other additives, are dissolved in organic solvents and applied onto substrates. After application, the solvent is evaporated to the atmosphere and a continuous coating film is left behind. The drawback of liquid coating is the high content of volatile organic solvent, which is just used for mixing and suspending paint ingredients and is evaporated after application. In addition, the overspray that doesn't get onto the target is non-recyclable. The use of organic solvents is not only harmful to the environment, but also a waste of money and energy (Weiss 1997).

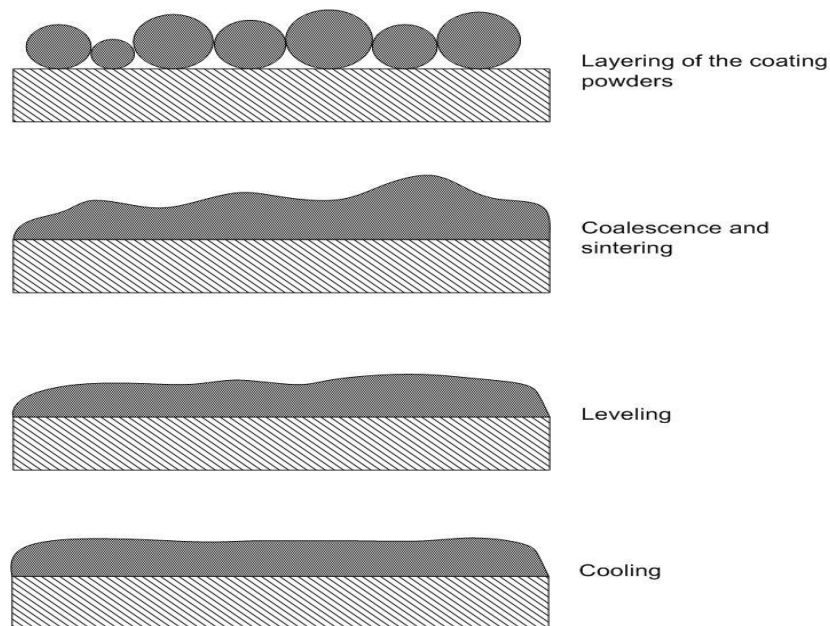
The technology of powder coating was first introduced in the 1950's as an alternative process to liquid coating. In powder coating, all the paint ingredients are dry-extruded together and ground into powders with absence of any solvent throughout the whole fabricating process. Then the powders are transported and applied onto the surface of substrate using fluidized bed (Gemmer 1995) or electrostatic spray techniques (Bailey 1998).

Figure 2.1 shows an example of a powder coating application process used in an automobile production line. At first, powdered paint is discharged from a storage hopper to a fluidized bed. The powder is fluidized by air and pneumatically transported to a spray gun. The particles are electrostatically charged by the electrostatic spray gun and sprayed onto a subject in a spray booth. The particles that are not fixed onto the subject are recycled back to the fluidized bed for further spraying. After spraying, the coated substrate is moved to an oven, where is heated with an appropriate temperature. During the curing process, powders begin to melt and level to a continuous and uniform film, as

shown in Figure 2.2. After cooling, a coating film for decoration and/or protection is produced.



**Figure 2.1 Schematic diagram of powder coating process**



**Figure 2.2 Schematic of film formation in powder coating (Sauer 2013)**

Ever since its first appearance, powder coating has garnered lots of attentions due to its numerous merits over liquid coating, which include: no emission of volatile organic compounds (VOCs), potential for 100% utilization of paint material and better substrate



protection (Misev 1991). In summary, the popular “four E’s” were introduced: ecology, economy, energy and excellence of finish (Bosschi 1986). Based on these advantages, powder coating has already been applied to coat appliances, furniture, architectural and building materials and the underhood parts and primer coats in the automotive industry. In these markets, powder coating has fully or partially replaced traditional liquid coating. Currently, powder coatings account for roughly 10% of the industrial paint market, and have experienced an annual growth rate between 10 and 13% over the last 20 years (Richart 2001). The most prominent uses of powder coating are lawn and garden equipment, architectural uses and general metal finishing (Richart 2001). The automobile industry is also an increasing market for powder coating, even though most consumption is limited mainly to underhood components. For instance, clear coats made by powder coating have been successfully applied in BMW’s 5 and 7 series vehicles (Biller 2006). Another potential market of powder coating lies in pharmacy industries, like the coatings on pharmaceutical dosage to control drug release rate (Sastry et al. 2000; Daniher and Zhu 2008).

## 2.2 Fine Powder Coating Technology

Despite all the advantages mentioned above, the application of powder coating is still limited and has not been widely adopted because of its inferior aesthetic appearance qualities in comparison to liquid coatings. Normally, the powder coatings provide a thicker film (60 to 100 microns) than liquid coatings (10 to 40 microns) and relatively poorer surface qualities, such as poor distinctness of image, poor gloss and heavy orange peel look (Zhu and Zhang 2005). These drawbacks are attributed to the large particle sizes (with  $D_{50}$  larger than 30 microns) and could be overcome by the size reduction, as shown in Figure 2.3 and Figure 2.4 (Zhu and Zhang 2005; Huang 2009).

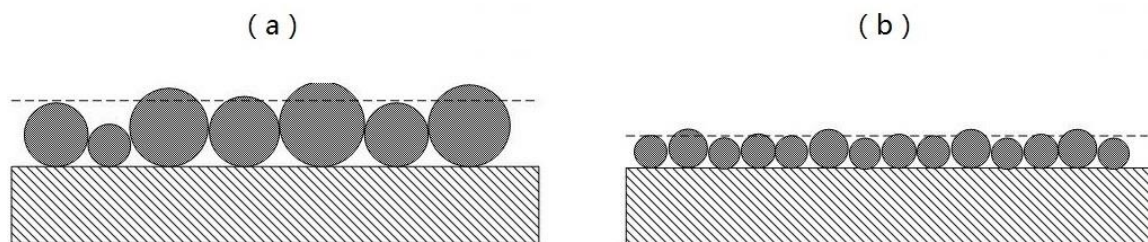


**Figure 2.3 Film thickness of (a) coarse powder film and (b) fine powder film (Huang 2009)**

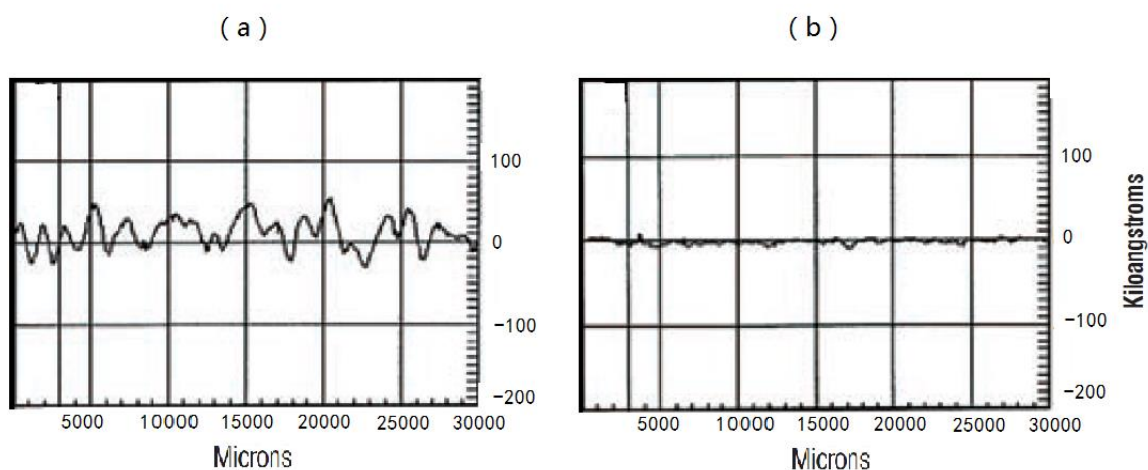


**Figure 2.4 Surface profiles of panels (a) coarse powder (b) fine powder (Zhu and Zhang 2005)**

Unfortunately, fine powders with  $D_{50}$  smaller than 25 microns are extremely cohesive due to strong interparticle forces. When the particle size goes down to a few microns, van der Waal's force, the largest interparticle force, becomes up to a million times greater than the force of gravity and makes the individual particles cling to each other (Visser 1989; Seville 2000; Kendall and Stainton 2001).

The cohesive nature of fine powder coating leads to another problem. In fluidization process, agglomeration of fine powder can generate slugging, in which the powders are lift up as a plug, or channeling, where the gas flows via channels inside the powder rather than passes through the voids between particles in the fluidization process, as shown in Figure 2.5, making the fine powder difficult to handle (Antony et al. 2004).

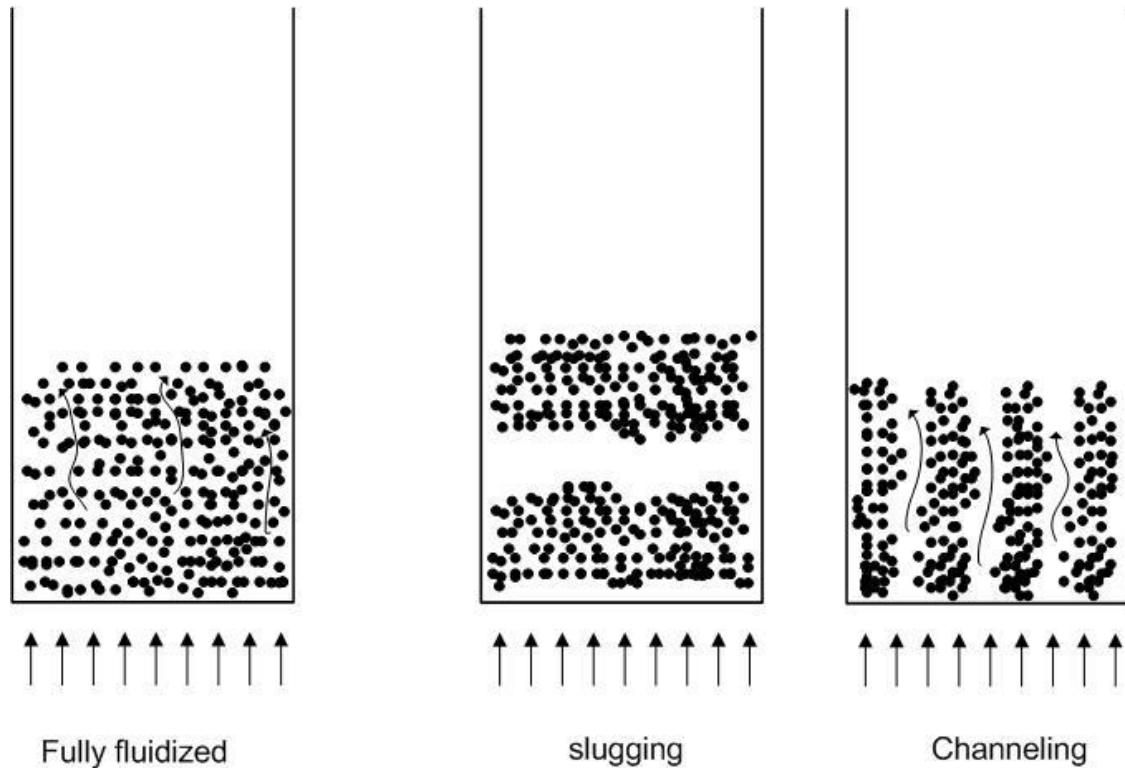


**Figure 2.5 Schematic of slugging and channeling**

Fluidizing the powder is the first step in powder coating application. Therefore, the poor flowability of fine powder greatly hinders the coating application. In this way, flow properties of powder play an important role in the application of powder coating. Table 2.1 shows powders can be categorized into five groups (Cheremisinoff and Cheremisinoff 1984), from very cohesive to very free-flowing, according to the angle of repose. Only the powder fair to passable flow can be fluidized and applied effectively. However, fine powders, mostly with angle of repose above  $45^\circ$ , even more than  $50^\circ$  in some circumstances, belongs to cohesive or very cohesive powder, which is difficult to be fluidized. The plugging or channeling occurred can make the application of powder coating stuck at the first step.

**Table 2.1 Classification of flow properties by angle of repose  
(Cheremisinoff and Cheremisinoff 1984)**

<b>Flow Properties</b>	<b>Angle of Repose(°)</b>
Very free-flowing	25-30
Free flowing	30-38
Fair to passable flow	38-45
Cohesive	45-55
Very Cohesive	55-70

### 2.3 Flow Additives for Fine Powder Coating

In response to the cohesive nature of fine powder, two methods had been used to improve the flow properties of such fine powder. One of them is applying extra forces, such as loading pressure (Kono et al. 1990), vibration (Xu and Zhu 2006), centrifugal force (Qian et al. 2001), magnetic assistance (Dave et al. 2000), acoustic and electric fields (Montz et al. 1989). These approaches do have some benefits, but with external excitations or addition of other materials like magnets. So they are a great consumption of external energy (Chen et al. 2008).

The other method is to use flow additives, or flow conditioners, to reduce the interparticle forces. Flow additives were first introduced to keep powders flowing evenly and/or increase flow rate through an orifice (Irani et al. 1960). Flow additives have been shown effective even in fine powder. By introducing a small amount of flow additive, the flowabilities of fine powders can be improved significantly (Hollenbach et al. 1983; Castellanos et al. 1999). Among the numerous additives, nano particles are widely accepted (Zhu and Zhang 2004). Although flow additives like nano-sized fumed silica can improve flowability and fluidizability of cohesive fine powders, the mechanism is not clearly understood. Some researchers believe that flow additive works as a “ball-bearing” or lubricant to reduce the internal friction (Hollenbach et al. 1983; Kono et al. 1989), as

shown in Figure 2.6 (a). While some believe that flow additive can reduce electrostatic charge (Dutta and Dullea 1990), as shown in Figure 2.6 (b).

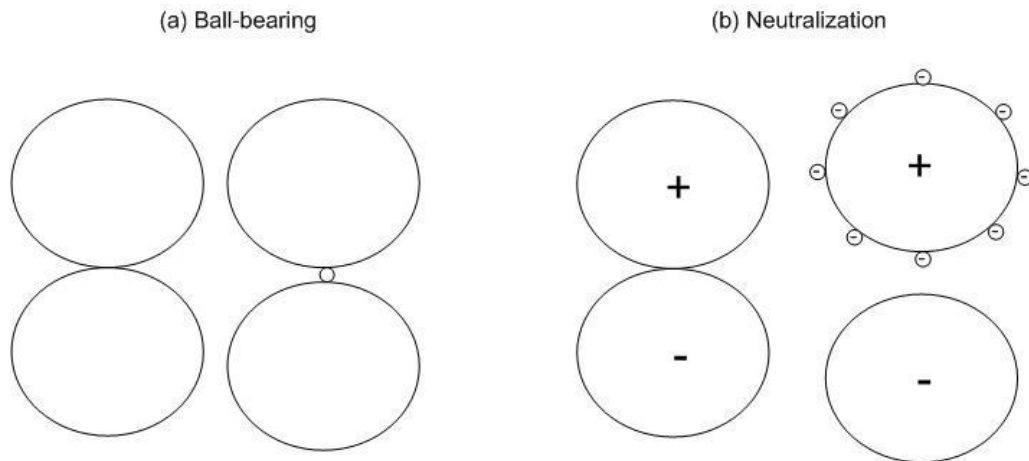


**Figure 2.6 Possible mechanism of flow additive**

However, most researchers believe that additive as a spacer, which cling onto the surfaces of host particles and increase the distance between or decrease the local radius of curvature and increase the hardness at the contact of two fine particles, thus reduce the van der Waal's force (Visser 1989; Rumpf 1990; Lauga et al. 1991; Xie 1997; Zhu and Zhang 2005; Huang et al. 2009; Kojima et al. 2013).

Yang et al (2005) studied the van der Waal's force between particles with and without additive and found that increasing the separation distance between host particles can significantly decrease the van der Waal's force. As shown in Figure 2.7, *A* and *B* represent powder particles, or host particles, while *c* represents flow additive, or guest particle. It's should be noted here that the actual particles are not spherical and the size of nano additive should be much smaller than powder particles. Case (a) and Case (b) show that the situations with and without additive respectively.

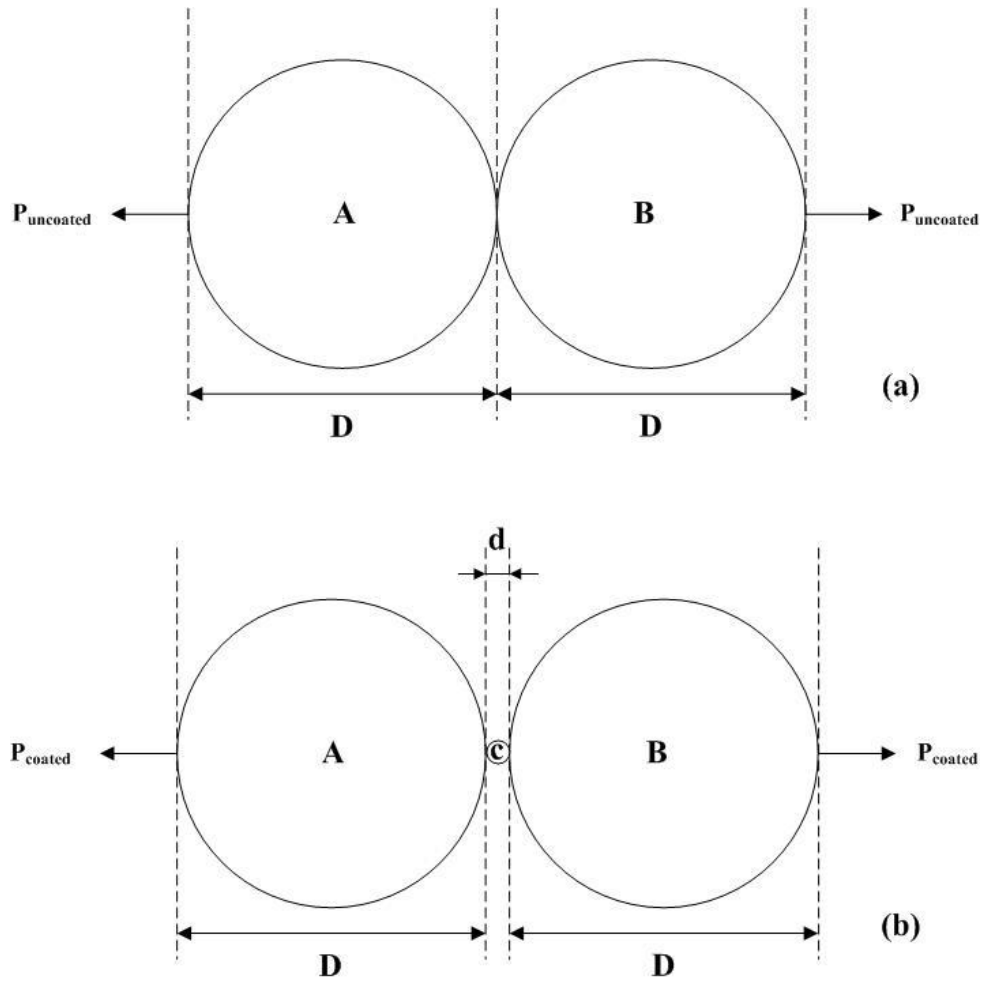


**Figure 2.7 Schematic diagram of cohesion forces between (a) host particles uncoated with additive (b) host particles coated with additive (Yang et al. 2005)**

In Figure 2.7 (a), two host particles are in direct contact without major deformation. The amount force needed to pull the two particles apart is estimated using the following equation (Hamaker 1937):

$$P_{uncoated} \approx \frac{A}{12} \frac{D}{2} \frac{1}{h_0^2} \quad (2-1)$$

where  $A$  is the Hamaker coefficient,  $h_0$  is the atomic scale separation distance between the two particles, which is normally between 0.165 and 0.4 nm (Fu 2010), and  $D$  is the diameter of host particles.

When the additive is added in, and a single guest particle is between the host particles, as shown in Figure 2.7 (b), the required amount force to pull the two particles apart is shown as follows (Rumpf 1990) :

$$P_{coated} \approx \frac{A}{12} \frac{dD}{d+D} \frac{1}{h_0^2} \quad (2-2)$$

Since the diameter of the guest particle,  $d$ , about 20 nm, is much smaller than the diameter of the host particle,  $D$ , about 20 microns,  $P_{coated}$  can be further simplified to:

$$P_{coated} \approx \frac{A}{12} d \frac{1}{h_0^2} \quad (2-3)$$

Divide Eq. (2-3) by Eq. (2-1), the ratio of separation force of coated and uncoated particles is:

$$\frac{P_{coated}}{P_{uncoated}} \approx 2 \frac{d}{D} \quad (2-4)$$

As the diameter of the nanoparticle  $d$  is hundreds or thousands of times smaller than the diameter of fine powder particles, the interparticle force should be reduced by hundreds or of thousands times comparing with the original force thus the flowability of fine powder is greatly improved.

With the remarkable effects of nanoparticle additive on flowability of the fine powder, many commercial nano particles, such as fumed silica, titanium dioxide and alumina oxide are employed as flow additives in fine powder coating processes. Studies have shown that additive materials (Huang et al. 2010), host particle materials (Elbichi and Tardos 1998), additive size (Chen et al. 2008), additive loading ratio (Danish and Parrott 1971) and mixing methods (Yang et al 2005) all influence the effectiveness of flow additive. The selection of flow additive should consider the application. For example, silica, titanium dioxide and aluminum oxide are preferred in general coating (Thomas et al. 2009).

However, there are also some drawbacks of using nanoparticles as flow additive, which mainly result from the differences in materials of additives and coating powders. All flow additives used currently are inorganic materials, while the coating powders are organic resins. In general, inorganic nanoparticles have an enormous specific surface area, the surface energy of the particle is high, and the chemical properties of the bare particle surface are very active, nanoparticles are easy to form aggregation or agglomeration (Rong et al.2006; Hong et al. 2007).

Those differences in materials can cause serious compatibility issues between inorganic additive and organic fine resin powders. Those agglomerates make the additives hard to be well dispersed onto the surface of additives, making the effect of nanoparticles as flow additive impaired. And more serious problems occurred during the curing process of powder coating. During the curing, agglomerates of additive are apt to “flow up” to the surface of resin fusion due to the different surface tension, resulting in the seeds on the final finish. In addition, the agglomerate of additive on top will repel resins with its relatively higher surface energy, leading to pinholes or craters. And the presence of organic additive will weaken the leveling of molten resin, increasing the roughness of coating finish. On the other hand, the organic additive affects the gloss at the same time because of its unique optical properties than resins.

## 2.4 Surface Modification of Nano-Additives

In order to improve the compatibility and dispersibility of inorganic additive in organic resin powders, a series of methods has been tried by researchers in two aspects: development of new compounding (dispersion) technique and surface pretreatment of nanoparticles (Rong et al. 2006). However, more efforts were laid on the latter aspect, which is surface modification of nano additive.

A method to coats inorganic particles with an organic layer onto the surface of inorganic particles was developed (Sato and Ruch 1980). By coating a thin “shell” on the surface of inorganic particles, the physical, chemical, structural and electronic properties of the



original particles can be modified to meet with various application requirements (Vollath and Szabo 1999; Ruys and Mai 1999). To encapsulate organic materials on inorganic additives, two methods can be employed. One is the dry method like physical vapor deposition (Zhang et al. 2000), plasma treatment (Hegemann et al 2003), anti-solvent process (Wang et al. 2004) and chemical vapor deposition (Nagel et al. 1982; Kong et al. 1998). The other is the wet method: solvent evaporation (Cohen et al. 2000; Hans et al. 2002) and sol-gel method (Brinker et al. 1990; J. Ruys and Mai 1999).

In the sol-gel method, the inorganic material is dispersed in an organic polymer solution, and the solution (or sol) evolves gradually towards the formation of a gel-like network. This technique offers several advantages because it only needs mild conditions like ambient temperature and constant stirring (Xia 2013). Thus there is no need to worry about activity of the polymer and the method is easy to process.

## 2.5 Summary and concluding remarks

Powder coating is the fastest growing finishing method in the coating industry. It is beneficial to the environmental as there is no emission of VOCs, and reduces the cost as the powder can be recycled. However, the application of coating powder is restricted to wheels, radiators, engine blocks, and so on, because of its thick film and poor aesthetic appearance.

All those drawbacks are attributed to the large particle sizes and could be overcome by the size reduction. The fine powders, which can achieve a relative thin coating finishing and good aesthetic appearance, are cohesive and experience poor flow in various processes due to the relatively larger interparticle forces.

Adding flow additive can increase the distance of powder particles and thus reducing the interparticle forces. In this way, the flow properties of fine powder can be effectively improved. However, the difference of material between inorganic additives and organic powders leads to serious compatibility issues like the “fish eye” or seeds on the coating surface.

To solve the compatibility problems of additives in powder coating technology, the inorganic particles are encapsulated with organic materials. By coating a thin “shell” on the surface of inorganic particles, the properties of the original particles can be modified and should meet with the properties of organic powders. However, that is still a hypothesis and there is no attempt to study to performance of the modified nano particle on improving the flowability and film qualities of the fine powders.

The train of thought in powder coating technology is summarized in Figure 2.8.

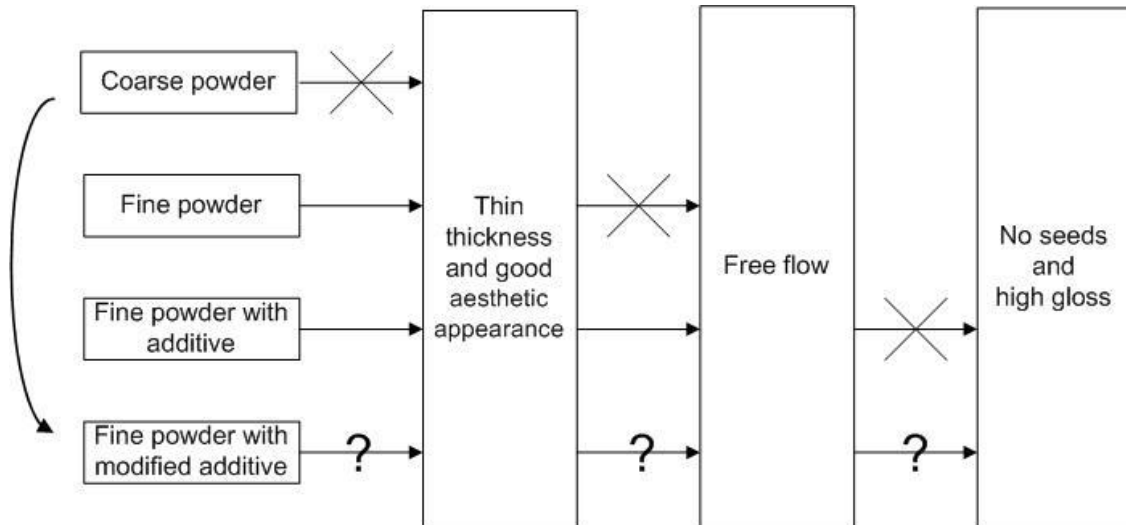


**Figure 2.8 Train of thought in powder coating technology**

## Chapter 3

### 3 Experimental Methods

This work focuses on a new modification technology for nano additives for fine powder coatings. The whole experimental work is divided into three stages:

Firstly, encapsulate the nano-size silica additives with polymer resin in different R-EA ratios, followed by incorporating the modified additives with coating powders in different additive loading ratios;

Secondly, evaluate the semi-static and dynamic flow properties of the coating powder samples by measuring the Angle of Repose and Avalanche Angle, respectively;

At last, study the film qualities of the coating films by measuring film gloss, roughness and the number of seeds of the film surface.

All the materials used in this work are listed in Table 3.1.

**Table 3.1 List of materials used in this work**

Materials		Model	Supplier	State/size
Commercial Coating Chips	Polyester	PE-0191-H	Prism	Chips
	Hybrid	HB-0101-H	Prism	Chips
Commercial Additive	Nano- Silica	AEROSIL®R972	Degussa	Powder 16 nm
Encapsulating Materials	Polyester	CRYLCOAT®2689-0	Cytec	Chips
	Hybrid	70 wt% of CRYLCOAT 316	Cytec	Chips
		30 wt% of D.E.R. <sup>TM</sup> 672U	Dow	Chips

## 3.1 Experimental Procedures

### 3.1.1 Modification of Nano-size Additives

The modification, or the encapsulation included four major stages which were dissolving, drying, milling and collection, as shown in Figure 3.1.

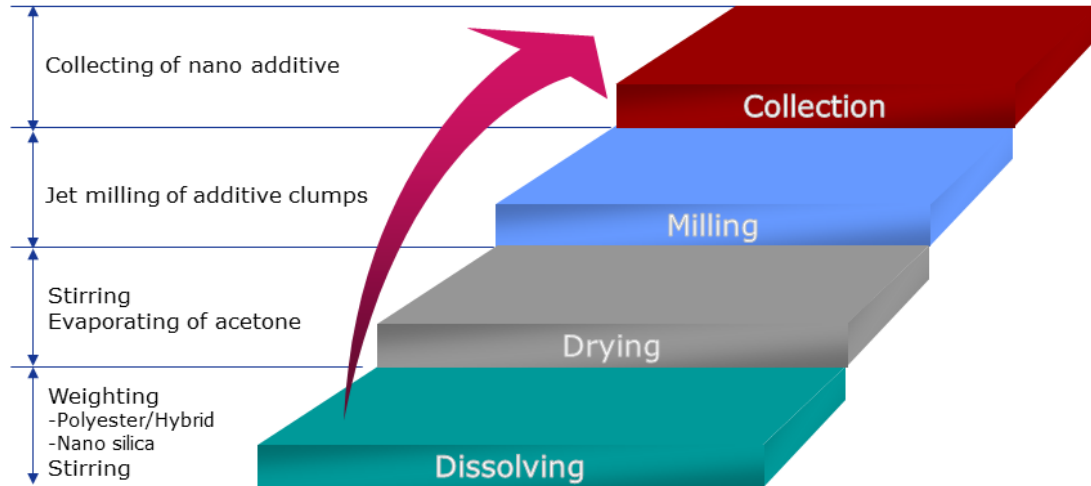


**Figure 3.1 Four stages for encapsulation of additive**

#### Stage 1-Dissolving

In this stage, given mass of resin (polyester or hybrid powder), which acted as the encapsulating material, was first dissolved into acetone. A magnetic stirrer apparatus was used to stir the solution for one hour at 200 rpm under the room temperature. Then followed by one hour ultrasonic bath until the resin was completely dissolved and the solution became clear and transparent. Then the silica additive was added in, kept on stirring for another twenty hours. The whole stage could be shown in Figure 3.2.

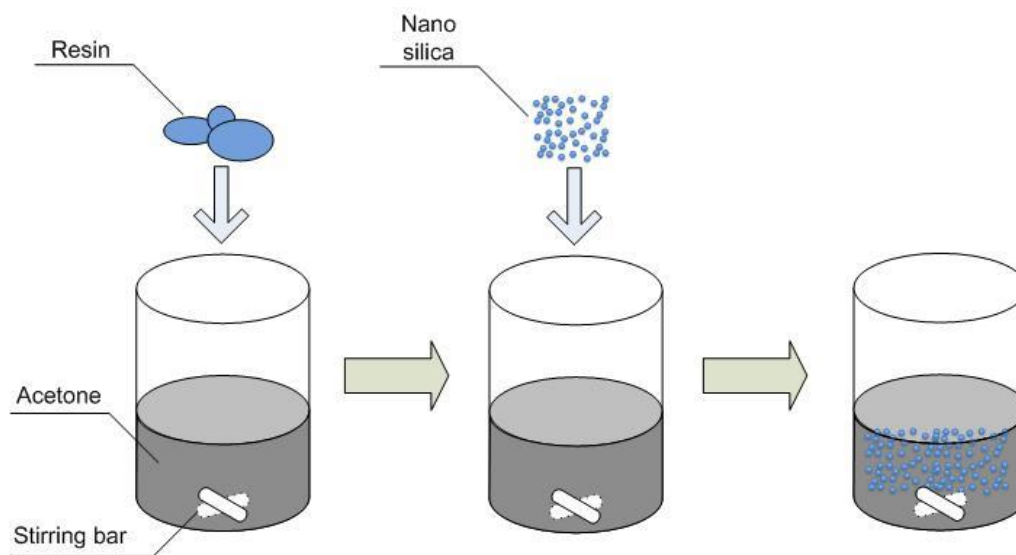


**Figure 3.2 Schematic of dissolving**

The mass of acetone was 7-8 times of the total mass of additive and encapsulating resin to ensure the silica additive could be mixed and dispersed well. The mass of resin and additive added in was depended on the specific mass ratios listed in Table 3.2,

**Table 3.2 Mass ratios of encapsulating resin to nano-size silica additive**

Description of Additive	Mass Ratio of Resin to Nano Silica
Polyester-5%	5:95
Polyester-10%	10:90
Polyester-15%	15:85
Polyester-20%	20:80
Hybrid-5%	5:95
Hybrid-10%	10:90
Hybrid-15%	15:85
Hybrid-20%	20:80

Stage 2-Drying

With the evaporation of the acetone, the solution gradually became dry and at last white mud. Then the mud was removed and tiled onto a 20x10cm plate, after one day natural dry at room temperature, all the acetone was evaporated and left with the encapsulated additive powder clumps.

### Stage 3-Milling

Since that ultrafine powder coating technology needs additive to be in nano size, the third step would be milling. A jet milling system developed by the Particle Technology Research Centre (PTRC) of the University of Western Ontario was used to grind the additive chips to nano size as shown in Figure 3.3.

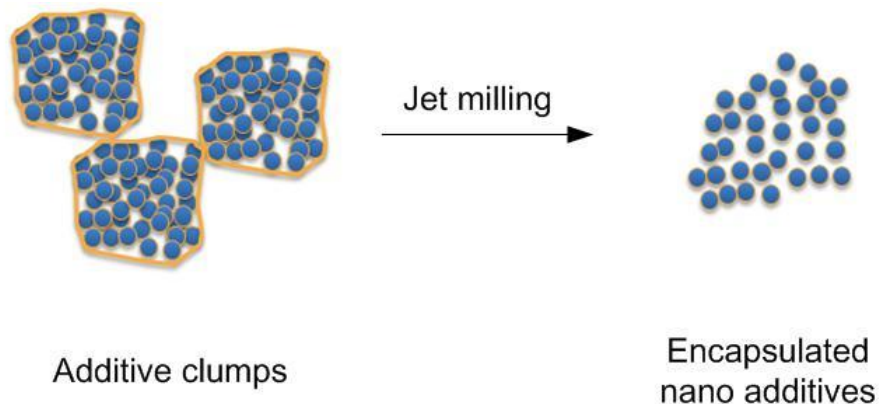


**Figure 3.3 Schematic of jet mill of additive clumps**

The jet mill system is shown in Figure 3.4. The additive particles or clumps were fed into the inlet by a vibrating feeder. Then the chips were sucked into the grinding chamber due to the negative pressure induced by the feeding air. In the chamber, the strong inter-particle collisions from opposed suspension jets crashed the particles into nano size. The ground particles were then separated by a cyclone and a filter. The coarse particles would be collected in a plastic barrel collector for the further milling, and other additive particles would be stopped by the HEPA filter. The additive particles left attached on the HEPA filter were the desired encapsulated additive with suitable particle size. In this process, the feeder was set to 0.1 g/s; the feeding air pressure was set to 20 psi; the two working air pressures were set to 20 psi.

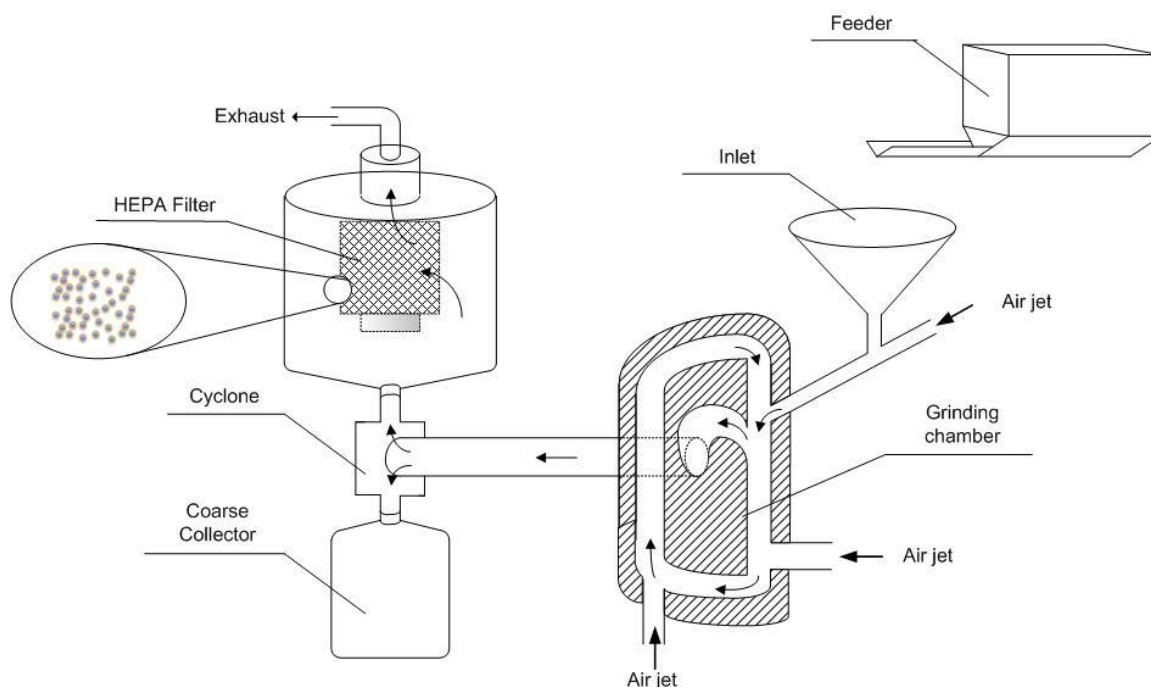


**Figure 3.4 Schematic of Jet Mill**

#### Stage 4-Collection

After jet milling, the desired particles were attached to the HEPA filter, which needs a collection system to manually collect the modified additive. A lab made device was used to transport the additive from the HEPA filter to a smaller filter, as shown in Figure 3.5. It consists of a canister and a cylindrical thimble filter. The canister is connected to vacuum to provide suction. Due to the exhaust flow, the additive on the HEPA filter from the jet mill was sucked into the canister and trapped by the thimble filter, with the clean air can come out from the canister with the exhaust flow. Then the thimble filter was detached from the canister and the additive was poured into sample bags.

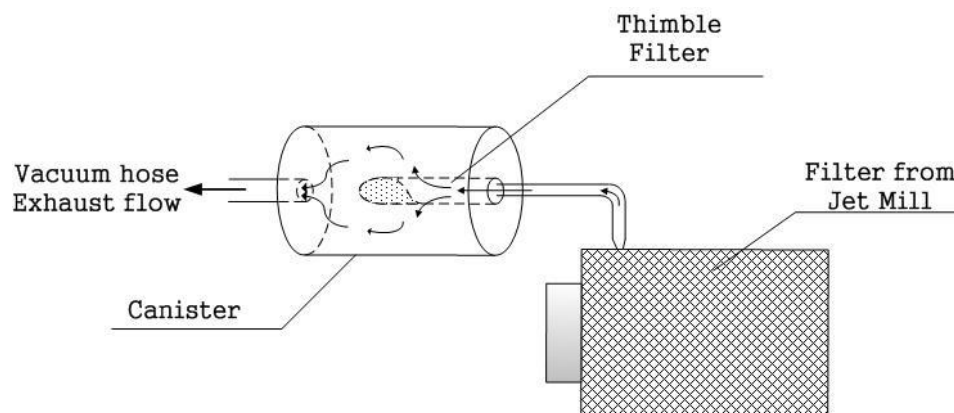


**Figure 3.5 Schematic of collector**

There were two encapsulating materials, polyester (PE) and hybrid (HB) resins and four Resin-to-Encapsulated Additive (R-EA) ratios for each of the two materials, which were, 5%, 10%, 15% and 20%. Each additive was named with the encapsulating resin material followed by the corresponding R-EA ratio, connected by “-”. For instance, PE-5% means the additive which was encapsulated with polyester resin with 5% in mass percent. Count in the control additive (with no resin), 9 different additives were studied in this research project, shown in Table 3.3.



**Table 3.3 List of additives prepared**

<b>Label</b>	<b>Encapsulating material</b>	<b>R-EA ratio(By mass)</b>
Control additive	N/A	0
PE-5%	Polyester	5%
PE-10%	Polyester	10%
PE-15%	Polyester	15%
PE-20%	Polyester	20%
HB-5%	Hybrid	5%
HB-10%	Hybrid	10%
HB-15%	Hybrid	15%
HB-20%	Hybrid	20%

### 3.1.2 Preparation of Coating Powder Samples

Preparation of coating powder samples consisted of two parts. The first part was grinding of the commercial coating chips to suitable particle size for the ultrafine powder coating technology. And the second part was mixing the coating powder with additive in different additive loading ratios.

#### Stage 1-Air Classifying Milling

Polyester and hybrid coating chips bought from the market were ground into fine powders with an Air Classifying Mill (ACM) (Donghui Powder Processing Equipment Co., China), as shown in Figure 3.6.



**Figure 3.6 Air Classifying Mill (ACM)**

Figure 3.7 shows how the ACM works. The chips were placed into the feed hopper and then fed into the grinding zone by a screw feeder. In the grinding section, the chips are contacted by the fast spinning grinding rotor and the size was reduced mainly by the impact of the materials against impactors and impact wall. The ground particles were then carried by the upward air flow to the classifier. In the classifying section, coarse particles were diverted back to grinding section for further reduction because the drag force produced by the air flow was smaller than centrifugal force from the rotation. Fine particles, on the other hand, passed through the classifier and then were carried by the air flow to the cyclone. The finest particles that could not be separated left through the top of the cyclone and are carried to the bag house. The rest particles were separated from the air flow and collected by the bag.

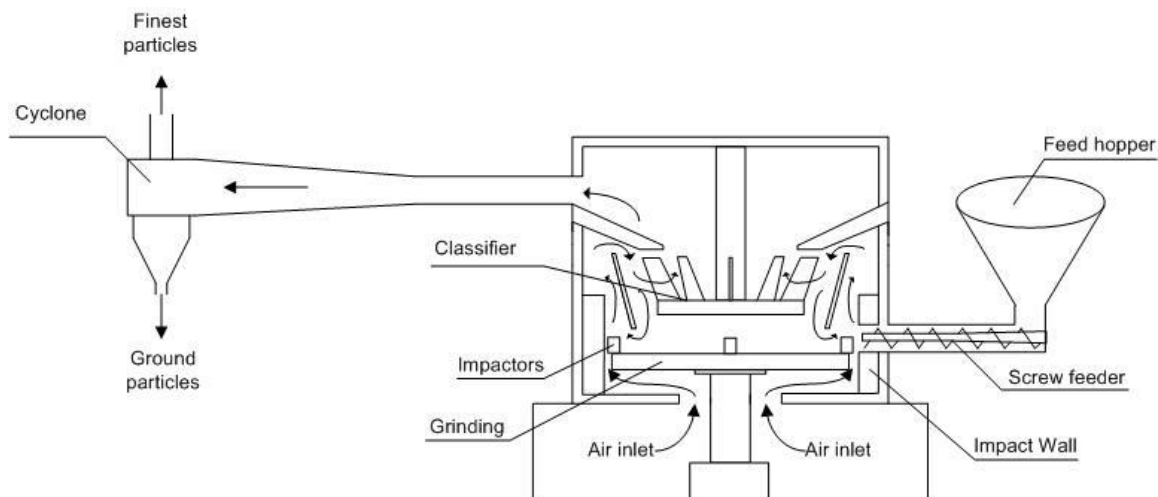


**Figure 3.7 Schematic of Air Classifying Mill**

For different powders, the operation conditions varied and had a great influence on the particle size as well as the particle size distribution. So adjustments were tried until the desired particle size and appropriate particle size distribution was accomplished. The specific conditions for the two coating powders are listed below in Table 3.4.

**Table 3.4 Operation conditions of ACM**

Conditions	Polyester	Hybrid
Fan speed, m <sup>3</sup> /s	24.8	26
Grinding rotor speed, rpm	8900	7800
Classifier speed, rpm	3700	3900
Feeder rate, kg/h	1.44	1.68

## Stage 2-Mixing

To ensure homogenously mixing powder with additive, manually pre-mixing and an ultrasonic-vibration sifter (VORTI-SIV Lab Models RBF-12, MM Industries, Inc., US), as shown in Figure 3.8, was used.



**Figure 3.8 Ultrasonic-Vibration Sifter**

As shown in Figure 3.9, coating powder was firstly placed in a plastic bag and then certain mass of additive was added in. After manually shaking the bag for ten minutes, the pre-mixed powder samples were placed on the sieve screen of ultrasonic-vibration sifter. The sieve screen was vibrated by a vibration motor as well as an ultrasonic vibrator. During the vibration and sieving process, additive agglomerations were broken and through the sieve screen to the collecting tray along with coating powder. After that, the powder from collecting tray was poured back onto the sieve screen. For the second time sieving, additive could be mixed uniformly and homogenously with the powder.

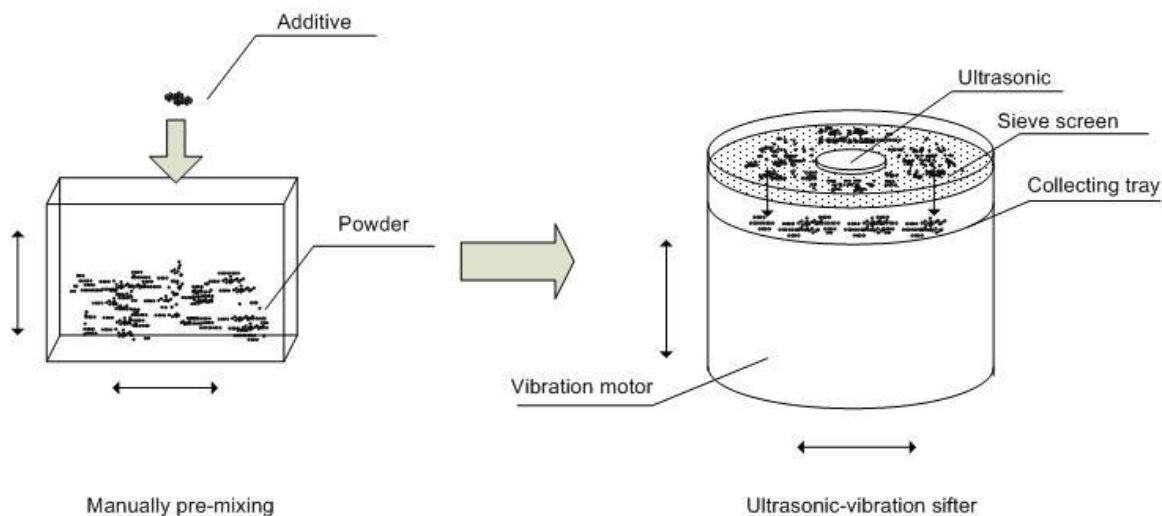


**Figure 3.9 Schematic of mixing**

In this work, polyester or hybrid coating powders from ACM and the corresponding additives (polyester coating powder was mixed with the additives encapsulated with polyester resin and the same with hybrid powder) were sieved twice with a 45 microns screen in four additive loading ratios, which were 0.15%, 0.3%, 0.5% and 0.8% by weight percent. In addition, coating powders were mixed with control additive in these four additive loading ratios too.

In total, 40 samples with additive were tested in this research project. To identify these samples clearly, each powder sample was named with the additive label followed by the corresponding additive loading ratio, connected by “-”. For instance, PE-5%-0.15% means that the polyester coating powder mixed with additive PE-5% in an additive loading ratio of 0.15%.

Below is a summary of all the samples and their composition, shown in Table 3.5.

**Table 3.5 List of all powder samples prepared**

<b>Label</b>	<b>Powder coating</b>	<b>Additive</b>	<b>Additive loading ratio</b>
PE-Control-0.15%			0.15%
PE-Control-0.3%	Polyester	Control	0.3%
PE-Control-0.5%		Additive	0.5%
PE-Control-0.8%			0.8%
PE-5%-0.15%			0.15%
PE-5%-0.3%	Polyester	PE-5%	0.3%
PE-5%-0.5%			0.5%
PE-5%-0.8%			0.8%
PE-10%-0.15%			
PE-10%-0.3%	Polyester	PE-10%	0.3%
PE-10%-0.5%			0.5%
PE-10%-0.8%			0.8%
PE-15%-0.15%			
PE-15%-0.3%	Polyester	PE-15%	0.3%
PE-15%-0.5%			0.5%
PE-15%-0.8%			0.8%
PE-20%-0.15%			
PE-20%-0.3%	Polyester	PE-20%	0.3%
PE-20%-0.5%			0.5%
PE-20%-0.8%			0.8%
HB-Control-0.15%			
HB-Control-0.3%	Hybrid	Control	0.3%
HB-Control-0.5%		Additive	0.5%
HB-Control-0.8%			0.8%
HB-5%-0.15%			
HB-5%-0.3%	Hybrid	HB-5%	0.3%
HB-5%-0.5%			0.5%
HB-5%-0.8%			0.8%
HB-10%-0.15%			
HB-10%-0.3%	Hybrid	HB-10%	0.3%
HB-10%-0.5%			0.5%

Label	Powder coating	Additive	Additive loading ratio
HB-10%-0.8%			0.8%
HB-15%-0.15%			0.15%
HB-15%-0.3%	Hybrid	HB-15%	0.3%
HB-15%-0.5%			0.5%
HB-15%-0.8%			0.8%
HB-20%-0.15%			0.15%
HB-20%-0.3%	Hybrid	HB-20%	0.3%
HB-20%-0.5%			0.5%
HB-20%-0.8%			0.8%

### 3.1.3 Spraying and Curing of Panel Samples

The effects of additive modification on the flow properties of fine powder could be evaluated by direct testing on the powder samples. However, to explore the effects of this additive encapsulation technology on the film qualities, the powder samples must be sprayed on the panels and form the coating films through the curing process.

#### Spraying

In this work, powder coating electrostatic spraying process was applied. The whole spraying process took place in a spray booth using an EasySelect-Cup Manual Powder Gun (ITW Gema GmbH, Switzerland). The powder spray gun was connected with external high voltage so the powder is firstly negative electrically charged. Then the powder was entrained by the high pressure air flow and sprayed towards the grounded aluminum panel. Part of powder particles could deposit on the target panel and stay by their electrostatic forces while others would miss the panel and be collected by the spray booth as reclaimed powder for recycle use.

The spray distance was set up to 20 cm. The work voltage was 30 kv to minimize the orange peel. The size of aluminum panel was 0.6\*51\*89 mm and was hung up by a grounded metal clip. And the powder was feed as a batch test. A schematic of spraying the panel is shown in Figure 3.10.

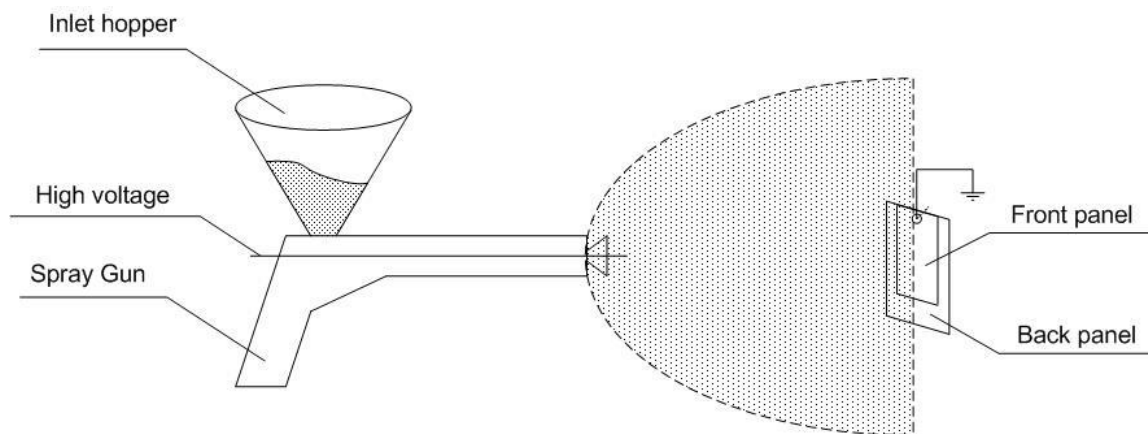


**Figure 3.10 Schematic of panel spraying**

Since that the thickness of the coating film plays a significant role on the film qualities, keeping the thickness of coating film on each panel consistent would be the key point to this work. To achieve consistent thickness of  $50 \mu\text{m}$ , a weight-control method was developed because the thickness of the coating film should have a linear relationship to the weight of the powder sprayed on the panel, theoretically. However, a portion of powder particles would travel around the panel and deposit on the back side, which makes the thickness of the film unrelated with the weight of panel. The solution to this problem was using a back panel. These two panels were hung together with no space between. So there was no powder particle on the back side of the front panel during the spraying. So only if the weight of powder on the front panel can be controlled to the same value before the curing, the goal of keeping the thickness of coating film uniform can be accomplished.

For polyester, the weight of powder sprayed on the panel was controlled at 0.32 to 0.33 g. For hybrid coating powder, the weight was controlled at 0.36 to 0.37 g, since that the density of polyester coating film is a little smaller than that of hybrid coating film.

## Curing

After spraying, a curing process was needed to form the film. During the curing, the powder on the panel would melt and flow out to form a coating film due to the high temperature. The crosslinking would happen between the polymers with higher molecular



weight being formed in a network structure. In this work, all panels were put into a bake oven with a temperature of 200 °C for ten minutes.

For each powder sample, three panels were sprayed and cured, giving a total of 120 panels in total to be measured. Among these panels, the thickness of the coating film was strictly controlled to ensure the comparability of effects of additive encapsulation on the film qualities.

## 3.2 Measurement Techniques

### 3.2.1 Measurement of Particle Size

The particle size of each powder, polyester and hybrid coating powder, was measured using laser diffraction method with a BT-9300S Laser Particles Size Analyzer, built by Baite Instrument Ltd., China, through the standard test procedure. The results were reported as three mean particle sizes,  $D_{10}$ ,  $D_{50}$  and  $D_{90}$ , which are respectively defined as the diameters at which 10%, 50% and 90% of particles by volume are smaller or equal to. Among the three diameters,  $D_{50}$  represents the medium particle size, while  $D_{10}$  and  $D_{90}$  indicate the amount of fine and coarse particles in the sample. The particle size distribution (PSD) was given as well.

### 3.2.2 Characterization for Flow Properties- Angle of Repose and Avalanche Angle

A series of tests were applied to evaluate the flow properties of the fine powders, including the test of Angle of Repose and Avalanche Angle.

#### Angle of Repose

The Angle of Repose was measured with a PT-N Powder Characteristic Tester (Hosokawa Micron Powder Systems Co., Summit, NJ, USA). Following the standardized testing procedures (ASTM D6363-08), the powders were loaded on a mesh and then dispensed through a glass funnel due to the vibration onto a circular plate. A conical heap would be formed with the falling of the powders until covers the whole area of the plate and no additional powder would be accumulated onto the heap. In other words, the

additional powder would slide down along the slope of the powder heap. Then the angle between the surface of the powder heap and the surface of the plate was defined as the Angle of Repose. A schematic diagram of AOR test is shown in Figure 3.11. To ensure the accuracy, 4-6 times were repeated following the same procedure and 3 of them with the difference smaller than 0.6 were applied. The average value of these 3 angles was recorded as the Angle of Repose of each powder sample.

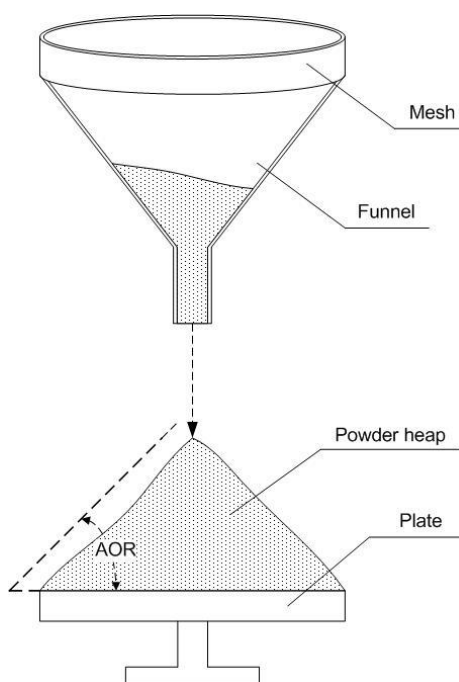


**Figure 3.11 Schematic of AOR Measurement**

### Avalanche Angle

The avalanche angle was measured with a Revolution Powder Analyzer (Mercury Scientific Inc., Sandy Hook, CT, US). In this test, a tapped volume of 120 ml powders, obtained by an accessory metal cup, was placed into an 11 cm diameter, 3.5 cm wide cylindrical drum with two transparent glass sides. Then the loaded drum was placed into the measuring bin of the Analyzer, where two computer controlled rollers would rotate the drum at various given speeds. The rotation speed would increase gradually to pre-mix

the powders and then stay at 0.6 rpm. The powders inside would be carried up by the side of the drum until collapse or avalanche. The behavior of the powders inside could be monitored and analyzed by a digital camera connected to a computer. With software supplied by the Analyzer manufacturer, the maximum angle between the powder surface and horizontal line before the avalanche was recorded as the Avalanche Angle (AVA). To ensure the accuracy, 200 avalanches were applied and the average Avalanche Angle was provided as the Avalanche Angle of each powder sample. The schematic diagram of Avalanche Angle measurement is shown in Figure 3.12 and Figure 3.13.

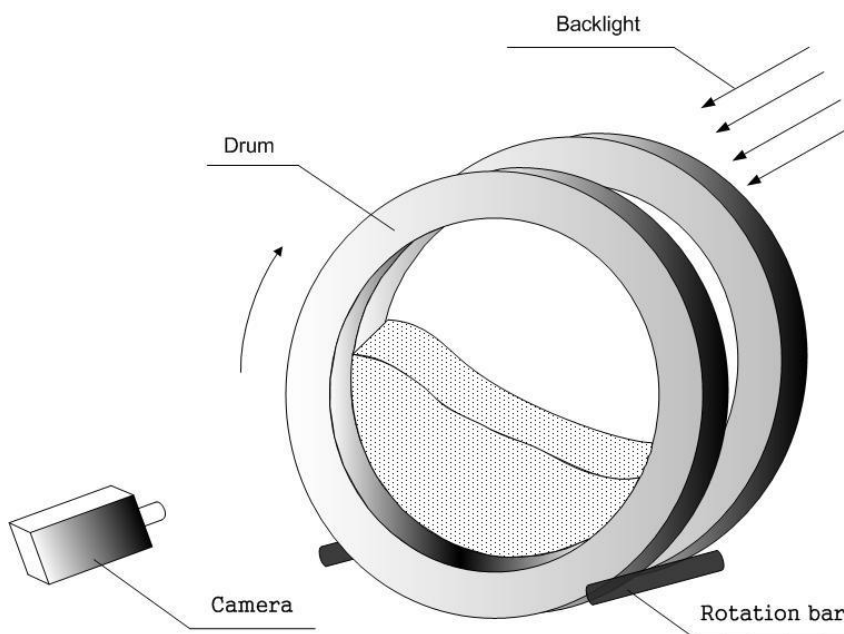


**Figure 3.12 Schematic of AVA Measurement**

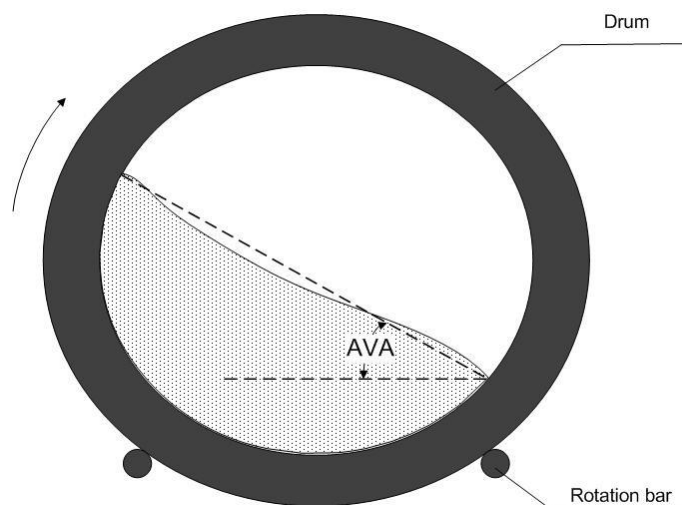


**Figure 3.13 Schematic of Avalanche Angle**

### 3.2.3 Evaluation of Film Qualities-Thickness, Gloss, Number of Seeds and Roughness

A series of tests was applied to evaluate the film qualities of the fine powder coating, including the test of thickness, gloss, number of seeds and roughness.

#### Thickness

The film thickness of each panel was measured by PosiTector® 6000 Coating Thickness Gauge (DeFelsko Corporation, US), as shown in Figure 3.14. A magnetic principle was used to measure the non-magnetic coatings. Since the coating film on the panel cannot be absolutely uniform, an average value of nine different parts on the whole panel was set to represent the thickness of the panel, as shown in Figure 3.15.



**Figure 3.14 Coating Thickness Gauge**

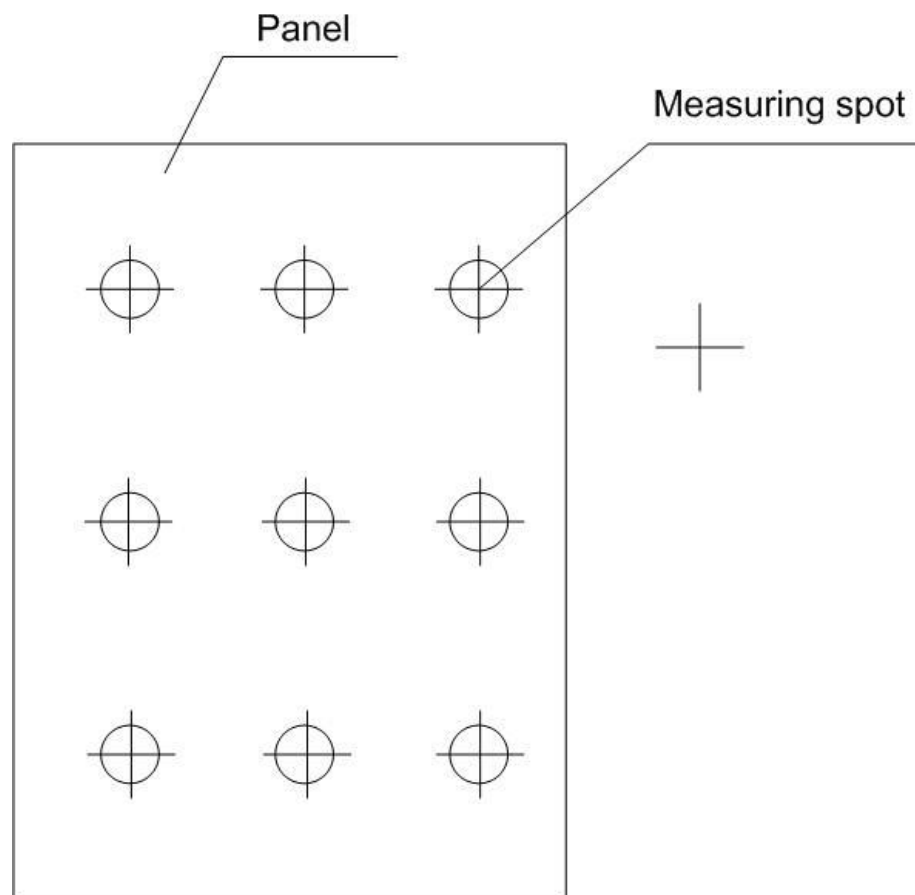


**Figure 3.15 Schematic of thickness measurement**

## Gloss

The gloss of coating film of each panel was measured by a Novo-Gloss<sup>TM</sup> (GENEQ Inc., CA). After the calibration of a standard black coating film of 93.3°, five different parts for each panel were measured at 60° measuring range and the average value was recorded as the film gloss of the coating film. Since three panels were sprayed and cured with the same powder samples, the average gloss of these three panels was used as the gloss of this specific powder sample. A schematic of gloss measurement is shown in Figure 3.10.

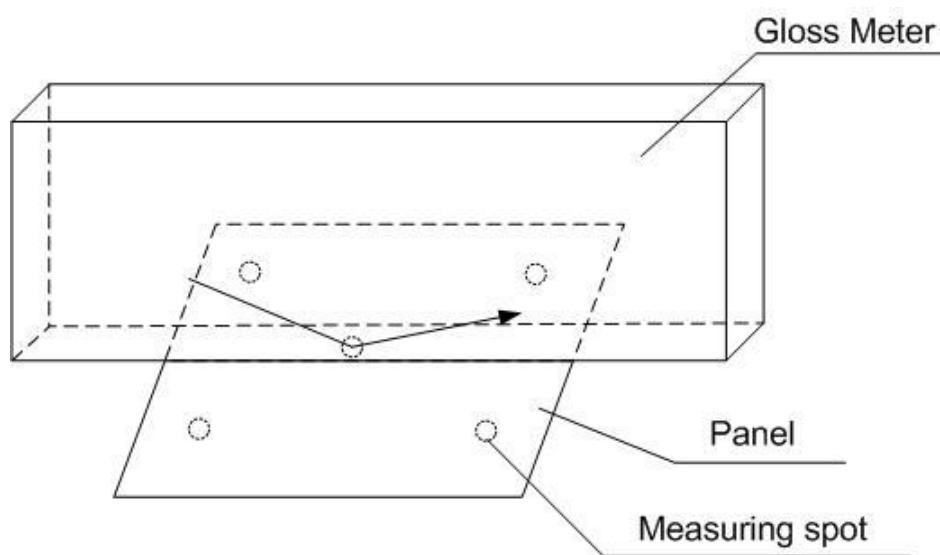


**Figure 3.16 Schematic of gloss measurement**

## Roughness

The roughness of film surface of coated panels was measured by a surface profiler, which was defined as  $R_a$ . The scan length is 5 microns and three scans were conducted for each panel sample and the average value was calculated, as shown in Figure 3.17. Afterwards, the average roughness of all the three panel samples coated with the same powder was used as the roughness of coating film.

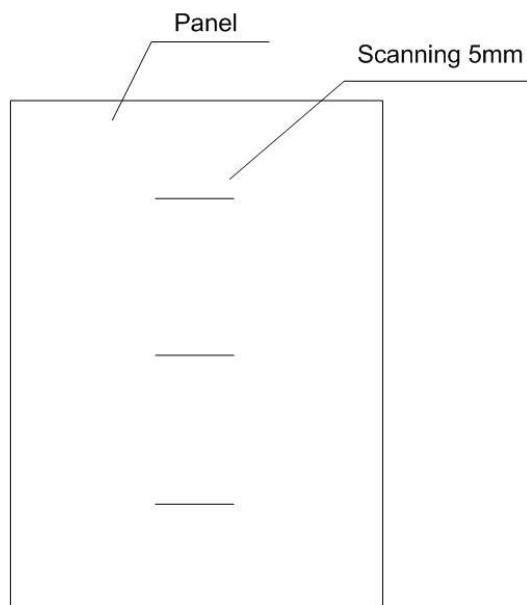


**Figure 3.17 Schematic of roughness measurement**

### Number of Seeds

Seed is a usually seen defect or fault on the coating film, especially for fine powder coating film because of the presence of additive agglomerates. The number of seeds which could be seen by the naked eye was recorded as the number of defects on coating film. Then the average number of seeds on the surfaces of three panels was used as the number of seeds for this specific powder sample.

## Chapter 4

### 4 Flow Characterization of Fine Powders with Modified Additives

#### 4.1 Introduction

In applications of fine powder coating, the flow properties always play a significant role throughout the whole process. For example, during the process of fluidization or pneumatic transportation, poor flowability will result in the powders tending to stick to the internal walls or clog up the transport lines, which will increase the frequency of pipeline clean. More importantly, uneven flow during the spraying of powders will ultimately lead to poor film qualities of the final products.

The flowability issues become more serious for Geldart's Group C powders, which comprise particles under 25-35 microns, or also referred to as fine powders. The interparticle forces, primarily the van der Waal's force, increase drastically when the particle size gets smaller, comparing to other forces exerted upon the particles. Fine powder is much more cohesive and more susceptible to form agglomerates than the coarse powder.

Numerous characterization techniques have been developed in the last decades, including Bed Expansion Ratio, Rotational Bed Expansion Ratio, Angle of Repose, Avalanche Angle, and Cohesion. However, confusion of inconsistent or even contradictory results from different characterization techniques can be seen. Previous work done by Krantz and Huang (Krantz et al. 2009; Huang et al. 2009) proposed an acceptable explain that each of them tests powder under a different condition. For example, the avalanche angle is measured under a more dynamic condition while the state of angle of repose is more likely to be considered as semi-static. The dynamic flow property is generally used as the indicator when powder flow under fluidization or pneumatic transportation while static flow property is more likely useful to investigate agglomeration issue (Fu 2010). As suggested by Krantz et al. (Krantz et al. 2009), there is not necessarily a relationship between any two of these characterization techniques, and the results under different



conditions are not interchangeable with each other. Thus, to fully evaluate the flow properties of fine powder, a single characterization method is not sufficient.

Due to the fact that the powder coating process is in semi-static and dynamic modes, two specific techniques were used in this work, which were Angle of Repose and Avalanche Angle. They represent semi-static flow property and dynamic flow property, respectively. For both of the techniques, a lower value means a better flow property.

In this section, three problems were explored:

1. If the encapsulation of flow additive has the effect on the flow properties and what is the optimum encapsulation ratio?
2. How much modified additive should be used in order to get the desired flow properties?

Two different resin bases were adopted to evaluate the effect of encapsulation on different powders, which may indicate broad application of this technology.

## 4.2 Effect of Resin-to-Encapsulated Additive Ratio on Flow Properties of Fine Powders

The additives were encapsulated with 2 resins (polyester or hybrid) in 4 Resin-to-Encapsulated Additive ratios. Thus there were 9 additives (8 modified additives and 1 control additive) studied in this work. Then the additive was incorporated into coating powder with corresponding resin base, in 4 additive loading ratios (control additive was employed in both of the resin based powders). In this way, all 40 samples prepared can be classified by resin bases, R-EA ratios and LOAs.

For each flow properties characterization, all of the 40 coating samples were tested. The results were compared with R-EA ratios and resin bases.

### 4.2.1 Semi-Static Flow Characterization

Semi-static flow property indicates how easily the powder flows in a relatively static condition, like in storage silos or spray gun hoppers. Generally, a poorer semi-static flow property means more energy is going to be consumed during the process.

In this work, the semi-static flow property was evaluated using Angle of Repose, which is a widely used characterization technique due to the convenience. It's known as a static flow measurement because when the powder particles land in a heap, the static interparticle forces cause the powder pile up as shown in Figure 3.11. However, there is also some kinetic energy impact on the heap when the powder falls down. Hence it is more likely to be referred to as semi-static flow property. The lower value of AOR, the better semi-static flow property the powder has.

Figure 4.1 illustrates the angle of repose values of polyester coating powder samples in relation to R-EA ratio. As expected, the encapsulation of additive does effectively affect the powder sample's angle of repose, or in other words, the powder's semi-static flow properties. Even though there exists LOA differences between powders, a general trend can still be observed. Angle of repose values firstly decrease with the increasing of R-EA ratio to a minimum value where R-EA ratio is around 10%. Further increase of R-EA ratio makes the AOR value increase and back to original level.

In details, from 0 to 5% of R-EA ratio, AOR of all those four groups of samples shows a relatively slow decrease rate and just decreased by around  $0.3^\circ$ . A small encapsulation level of 5% has rare effects on the semi-static flow property as the AORs almost stay at the same values as those of the control samples. From 5% to 10% of R-EA ratio, the effect is more apparent. For instance, the samples with 0.5% LOA have a dramatic drop of AOR by  $3.01^\circ$ , from  $41.24^\circ$  to  $38.23^\circ$ , representing a significant improvement on the semi-static flow properties. For the other three groups, the encapsulation on additive also make AOR lower than  $42^\circ$ , which is the maximum AOR that agglomeration would not occur during the application of powder coating according to Huang et al. (Huang et al. 2009). When the R-EA ratio is higher than 10%, AORs of powders with LOA of 0.15%, 0.3%, and 0.5% increase with the further increasing of R-EA ratio, samples blended with 0.15% additive even show higher AORs than those of the control samples. The powder with LOA of 0.8% shows a delayed trend: AOR continuously decreases until staying at a relatively constant value. Through comparisons of these LOAs curves, it can be drawn that the optimum R-EA ratio to get the best semi-static flow property for polyester based powder is 10%.

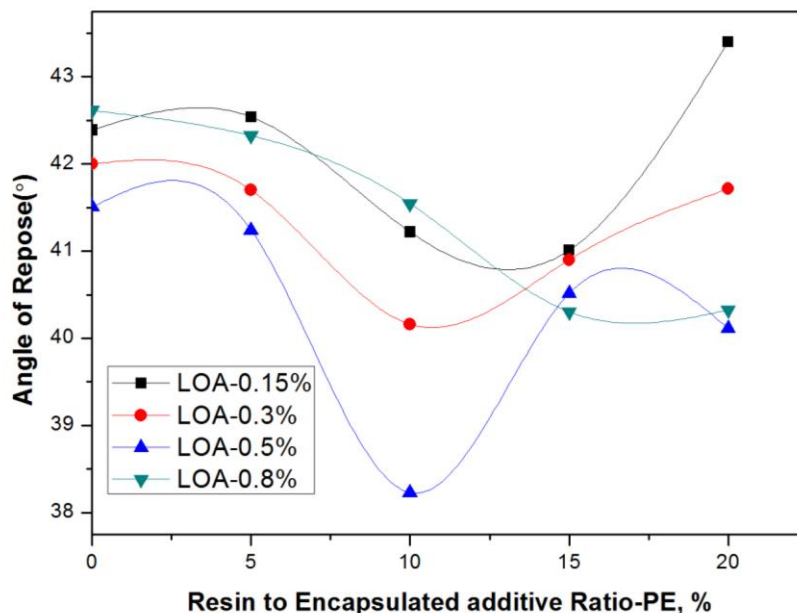


**Figure 4.1 Effects of R-EA ratio on AOR-PE  
(Additives were encapsulated with PE.  
Encapsulated additives were incorporated into PE powder)**

Change of additive encapsulation material and resin base of powder also affects the curves of AOR with respect to R-EA ratio. When additives were encapsulated with hybrid resin and loaded into hybrid based powder, the effects of R-EA ratio on AOR is shown in Figure 4.2. AOR of hybrid coating samples shares similar trends to polyester. AORs firstly decrease slowly with the increasing of R-EA ratio until a minimum value is reached when R-EA ratio is around 10%. After that, further increasing of R-EA ratio makes the AOR value increase and then stay at a constant value.

Several differences can also be seen between the polyester and hybrid coating samples. Firstly, the effect of R-EA ratio on decreasing AOR is more remarkable than that of polyester samples. For instance, the maximum reduction of AOR ( $6.11^\circ$ ) is larger than that of polyester powders ( $3.01^\circ$ ). Secondly, when the R-EA ratio is above 10%, the differences of AOR between each sample group, which are up to  $2^\circ$ , are more significant than those of polyester samples. At last, from 0% to 5% of R-EA ratio, instead of staying the same value, AORs of hybrid samples demonstrate higher decreasing rates. An exception is also found in hybrid samples, the powder with LOA of 0.15% reaches the lowest value when the R-EA ratio is only 5%.

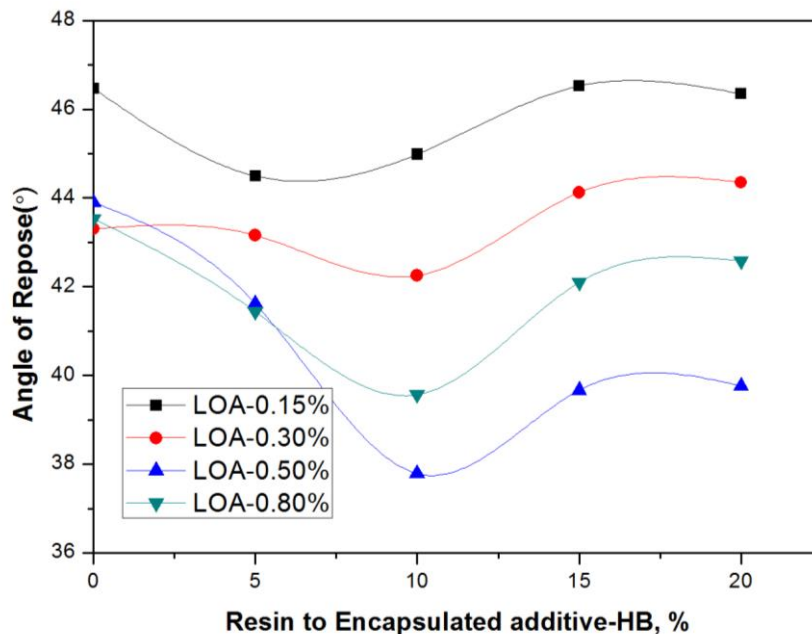


**Figure 4.2 Effects of R-EA ratio on AOR-HB  
(Additives were encapsulated with HB.  
Encapsulated additives were incorporated into HB powder)**

The difference can be attributed to different resin bases of these two powders themselves, one is polyester based while the other is hybrid based. Another possible reason is that the difference of the additives. The additives employed in polyester based powder are encapsulated with polyester resin, while the additives used in hybrid based powder are modified by hybrid resin. In addition, even though these two coating powders have the same particle size  $D_{50}$ , the difference between particle size distribution can partially influence the flow properties.

The trend is clear enough to validate our hypothesis. The encapsulation of flow additives does enhance the semi-static flow property of fine powders. The maximum effect could be reached when the additive is encapsulated with a suitable R-EA ratio, which may vary from different powder resin base or additive loading ratio. From our case, an R-EA ratio of 10% can be considered as a preferential choice for both HB and PE.

### 4.2.2 Dynamic Flow Characterization

Unlike Angle of Repose (AOR), the Avalanche Angle (AVA) measurement evaluates powders in a dynamic state with more kinetic energy acting on the powder particles, as shown in Figure 3.11 and Figure 3.12. As a consequence, AVA is commonly regarded as an indicator of dynamic flow property. Same as AOR, a lower value of AVA means a better dynamic flow property of powder.

Figure 4.3 shows the AVA values of polyester coating samples with respect to R-EA ratios. Similar to AOR, a concave curve trend is observed. From 0 to 10% of R-EA ratio, the AVA values of all the four samples decrease with the increasing of R-EA ratio until the minimum values could be obtained. For samples with LOA of 0.3%, 0.5% and 0.8%, the decreasing rates of AVA were similar to each other, indicating that encapsulation has a similar effect on these three samples. For samples with LOA of 0.15%, AVA reduction is much larger than that of other samples. When the R-EA ratio is above 10%, AVA begins to increase as the increasing of the R-EA ratio to different extents. For powder samples with LOA of 0.3%, excessive encapsulations even result in a worse flow property than the control samples.

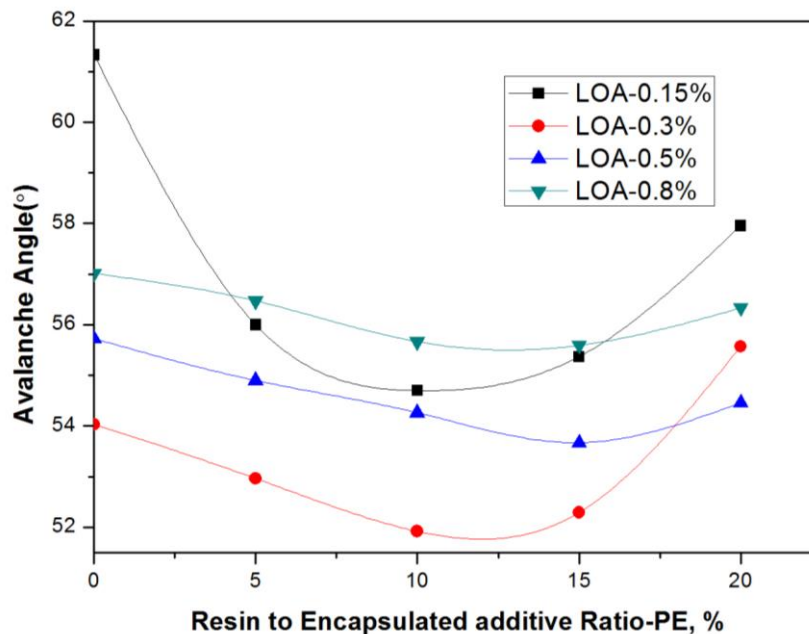


**Figure 4.3 Effects of R-EA ratio on AVA-PE  
(Additives were encapsulated with PE.  
Encapsulated additives were incorporated into PE powder)**

Change of additive encapsulation material and resin base of powder also affects the curves of AVA. The effects of R-EA ratio on AVA of hybrid coating powder samples are illustrated in Figure 4.4. As expected, an overall trend is clear to validate the effects of R-EA ratio. In general, the AVA values of all the samples decrease at first with the increasing of R-EA ratio to the minimum values and then increase with excessive R-EA ratios.

However, it's noticed that the effects are not as effective as what we found in polyester powders. At the same LOA of 0.3%, the largest drop of AVA in hybrid powders is around  $1^\circ$  while the AVA values of polyester powders experience a drop of  $2^\circ$ . Another difference is the optimum R-EA ratio. For powder samples with LOA of 0.3% and 0.5%, AVA reaches the minimum value when R-EA ratio is around 5% instead of 10%, which is the optimal R-EA ratio in polyester samples. It seems that less encapsulation is required to improve the dynamic flow property of hybrid powder when the LOA is 0.3% or 0.5%. The AVA of powder samples with LOA of 0.8% shows an inverse trend. The

AVA increases with the increasing of R-EA ratio to a maximum value and then decreases back to original value.

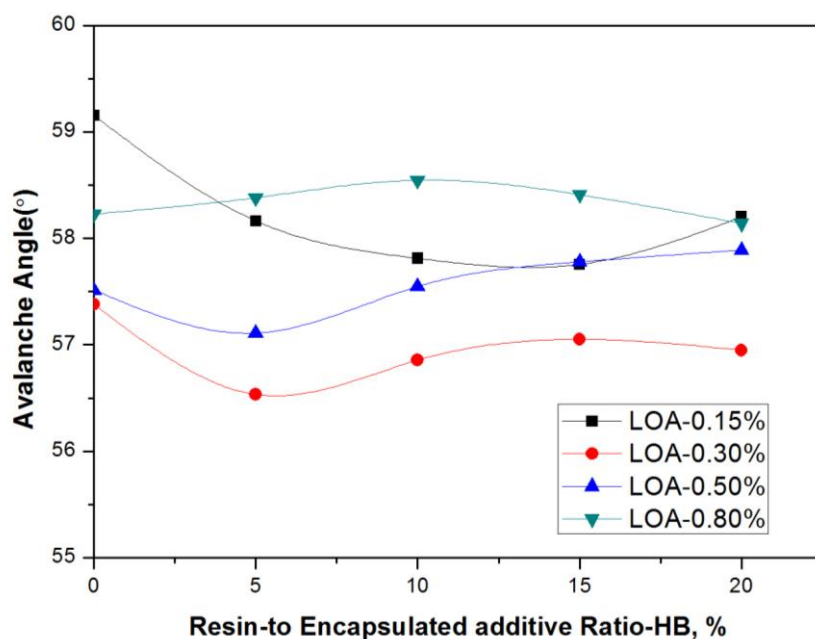


**Figure 4.4 Effects of R-EA ratio on AVA-HB  
(Additives were encapsulated with HB.  
Encapsulated additives were incorporated into HB powder)**

Resin-to-Encapsulated Additive ratio has effects on both semi-static and dynamic flow properties. The effect is observed for both the polyester based and hybrid based powders. In conclusion, the flow properties of fine powder improve with the increasing of R-EA ratio to an optimum value, where further encapsulation results in worse flow properties. The critical R-EA ratio is different for each powder, each loading ratio and each flow measurement.

To explain the variation of flow properties stated above, a general principle of flow additives should be introduced. Figure 4.5 shows a TEM image of nano-silica additive. It's clear to see that instead of functioning as individual particles, the nano-silica additive particles form agglomerates with branches like a “tree structure”. This “tree structure” can attach onto the surface of powder particles (the host particles). The presence of these “tree structure” can effectively increase the distance between the powder particles and

thus reduce inter-particle forces between the host particles, so as to improve the flow properties of fine powder.

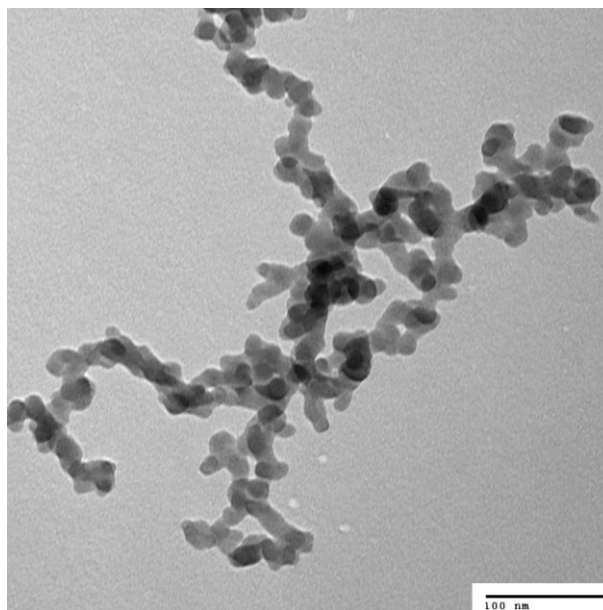


**Figure 4.5 TEM image of control additive (180k magnificant)**

However, a side effect is also noticed. The agglomerates on the surface of different host particles can join together due to the strong attraction between nano particles. “Chains” or “bridges” of agglomerates can be formed between two host particles, as shown in Figure 4.6. In order for the particles to have a relative movement (flow), a strong shear strength is needed to break the connection between these two host particles, which leads to the decrease of the flow property.

In general, 2 competitive effects of additive both work on the flowabilities of fine powder:

1. The agglomerates of additives can increase the distance of two host particles, thus decrease the inter-particle forces;
2. The agglomerates of additives can jointed together as a “chain” between host particles which requires strong shear strength to break.



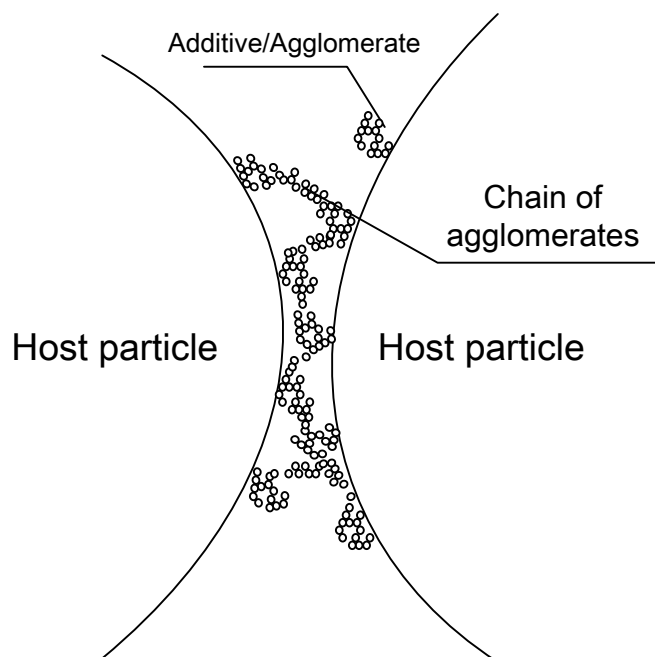


**Figure 4.6 Schematic of “Chain” effect of additive**

TEM images of additives after encapsulation can be seen in Figure 4.7. Additives were encapsulated with polyester or hybrid resin in different R-EA ratio. Comparing with Figure 4.5, it's clear to see that the “tree structure” remained after encapsulation. Based on the manually measurement of the diameter of additive particles, it's observed that the size of each additive particle increased significantly after encapsulation and a larger R-EA ratio corresponds to a bigger size of additive.

Given the fact of diameter increasing, we can sure that the silica particles are encapsulated by the resin. Thus, an acceptable explanation can be drawn here. The resin encapsulation reduces the attraction between silica agglomerates, making it easier to break the “chain” between the host particles, so as to improve the flow properties. That is why the samples with R-EA ratio of 5% and 10% show prior flow properties than the control sample.

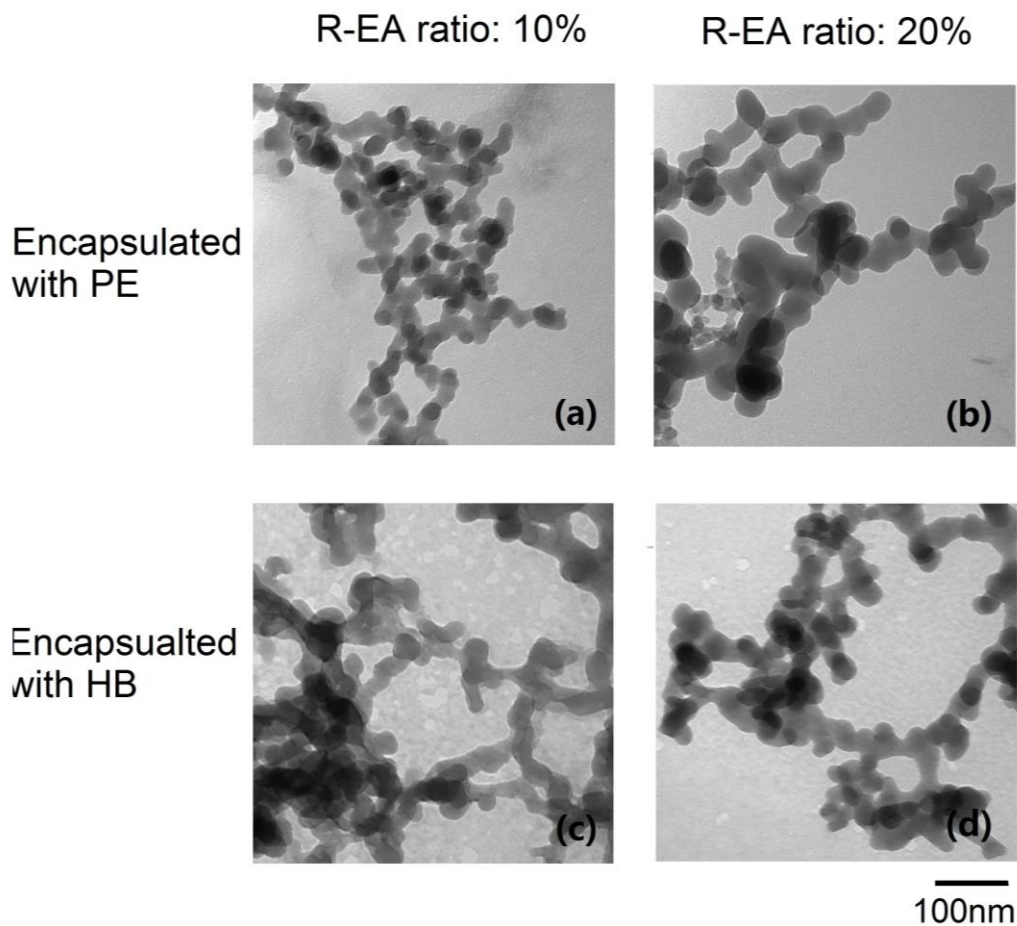


**Figure 4.7 TEM images of encapsulated additives**  
**(a) additive encapsulated with PE with R-EA ratio of 10%**  
**(b) additive encapsulated with PE with R-EA ratio of 20%**  
**(c) additive encapsulated with HB with R-EA ratio of 10%**  
**(d) additive encapsulated with HB with R-EA ratio of 20%**  
**(180k magnification)**

The increasing of the additive diameter can also be confirmed by the SEM images of powders loaded with different additive, as shown in Figure 4.8. The average size of additive agglomerates attached on the surface of host particle increased with the increase of R-EA ratio.

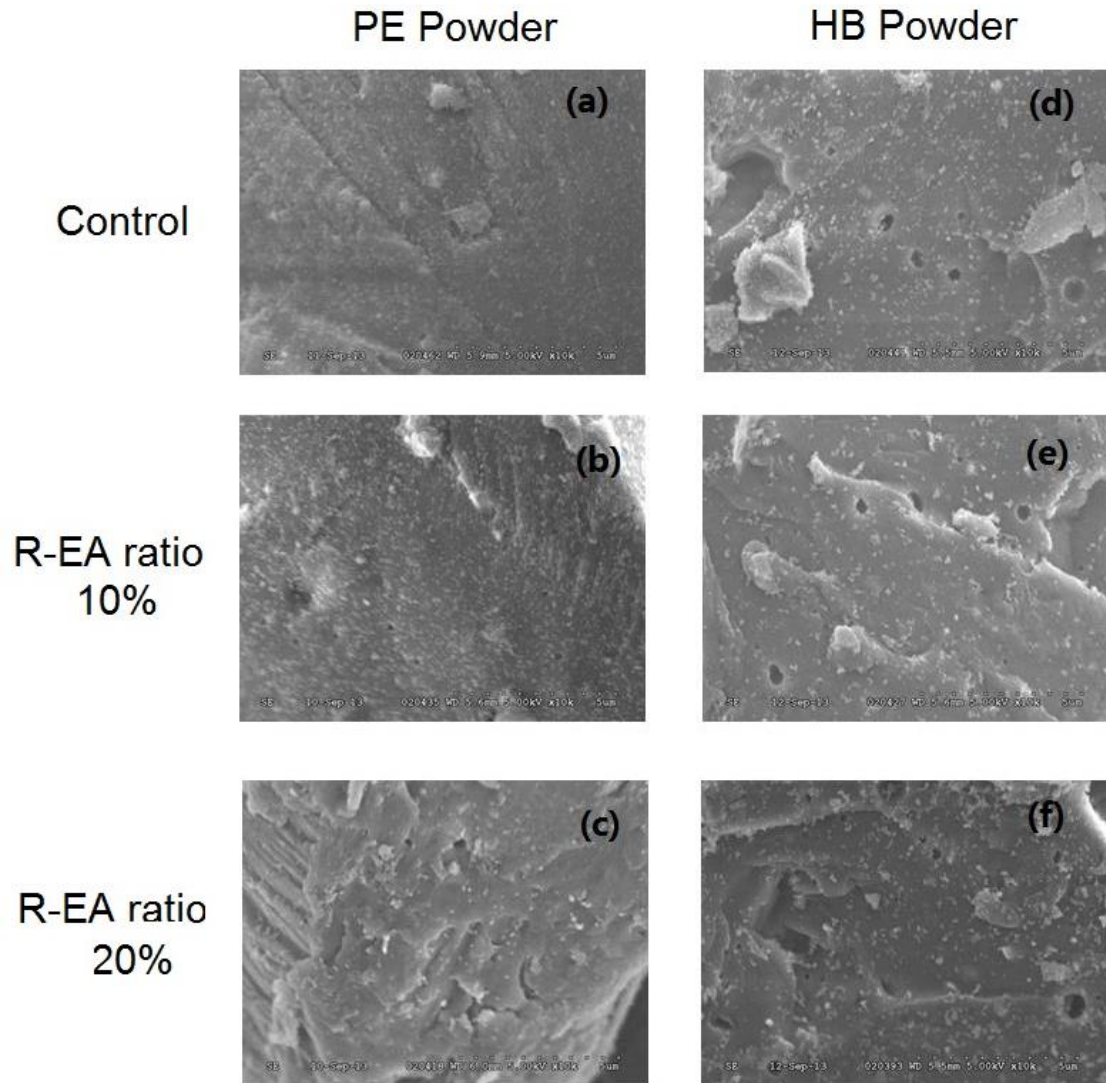


**Figure 4.8 SEM images of powder loaded with modified additive with LOA of 0.3%**

- (a) PE powder with control additive**
  - (b) PE powder with additive in R-EA ratio of 10%**
  - (c) PE powder with additive in R-EA ratio of 20%**
  - (d) HB powder with control additive**
  - (e) HB powder with additive in R-EA ratio of 10%**
  - (f) HB powder with additive in R-EA ratio of 20%**
- (10k magnification)**

However, the thickness of resin encapsulation reaches a certain level if R-EA ratio is too high, for example, 20% which can be seen in Figure 4.8 (b) and Figure 4.8 (d). The resin “shell” reduces the attraction between agglomerate and host particles. Thus there are less additive agglomerates attached to the surface of the host particles, as shown in Figure 4.8

(c) and Figure 4.8(f). As a result, the dominating contact between host particles return back to direct contact, results in worse flow properties.

In addition, with excess resin, several silica particles may be connected and combined by resin together. More shear strength is required to break the resin connection, as shown in Figure 4.9. As a consequence, the flowabilities of fine powder are reduced.

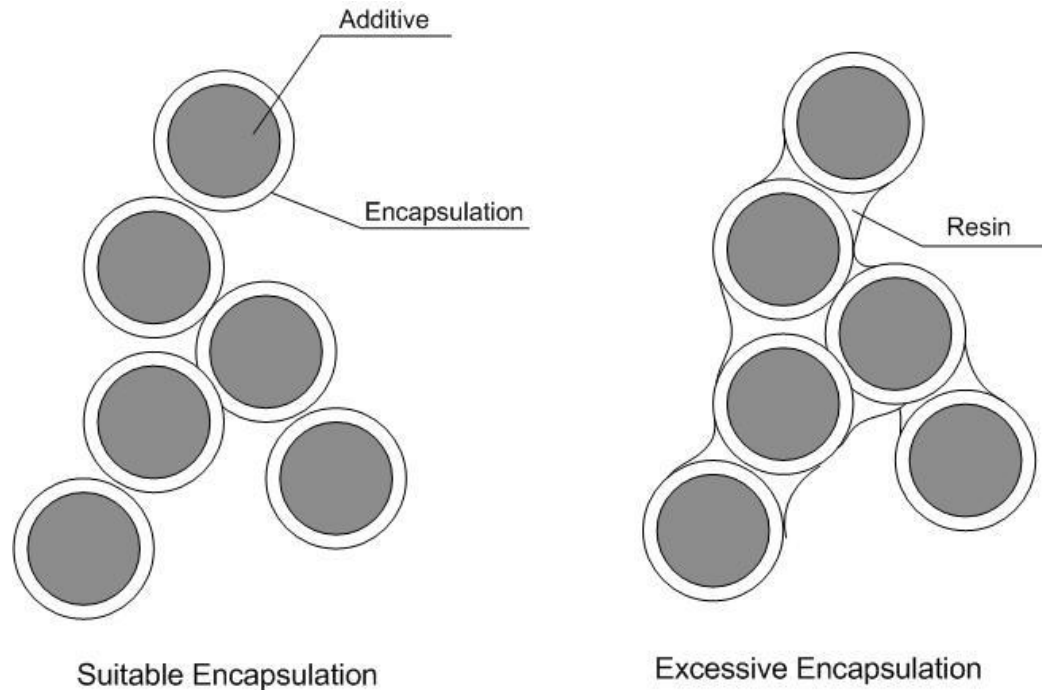


**Figure 4.9 Schematic of suitable and excessive encapsulation on additive**

### 4.3 Effect of Loading Ratio of Additive on Flow Properties of Fine Powders

From the above findings, it is found that the loading ratio of additive also has a significant effect on the semi-static or dynamic flow property of fine powder. For example, for the AOR of polyester powder samples with the same R-EA ratio, the powder with LOA of 0.5% shows a drastic improvement on semi-static flow property than the powder with LOA of 0.8%. In other words, even with the same additive, the flow property of fine powder can vary with the additive loading ratio.

In this section, the effect of loading ratio of additive on flowability of polyester based and hybrid based fine powder is evaluated by comparing the AOR and AVA values under different LOAs.

### 4.3.1 Semi-static Flow Characterization

Semi-static flow property indicates how easily the powder flows in a relatively static condition, like in storage silos or spray gun hoppers. In this work, semi-static flow property was represented by Angle of Repose, which is a widely used characterization technique due to the convenience, as shown in Figure 3.11. The lower value of AOR, the better semi-static flow property the powder has.

AORs of polyester samples were measured as a function of additive loading ratio in Figure 4.10. Even though some overlaps among the samples with different R-EA ratio, the trend is quite clear. With the increasing of additive loading ratio, AOR decreases drastically at the very beginning and reaches a minimum value at around LOA of 0.5% and then increases in reverse. From 0 to 0.15%, the AOR of all samples decreases drastically with a drop of 5-8°, which means that a tiny percentage as small as 0.15% of additives, regardless of being encapsulated or not, improves the semi-static flow property significantly. From 0.15% to 0.3%, the AOR of all samples was still decreasing, while the rate is smaller. From 0.3% to 0.5%, the AORs of the control sample, samples with R-EA ratio of 5% and 15% almost stay constant. The AORs of the other samples keep decreasing and minimum values can be obtained when the LOA is 0.5%. For the powder with R-EA ratio of 10%, the improvement of flow property is particularly significant with the minimum AOR among all the samples. When the LOA is above 0.5%, increasing additive loading ratio from 0.5% to 0.8% makes AOR higher, in other words, the semi-static flow property worse. Even though, the semi-static flow property of those powders is still much better than the powder without additive.

Overall, for polyester based fine powder, the presence of additive can improve the semi-static flow property and there exists an optimum LOA, which is around 0.5%, to get the best semi-static flow property.

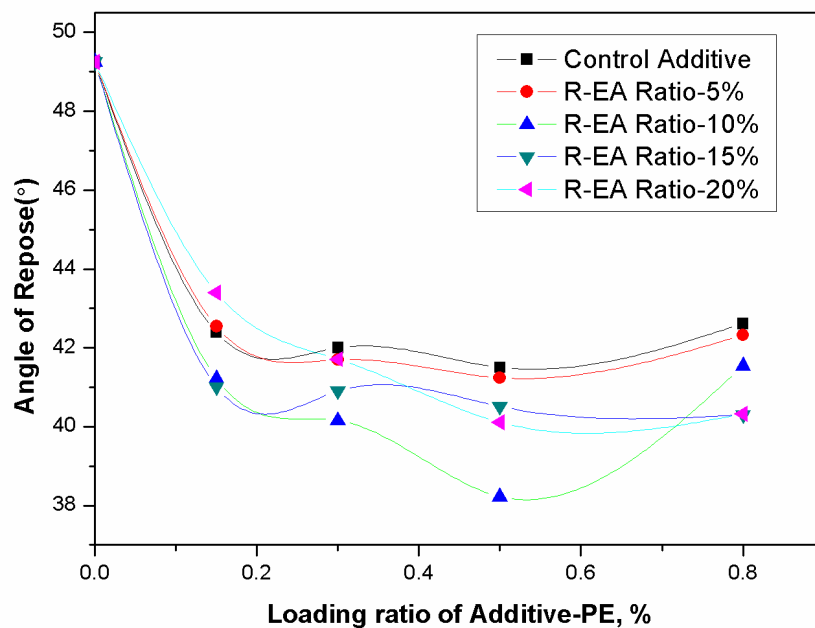


**Figure 4.10 Effects of LOA on AOR-PE  
(Additives were encapsulated with PE.  
Encapsulated additives were incorporated into PE powder)**

After changing the resin base of powder samples from polyester to hybrid, the same trend can be observed as shown in Figure 4.11. AOR decreases with the increase of LOA until the minimum value is obtained when the LOA is around 0.5%. Further increasing of LOA results in higher values of AOR.

However, a same but more obvious phenomenon happens with the new powder resin base. For the powder sample with control additive, AOR stops decreasing and becomes relatively stable when the LOA is above 0.3%. For the powder samples with modification additive, AOR keeps decreasing until the LOA reaches 0.5%, where the minimum value is obtained.

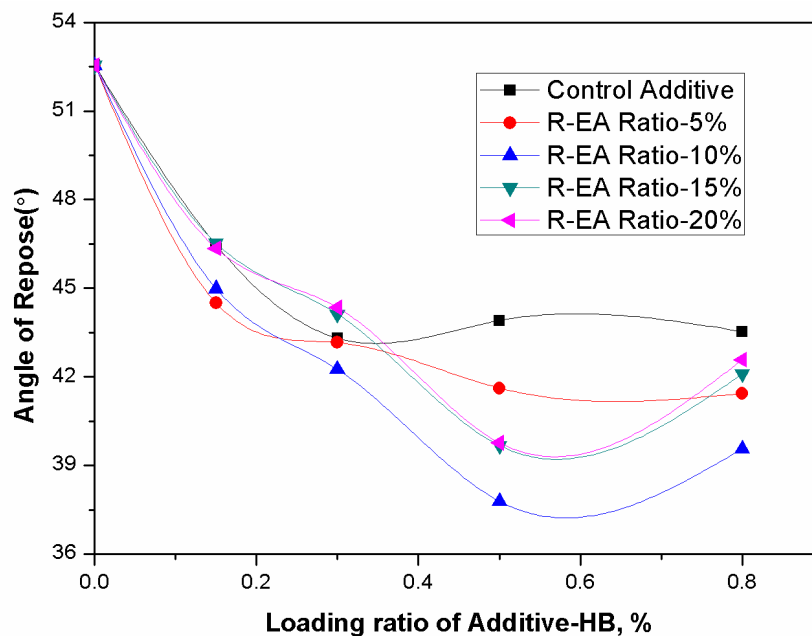


**Figure 4.11 Effects of LOA on AOR-HB  
(Additives were encapsulated with HB.  
Encapsulated additives were incorporated into HB powder)**

In general, there is an optimum LOA for each of the samples to get the minimum AOR. However, the optimum LOA varies from what kind of additive is loaded in. For the powder with control additive, the optimum LOA is 0.3%. While for the powder samples with encapsulated additive, the optimum LOA is increased to 0.5% and much better semi-static flow property can be achieved.

#### 4.3.2 Dynamic Flow Characterization

Unlike Angle of Repose (AOR), the measure of Avalanche Angle (AVA) is under a more dynamic state with more kinetic energy acting on the powder particles. As a consequence, AVA is commonly regarded as an indicator of dynamic flow property. A lower value of AVA means a better dynamic flow property of powder.

Figure 4.12 illustrates the effects of loading ratio of additive on the AVA of polyester powder samples. AVAs of all the samples decrease as increasing the LOA at the first beginning. 0.3% is the optimum LOA except for the sample with R-EA ratio of 20%, where the lowest AVAs were achieved. When the LOA is above 0.3% (0.5% for sample

with R-EA ratio of 20%), AVAs increase as we have seen for many times from the previous characterizations. When the LOA is above 0.5%, AVAs keep increasing while the increasing rates are decreasing.

It can be noticed that AVAs of powder without additive (LOA of 0) are not measured. This is because the fine powder with  $D_{50}$  less than 30 microns is so cohesive that gets agglomeration easily. When measuring the AVA of such powder using the Revolution Powder Analyzer (Mercury Scientific Inc., Sandy Hook, CT, US), the big agglomerates of fine powder adhered on the glass sides of the drum and made the glass surface unclear, which makes it impossible to get reasonable results. However, the results from the other samples are clear enough to show a meaningful trend.

Change of additive encapsulation material and resin base of powder also affects the curves of AVA. In Figure 4.13, the relationship of AVA and LOA for hybrid based powder samples is evaluated. As expected, AVA decreases as the increasing of LOA until the optimum AVA is reached when the LOA reaches at 0.3%. Afterwards, further addition of additive leads to higher values of AVA.



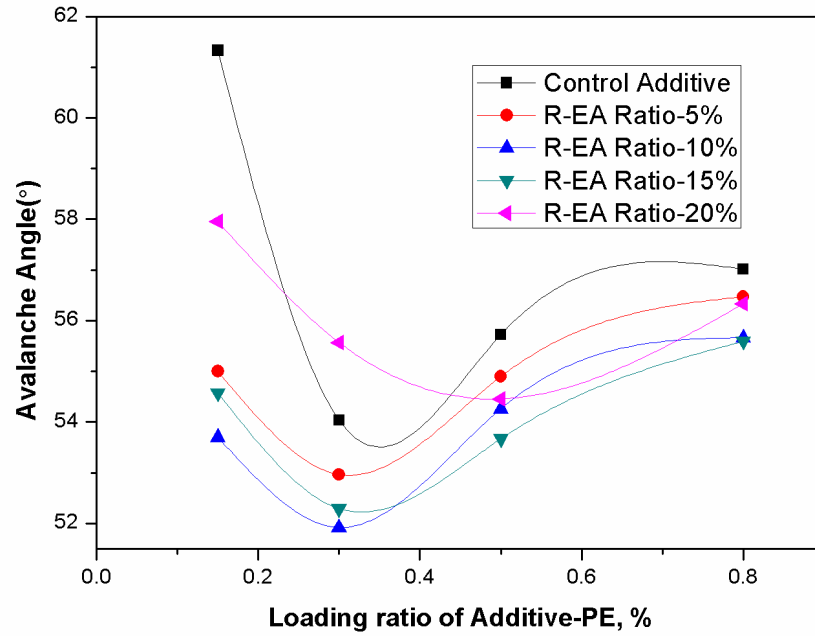


**Figure 4.12 Effects of LOA on AVA-PE  
(Additives were encapsulated with PE.  
Encapsulated additives were incorporated into PE powder)**

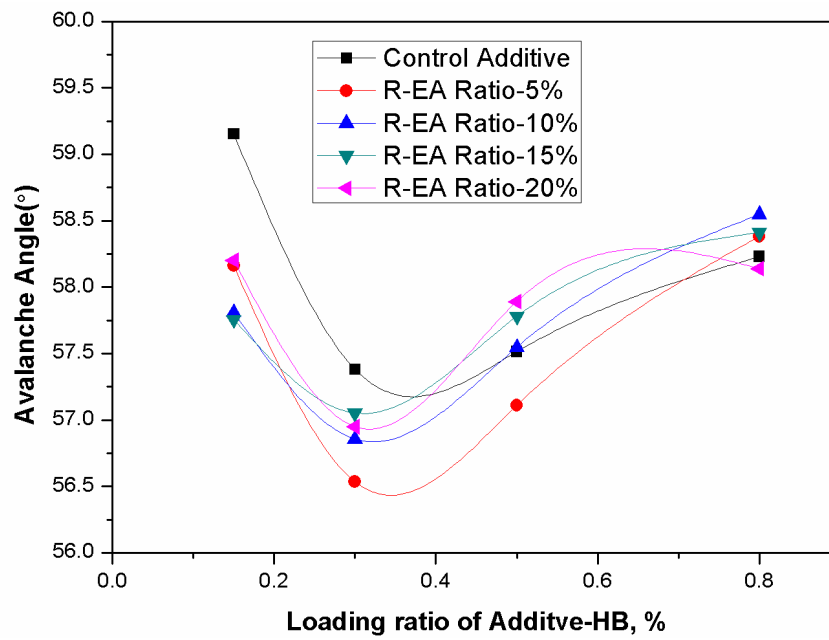


**Figure 4.13 Effects of LOA on AVA-HB  
(Additives were encapsulated with HB.  
Encapsulated additives were incorporated into HB powder)**

An explanation to the effects of LOA on the flow property is drawn here. With an LOA as low as 0.15%, the additive agglomerates can just cover a small portion of host particle surface. As a result, most contacts of host particles still remain as direct contact between polymer particles, corresponding to bad flow properties, as shown in Figure 4.14 (a). Increasing the LOA, the number of agglomerates on the surface is increased, which can be seen in Figure 4.15. The agglomerates of additive can convert most direct contacts between host particles to indirect contacts separated by silica additive, as shown in Figure 4.14 (b). However, when the LOA is excessive, there are too many agglomerates on the surface of powder, as shown in Figure 4.15 (b) and Figure 4.15 (d). As discussed before, agglomerates on the surfaces of neighboring host particles can connect as “chains” or “bridges” because of the strong attraction forces as shown in Figure 4.14 (c). As such, higher shear strength is needed to break down the connections and make host particles flow.

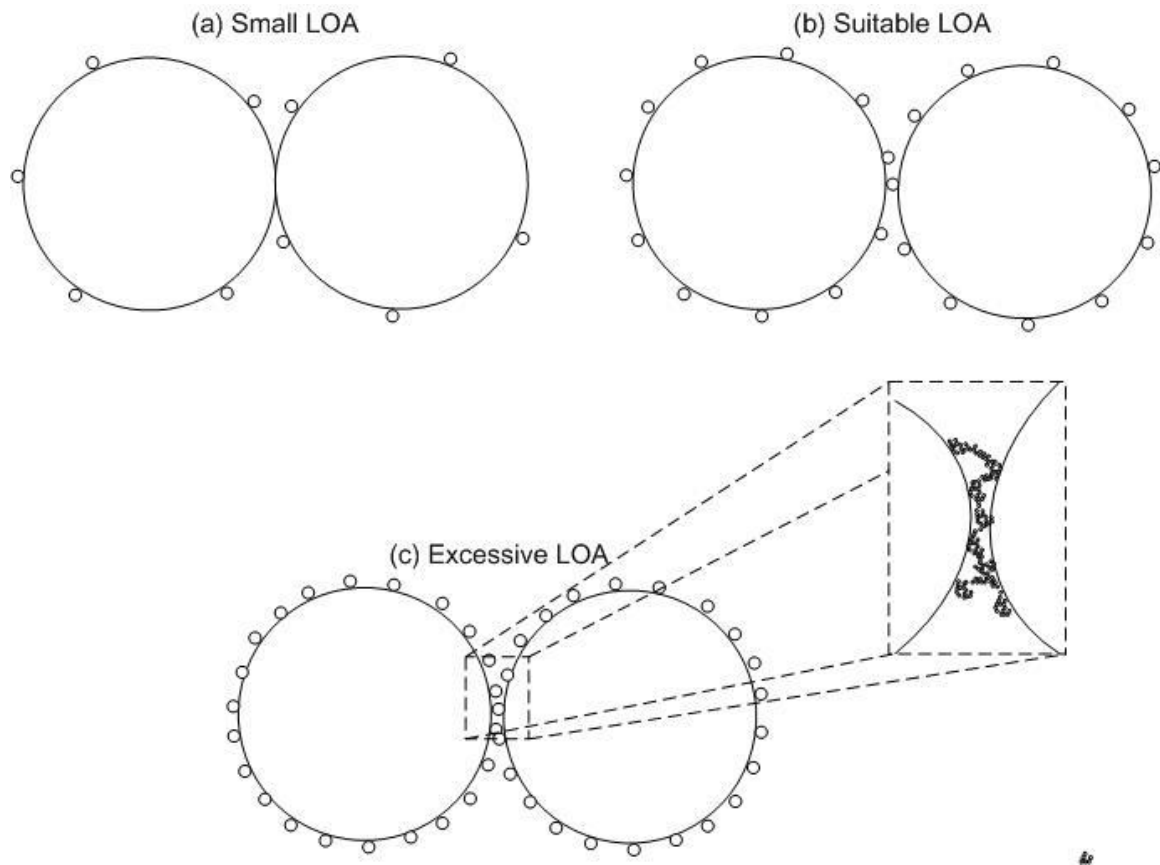


**Figure 4.14 Schematic of contacts of particles under different LOA**

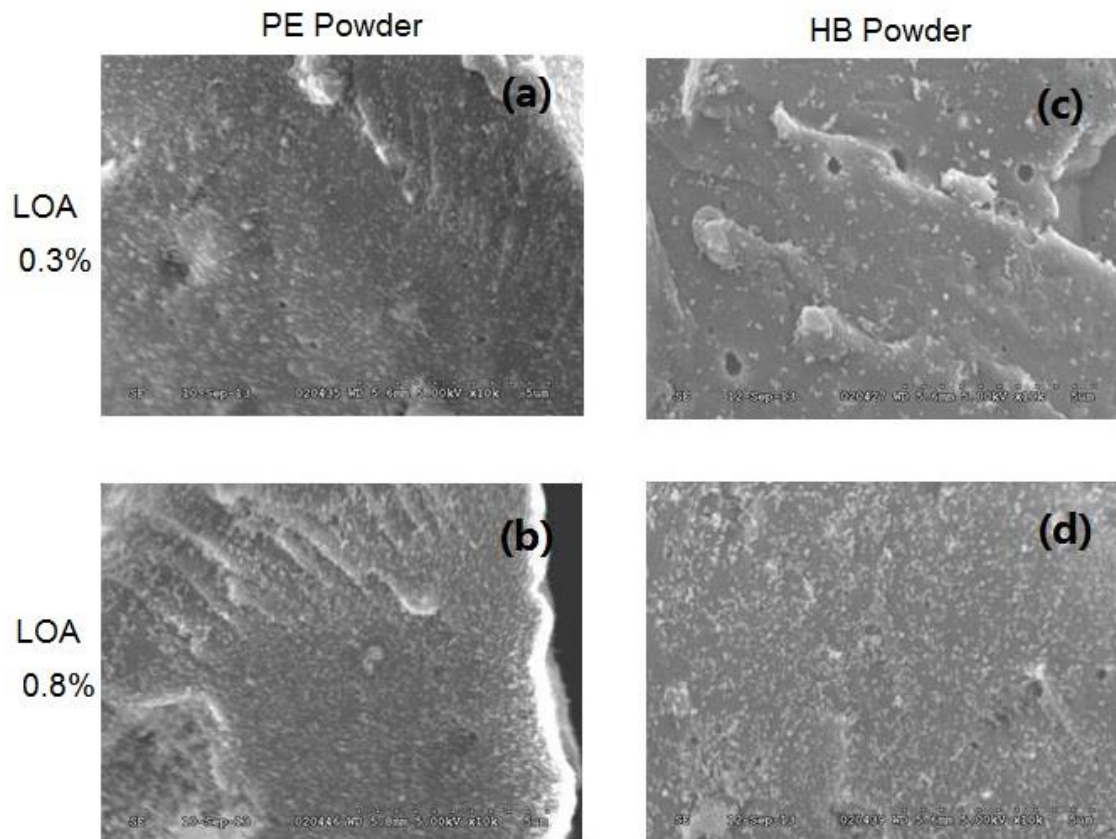


**Figure 4.15 SEM images of powder loaded with modified additive with R-EA ratio of 10%**

- (a) PE powder with LOA of 0.3%**
  - (b) PE powder with LOA of 0.8%**
  - (c) HB powder with LOA of 0.3%**
  - (d) HB powder with LOA of 0.8%**
- (10k magnification)**

#### 4.4 Chapter Summary

In this chapter, semi-static and dynamic flow properties of 40 powder samples (The additives were encapsulated with 2 resins in 4 R-EA ratios. Each additive was incorporated into coating powders in 4 LOAs) are investigated based on the different resin bases, R-EA ratios and LOAs.

At a fixed additive loading ratio, both AOR and AVA of these two resin bases decrease as the increasing of R-EA ratio to minimum values. After that, further increasing of R-EA ratio makes the AOR and AVA increase back. To get the minimum AOR, the optimum R-EA ratio is around 10% (for both of the polyester and hybrid based powder samples).

To get minimum AVA, the optimum R-EA ratio is around 10% (for polyester based powder) or 5% (for hybrid based powder).

For a certain R-EA ratio, both AOR and AVA of the two resin bases initially decrease as the increasing of LOA to minimum values and then increase back with further increasing of LOA. The optimum LOA is 0.5% (for AOR) or 0.3% (for AVA), regardless of powder resin base.

There is a series of optimum combinations of R-EA ratio and LOA for these two resin bases based on semi-static or dynamic flow property, as shown in Table 4.1.

**Table 4.1 Optimum conditons for best flow properies of fine powder**

Samples	Semi-static flow property	Dynamic flow property
Polyester samples	R-EA ratio: 10%	R-EA ratio: 10%
	LOA: 0.5%	LOA: 0.3%
Hybrid samples	R-EA ratio: 10%	R-EA ratio: 5%
	LOA: 0.5%	LOA: 0.3%

## Chapter 5

### 5 Film Quality Characterization of Fine Powders with Modified Additives

#### 5.1 Introduction

Beside flow properties, the industries are also interested in the film appearance of powder coating, such as the roughness, clarity, color, gloss and opacity of coatings etc. (Biris et al. 2001). Like in automotive applications, a high gloss, smooth finish is preferred to provide a high distinction of image. Therefore, film appearance qualities are major parts of research in the fine powder coating.

Even the facts that fine powder coating brings a smoother surface and thinner film than the traditional powder coating, limitations of this innovation still exist. The presence of nanoparticle additive, which is required to make the cohesive fine powder flow and fluidize well during the application, leads to a series of compatibility issues between the additive and fine powder.

That incompatibility of additive and fine powder is inherent from the difference of materials, i.e., the additive is made from inorganic materials and fine powder is mainly composed of organic resins. The inorganic additives have a higher surface tension, leading to a poor wettability of nano additive particles, or the agglomerates of additive. Therefore, the additive/agglomerate cannot be wet by the molten resin and become well dispersed in the cured coating film. In addition, nano additive particles, or the agglomerates are apt to flow “up” to the surface of coating film, resulting in seeds on the final finishing as shown in Figure 5.1.

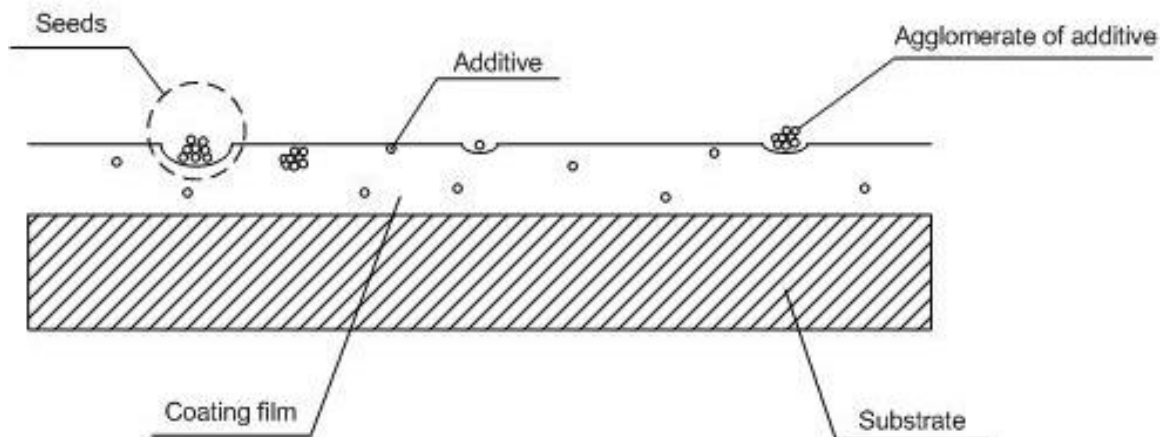


**Figure 5.1 Schematic of seeds on film surface**

If the organic additive is used, this will increase the viscosity of the coating during the curing process and weak the leveling of melted resin, increasing the roughness of coating finish. The leveling of melted resin can be seen in Figure 2.2.

The inorganic additive also affects the gloss because the micro-structure formed on the film surface due to the incompatibility, as shown in Figure 5.1. Therefore, the film of fine powder coating with inorganic additive always exhibits reduced gloss.

In this work, an encapsulation technology was used to solve all these compatibility problems. By encapsulating the inorganic nanoparticle additive with organic resins, the surface of nanoparticle is modified to have the similar surface tension as the organic powder particles. As a result, improved compatibility of nano additives would lead to better dispersion of additive in the cured film, thus enhancing the film qualities of coating film.

To explore the effects of this additive encapsulation technology on film qualities, the powder samples must be sprayed on the panels and coating film has to be formed through the curing process. For each powder sample, three panels were sprayed and cured. The film thickness of each panel was strictly controlled by a weight-control method to get a consistent thickness. Then the film qualities of coated panels were studied by the characterizations of gloss, roughness and the number of seeds.

## 5.2 Effect of Resin-to-Additive Ratio on Film Qualities of Fine Powders

The additives were encapsulated with 2 resins (polyester or hybrid) in 4 Resin-to-Encapsulated Additive (R-EA) ratios. Thus there were 9 additives (8 modified additives and 1 control additive) studied. Then the additive was incorporated into coating powder with corresponding resin base, in 4 Loading ratios of Additive (LOAs). Control additive was employed in both of the two resin based powders. For each of the 40 powder samples, three panels were sprayed to test the film qualities. In this way, 120 panels were prepared.

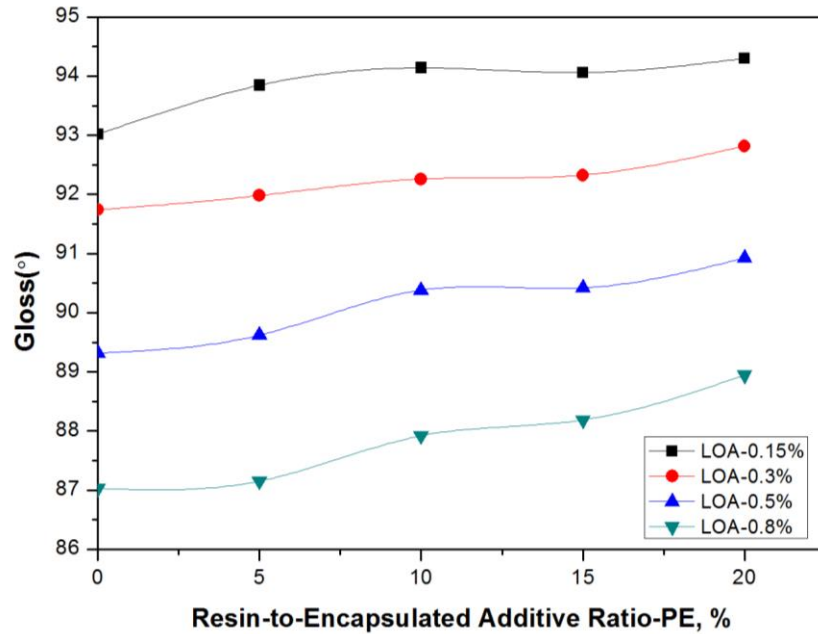
For each characterization test, all the 120 panels were tested. The results were compared with R-EA ratios and resin bases.

### 5.2.1 Gloss

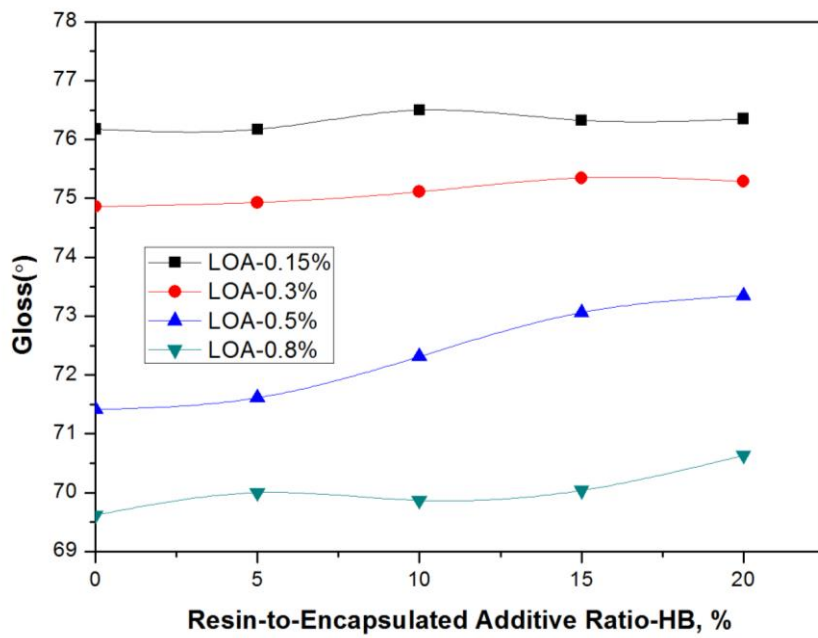
The value of gloss of 120 samples was measured using a gloss meter, as described in Figure 3.16, by evaluating the reflection of light in a certain angle of 60°.

Figure 5.2 and Figure 5.3 show the gloss of films on panels coated with different powder samples, as a function of R-EA ratio of additive used in coating powder. It's clear that all the samples, regardless of powder resin bases or LOA, have a general trend of increased gloss with increasing R-EA ratio. The increasing rates are almost constant and are independent from additive loading ratio, since the lines are almost linear and parallel to each other.

Following this trend, further increase of R-EA ratio is expected to keep increasing the gloss. However, the samples with R-EA ratio as high as 20% already exhibit really bad flow properties. From the analysis in Chapter 4, excess R-EA ratio results in even worse flow properties, which is not what the industries want to see. Therefore, it's necessary to consider both the gloss and flow properties and find out an optimum R-EA ratio. In this work, R-EA ratio of 10% is preferred, because it's best for the flow properties and acceptable for the gloss.



**Figure 5.2 Effects of R-EA ratio on gloss-PE  
(Additives were encapsulated with PE.  
Encapsulated additives were incorporated into PE powder)**



**Figure 5.3 Effects of R-EA ratio on gloss-HB  
(Additives were encapsulated with HB.  
Encapsulated additives were incorporated into HB powder)**



It is well known that additive in the coating film can significantly impair the gloss, so what really matters is the proportion of net silica in film. At a fixed additive loading ratio, a larger R-EA ratio means fewer silica additive is used in the powder samples. Therefore, the gloss is improved because less silica was in the final film. For further explanation, the net silica to powder coating ratio is introduced in this work, which equals to  $LOA \cdot (1 - R-EA \text{ ratio})$ . For instance, for the sample with R-EA ratio of 20% and LOA of 0.5%, the net silica to powder coating ratio is equal to  $0.5\% \cdot (1 - 20\%)$ , which is 0.4%. In this way, an evaluation of gloss as a function of net silica to powder coating ratio is shown in Figure 5.4. Gloss decreases with the increasing of net silica to powder coating ratio, conforming our hypothesis. More importantly, it is found that there is a linear relationship between the gloss and net silica to powder coating ratio.

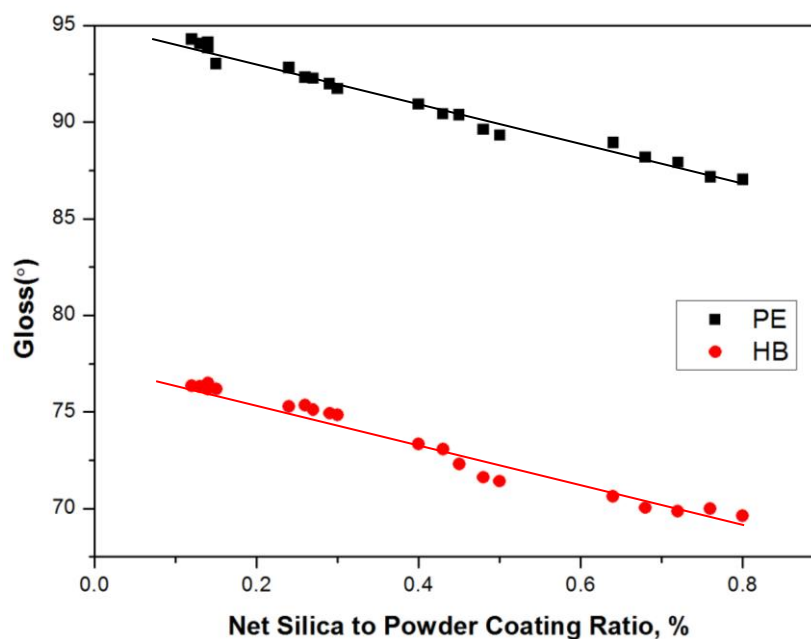


**Figure 5.4 Effects of net silica to powder coating ratio on gloss**

### 5.2.2 Roughness

Film appearance was also characterized using surface roughness. In facts, the smoothness of film surface can be divided into two spatial frequencies, short wave (characterized by the roughness  $R_a$ ) and long wave (characterized by waviness  $R_z$ ) as shown in Figure 5.5 (Biris et al. 2001). The long wave in millimeters represents the orange peel texture on the surface. The short wave is related with the gloss to certain extent, since the value of gloss

can indicate the flatness of the film in micron to nano meter level. In this work, the roughness is characterized as short wave because the scan length of surface profiler was 5 mm, which is not long enough to describe the long wave, as shown in Figure 3.17.

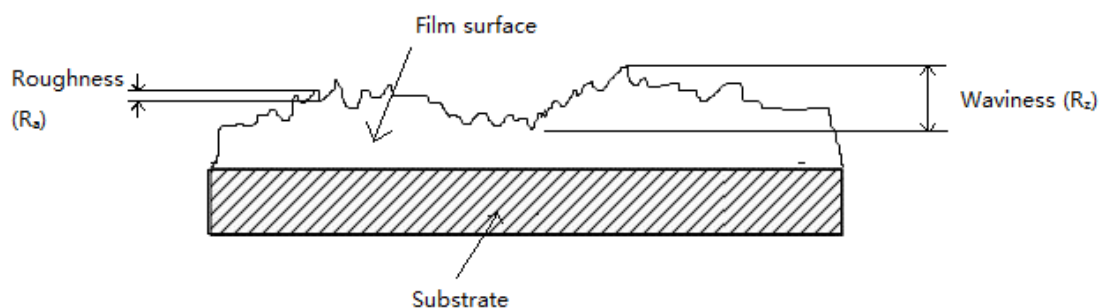


**Figure 5.5 Cured film surface characterized by roughness ( $R_a$ ) and waviness ( $R_z$ ) (Biris et al. 2001)**

In this work, not all of the panels were tested. To save time and cost, only twenty panels with R-EA ratio of 0, 10% and 20% and LOA of 0.3% and 0.5%, which are sufficient to give a big picture of the trend, were chosen in this work.

The results are listed in Figure 5.6 and Figure 5.7. As with gloss, roughness of both polyester and hybrid based coating was found to reduce with the increasing R-EA ratio, regardless of LOAs.

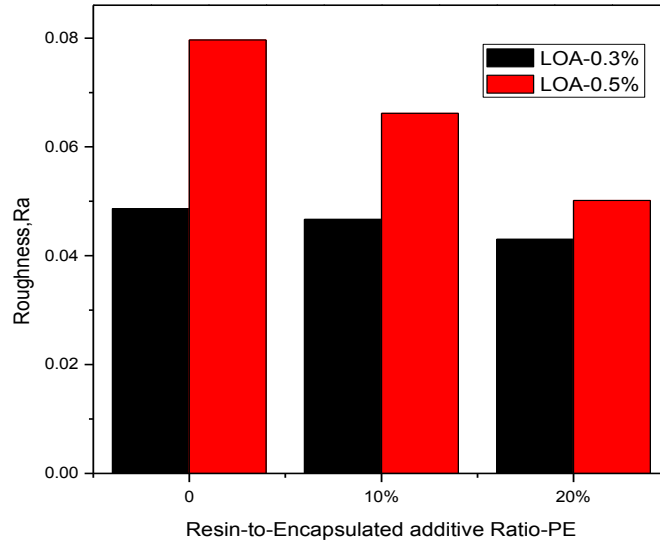


**Figure 5.6 Effects of R-EA ratio on roughness-PE  
(Additives were encapsulated with PE.  
Encapsulated additives were incorporated into PE powder)**

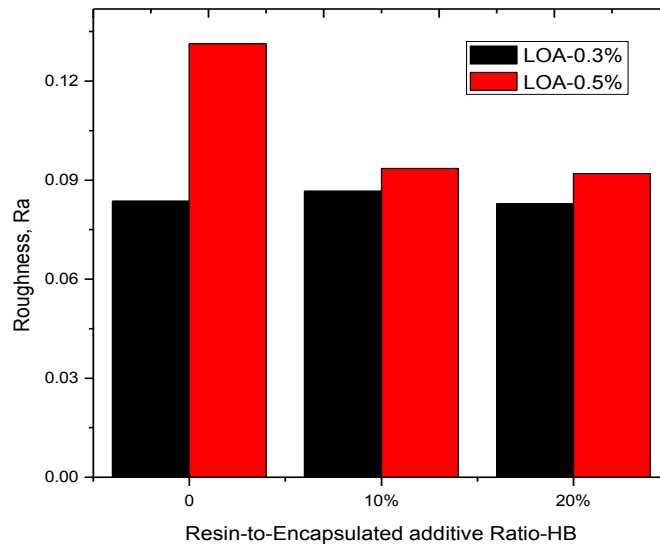


**Figure 5.7 Effects of R-EA ratio on roughness-HB  
(Additives were encapsulated with HB.  
Encapsulated additives were incorporated into HB powder)**

### 5.2.3 Number of Seeds

With the incompatibility of additive to powder coating, the additives or agglomerates of additives can flow “up” to the surface of coating film during the curing process, causing the seeds on the film surface, as shown in Figure 5.1. So the quality of finish was evaluated by counting the number of seeds on the coating layer, as described in Chapter 3.

Figure 5.8 and 5.9 show the number of seeds on the panel samples with respect to R-EA ratio. One should note that for all the samples, a general trend can be seen. Comparing with the samples with control additive, the number of seeds decreases with the increase of R-EA ratio from 0% to 10%. The smallest number of seeds can be achieved when R-EA ratio is around 10%. When the R-EA ratio is above 10%, the number of seeds starts to increase with increasing the R-EA ratio. The optimum R-EA ratio for the least number of seeds is 10%, for both of the two resin bases and all the LOAs.

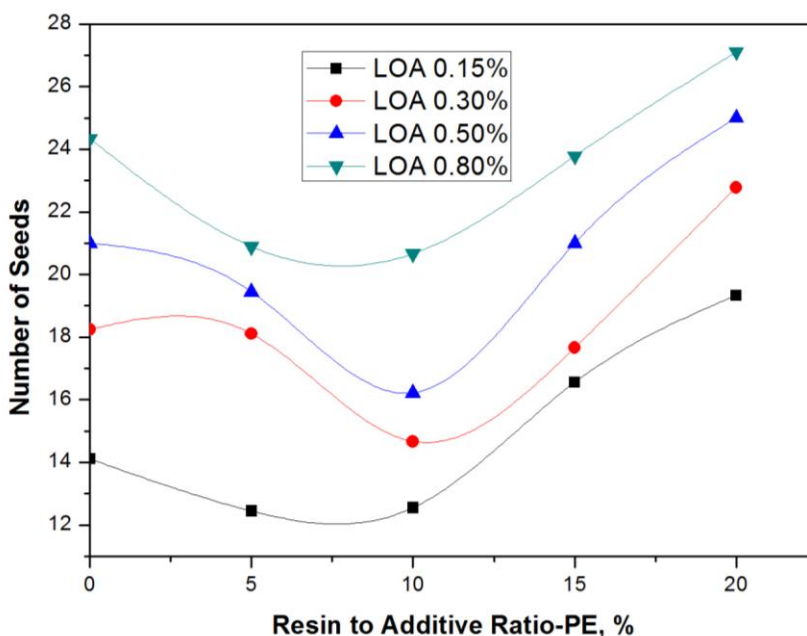


**Figure 5.8 Effects of R-EA ratio on number of seeds-PE  
(Additives were encapsulated with PE.  
Encapsulated additives were incorporated into PE powder)**

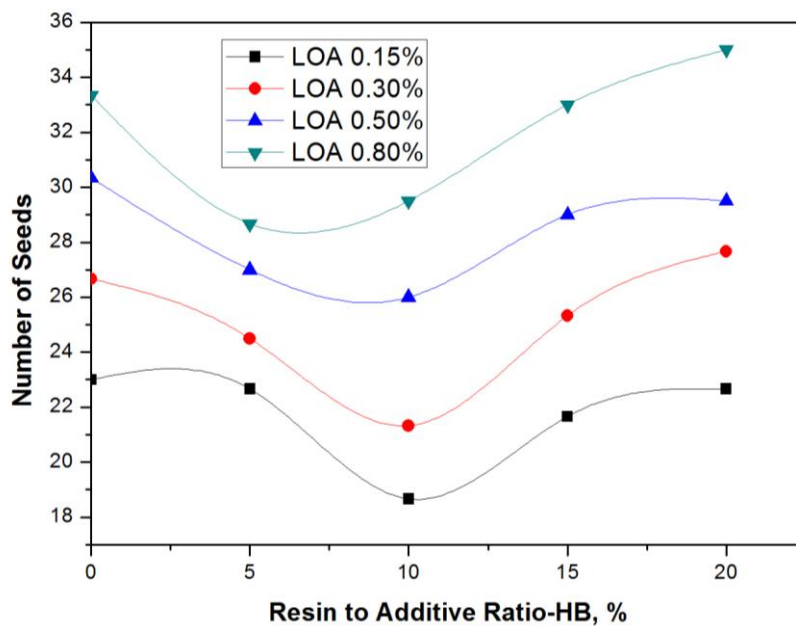


**Figure 5.9 Effects of R-EA ratio on number of seeds-HB  
(Additives were encapsulated with HB.  
Encapsulated additives were incorporated into HB powder)**

It's should be noted here that since the seeds are counted by naked eyes, which much depends on the operator's own standard or experience. So even for the same panel, the exact number of seeds for each count may vary. However, the changes of numbers of seeds from different are quite noticeable for the same examiner. Therefore, only if it is the same person counting the number following the same standard, the results are reliable.

To find out the major reasons contributing to this trend, the mechanism of seeds is introduced here. All flow additives used nowadays are inorganic materials while the powder coatings are mainly composed of organic materials. The great differences in physical and chemical properties between inorganic additive and organic resin lead to the compatibility issues. In details, the inorganic additive has a poor wettability due to the higher surface tension. Therefore, the additive cannot be wet by the fused resin and be well dispersed in the cured coating film. In addition, agglomerates formed by strong attraction force between additive particles make the wetting of additive more difficult. As a consequence, the nano additive particles, or the agglomerates of additive are apt to flow "up" to the surface of coating film, resulting in seeds on the final finishing.

By encapsulation, the surface of inorganic additive is covered by organic resins, which makes the modified additive compatible with the fine powders, overcoming the compatibility issues from the beginning. With the same surface tension, modified additive can be wet by the fused resin and dispersed well in coating film. In addition, the modification increase the distance between nano silica, thus reduces the attraction force between. Therefore, the agglomerates formed are easier to be broken during the curing process. Then the individual particles can be wet by the melted resin and dispersed well.

Excessive encapsulation has the reverse effects on film quality. That is because, when resin to modified additive ratio is high enough, silica additive particles are connected together by excessive resin, as shown in Figure 4.9. The resin connections are difficult to break during the curing process. Therefore, additive cannot be wet and dispersed well, leading to the seeds on the film surface.

## 5.3 Effect of Additive Loading Ratio on Film Qualities of Fine Powders

From the above findings, it is found that the LOA also has effects on film quality of fine powder. In this section, the effects of LOA on film qualities are studied by comparing the gloss, roughness and number of seeds under different LOAs.

### 5.3.1 Gloss

The effect of LOA on the gloss was shown in Figure 5.10 and Figure 5.11. For both of the resin bases, gloss of panel samples decreases with the increasing of LOA. That trend agrees with the theory of net silica to powder coating ratio, which is  $LOA \cdot (1 - R-EA \text{ ratio})$ . At a fixed R-EA ratio, large LOA corresponds to higher net silica to powder coating ratio. More silica results in reduced gloss.

Following this trend, a LOA as low as possible is preferred. However, LOA less than 0.3% is not adequate to improve the flow properties of the fine powder. Based on the overall consideration of flow properties and gloss, LOA of 0.3% or 0.5% is chosen as the optimum LOA, for polyester based or hybrid based powder respectively.

### 5.3.2 Roughness

Figure 5.12 and Figure 5.13 show the effects of LOA on the roughness. Since samples with LOA of 0.15% and 0.8% show really bad flow abilities, only 0.3% and 0.5% are evaluated in this work. For both polyester and hybrid bases, samples with LOA 0.5% have larger roughness over the samples with LOA 0.3%, which means that samples with LOA of 0.3% have a smoother surface than samples with LOA of 0.5%. Therefore, LOA of 0.3% is preferred to achieve a smoother surface.

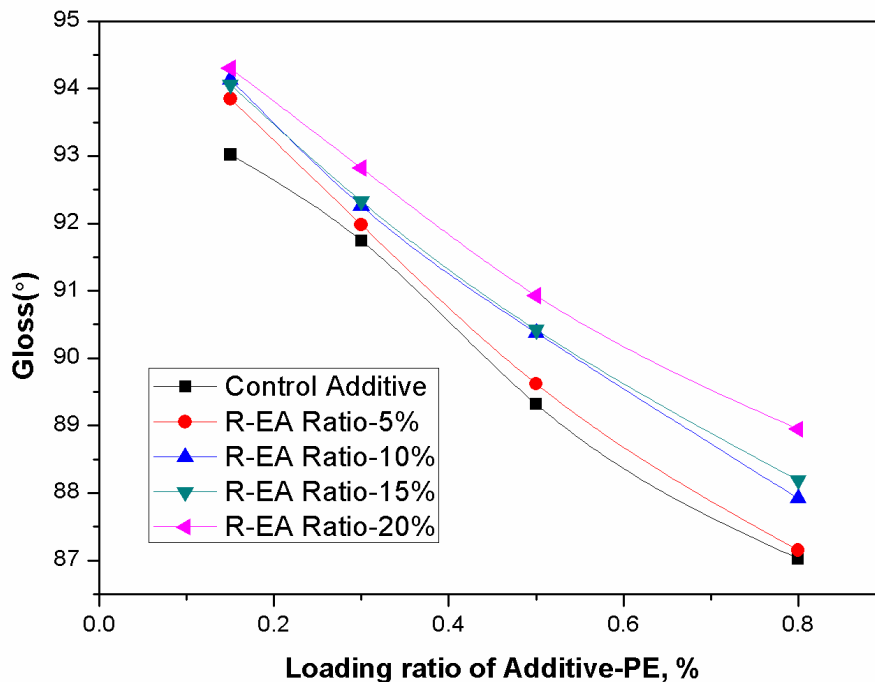


**Figure 5.10 Effects of LOA on gloss-PE  
(Additives were encapsulated with PE.  
Encapsulated additives were incorporated into PE powder)**

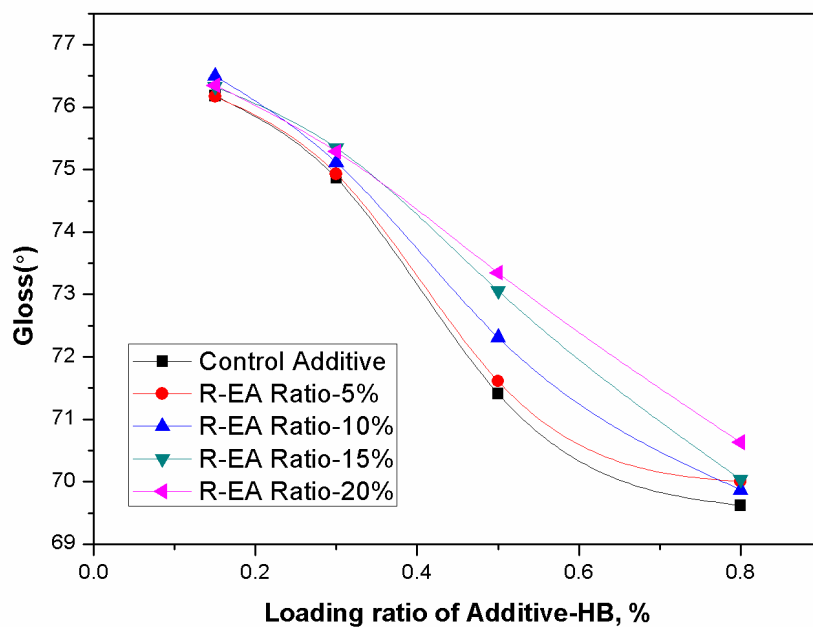


**Figure 5.11 Effects of LOA on gloss-HB  
(Additives were encapsulated with HB.  
Encapsulated additives were incorporated into HB powder)**



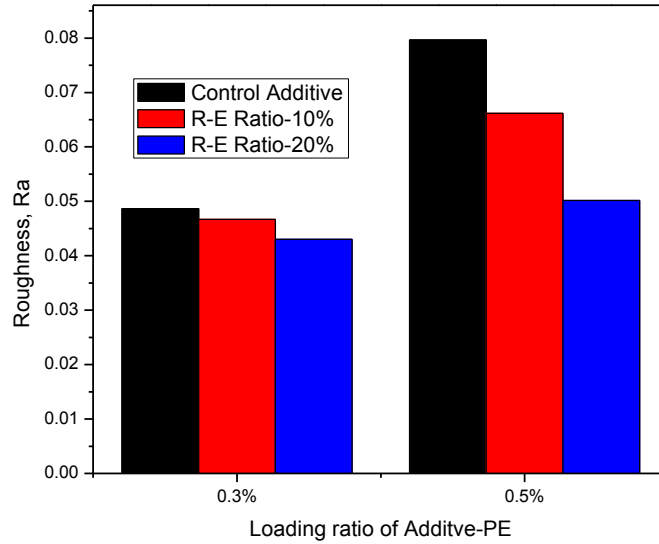


**Figure 5.12 Effects of LOA on roughness-PE**  
(Additives were encapsulated with PE.  
Encapsulated additives were incorporated into PE powder)

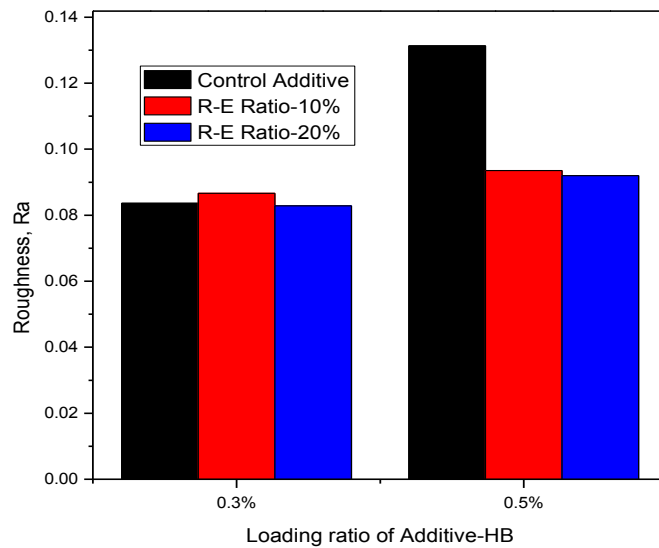


**Figure 5.13 Effects of LOA on roughness-HB**  
(Additives were encapsulated with HB.  
Encapsulated additives were incorporated into HB powder)

### 5.3.3 Number of Seeds

Figure 5.14 and Figure 5.15 show the number of seeds on the panel samples under different LOAs. For both of two resin bases, an overall trend is clear. Same with the control sample, the number of seeds of the samples with modified additive increases with the increase of LOA, which means that more additive results in more seeds on the film surface.

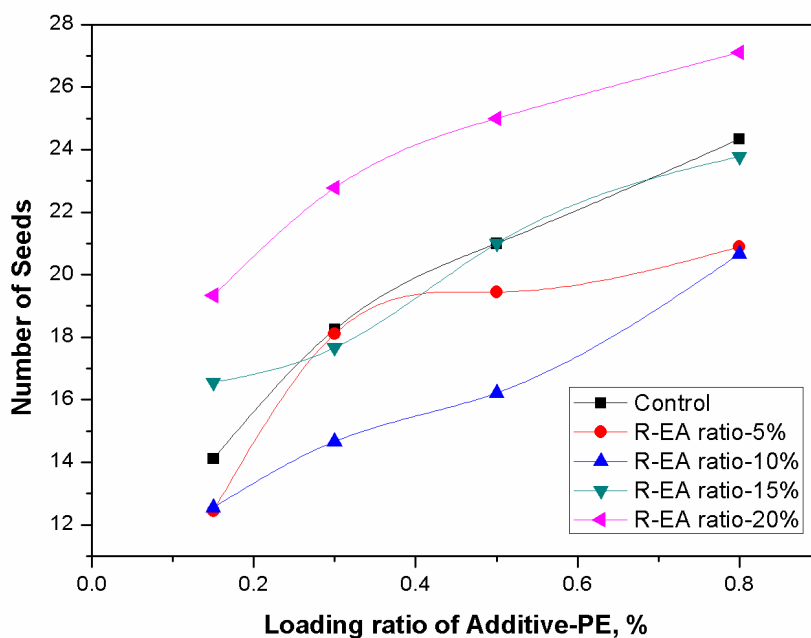


**Figure 5.14 Effects of LOA on number of seeds-PE  
(Additives were encapsulated with PE.  
Encapsulated additives were incorporated into PE powder)**

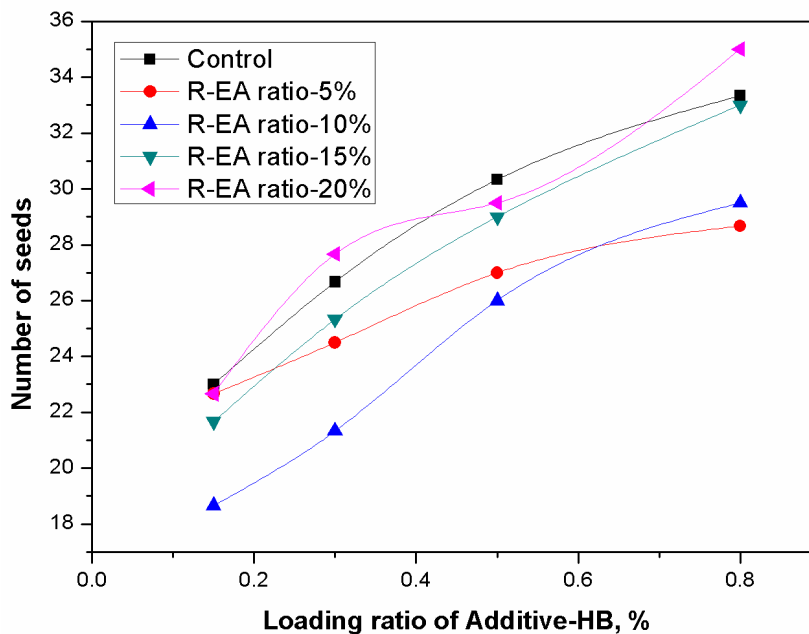


**Figure 5.15 Effects of LOA on number of seeds-HB  
(Additives were encapsulated with HB.  
Encapsulated additives were incorporated into HB powder)**

The explanation why larger LOA causes more seeds on the film surface is that the incompatibility issues are magnified with more additives being added in. And in addition, the concentration of additive in the powder samples affects the levelling of polymer to a higher extent.

However, another compromise has to be made. To make sure that fine powder can be fluidized well, suitable LOA has to be employed. Even though these additive can cause seeds on the film surface. Considering both the effects of LOA on the flow properties and film qualities, LOA of 0.3% or 0.5% is preferred to achieve the best flow properties and controllable number of seeds on the coating surface.

## 5.4 Summary

In this chapter, film quality characterizations such as gloss, roughness and number of seeds on the panel surface of 120 coated panel samples (The additives were encapsulated with 2 resins in 4 R-EA ratios. Each additive was incorporated into coating powders in 4 LOAs. Each coating powder was sprayed on 3 panels) are investigated based on the different R-EA ratios and LOAs.

At a fixed LOA, gloss increases with the increase of R-EA ratio for both two resin bases. However, after introducing net silica to powder coating ratio, gloss was found to decrease with the increasing of the net silica to powder coating ratio, which means that gloss is be inversely proportional to the net silica proportion. Roughness decreases as increasing the R-EA ratio. Number of seeds on the film surface, however, decreases with R-EA ratio increases from 0% to 10%, where a minimum number is achieved. When the R-EA ratio is above than 10%, seed number begins to increase with further increase of R-EA ratio. Therefore, R-EA ratio of 20% is required to get the highest gloss, while R-EA ratio of 0% is preferred to get best smoothness, and the optimum R-EA ratio for the least number of seeds is 10%.

At a certain R-EA ratio and for both powder resins, gloss decreases as LOA increases. On contrary, roughness and number of seeds increase with the increasing of LOA. More additive results in poorer gloss, higher roughness and more seeds on the film surface.

Additive is necessary to make the fine powder be fluidized in fine powder coating technology. Without adequate additive being added in, the fine powder is too cohesive to be fluidized and used. As a consequence, a compromise must be made between flow property and film quality.

## Chapter 6

### 6 Conclusions and Recommendations

#### 6.1 Conclusions

Due to the improvements on film uniformity and thickness reduction, fine powder coating (*D50* smaller than 25 microns) has great potential to be widely used in the near future. However, the inherent cohesive property of these Group C powders makes them difficult to handle and utilize. To overcome this limitation, much smaller nano sized additive is used to significantly improve the flow properties of fine powders. But all of the additives employed currently are inorganic materials, which are incompatible with the organic coating materials. The compatibility issues will greatly affect the film qualities of the powder coating.

In this work, a new encapsulation method was developed to solve the compatibility problem between inorganic additive and organic resin, and to improve the flow properties of fine powders. The optimum conditions for encapsulation level and additive loading ratio were also determined by considering both flow properties and film qualities.

##### 6.1.1 Flow Characteristic of Coating Powder

The encapsulation of nano additive and the effects on semi-static (represented by Angle of Repose, AOR) and dynamic (represented by Avalanche Angle, AVA) flow properties of fine powder were studied. The encapsulation on nano additive improves both the semi-static and dynamic flow properties. And the Resin-to-Encapsulated Additive ratio (R-EA ratio) and Loading ratio of Additive (LOA) both have an effect on the flow properties of fine powder.

At a fixed LOA, both AOR and AVA of these two resin bases decrease with increasing R-EA ratio to minimum values. Further increasing of R-EA ratio makes the AOR and AVA increase back. For semi-static flow, the optimum R-EA ratio is around 10% (for both of the polyester and hybrid based powder samples). To get minimum AVA, the

optimum R-EA ratio is around 10% (for polyester based powder) or 5% (for hybrid based powder).

At a fixed R-EA ratio, both AOR and AVA of the two resin bases initially decrease as the increasing of LOA to minimum values and then increase back with further increasing of LOA. The optimum LOA is 0.5% (for AOR) or 0.3% (for AVA), regardless of powder resin base.

For industrial applications, R-EA ratio of 5% to 10% and LOA of 0.3% to 0.5% are suggested, depending on the specific resin base and flow characteristic.

### 6.1.2 Film Characteristic of Coating Film

The effects of encapsulated nano additive on film qualities were also investigated. By studying the gloss, roughness and the number of seeds on the coating film, the results show that the encapsulation on the additive also affects the surface appearance of coating film.

At a fixed LOA, gloss increases with the increase of R-EA ratio for both two resin bases. Roughness decreases as increasing the R-EA ratio. Number of seeds on the film surface, however, decreases with R-EA ratio increases from 0% to 10%, where a minimum number is achieved. When the R-EA ratio is above 10%, seeds number begins to increase with the further increase of R-EA ratio.

At a fixed R-EA ratio and for both two powder resins, gloss decreased as the increase of LOA. On contrary, roughness and number of seeds increase with the increasing of LOA.

However, additive is mandatory to make the fine powder be fluidized in fine powder coating technology as discussed before. So compromises have to be made to reach the balance of flow properties and film qualities. For industrial applications, R-EA ratio of 10% and LOA of 0.3% are preferred because these conditions exhibit the best flow properties and least number of seeds. Besides, the resulting significant improvements of gloss and smoothness over the control samples are adequate in the industries.

## 6.2 Recommendations

For future work, the following recommendations are given.

1. The effect of encapsulation was only evaluated by only one flow additive in this work, which is nano silica. Such effect should be validated by the research on some other additives, for example, nano aluminum oxide.
2. Only one particle size, which is 22 microns, was studied in current work. Finer powder with  $D_{50}$  less than 20 microns is suggested to be estimated in future works because finer powder can provide thinner coating film.
3. The mixing method employed in this work was using an ultrasonic-vibration sieve, which requires addition time and energy to disperse additive into coating powder. In future works, it is suggested to incorporate the additive during the grinding process of fine powders with ACM. This new method may save lots of mixing time and achieve a more uniform dispersion of additive.

## References

- Alexandre, M., & Dubois, P. (2000). Polymer-layered silicate nanocomposites: preparation, properties and uses of a new class of materials. *Materials Science and Engineering: R: Reports*, 28(1), 1-63.
- Antony, S. J., W. Hoyle, et al. (2004). *Granular Materials: Fundamentals and Applications*, Royal Society of Chemistry.
- Ajbar, A., Alhumazi, K., & Asif, M. (2005). Improvement of the fluidizability of cohesive powders through mixing with small proportions of group a particles. *The Canadian Journal of Chemical Engineering*, 83(6), 930-943.
- Bailey, A. G. (1998). The science and technology of electrostatic powder spraying, transport and coating. *Journal of electrostatics*, 45(2), 85-120.
- Biller, K. (2006). OEM Automotive Powder Coatings. *Industrial Paint & Powder*, 82(7), 15-18.
- Biris, A. S., Mazumder, M. K., Yurteri, C. U., Sims, R. A., Snodgrass, J., & De, S. (2001). Gloss and texture control of powder coated films. *Particulate science and technology*, 19(3), 199-217.
- Bocchi, G.J. (1986). *Modern Paints and Coatings*, 76, 44.
- Brinker, C. J., & Scherer, G. W. (Eds.). (1990). *Sol-gel science: the physics and chemistry of sol-gel processing*. Access Online via Elsevier.
- Carr, R. L. (1965). Evaluating flow properties of solids. *Chem. Eng*, 72(2), 163-168.
- Carson, M. A. (1977). Angles of repose, angles of shearing resistance and angles of talus slopes. *Earth Surface Processes*, 2(4), 363-380.
- Castellanos, A., Valverde, J. M., Pérez, A. T., Ramos, A., & Watson, P. K. (1999). Flow regimes in fine cohesive powders. *Physical review letters*, 82(6), 1156.
- Chen, Y., Yang, J., Dave, R. N., & Pfeffer, R. (2008). Fluidization of coated group C powders. *AIChE Journal*, 54(1), 104-121.
- Cheremisinoff, N. P. and P. N. Cheremisinoff. (1984), *Hydrodynamics of gas-solids fluidization*.
- Cohen, H., R. J. Levy, J. Gao, I. Fishbein, V. Kousaev, S. Sosnowski, S. Slomkowski and G. Golomb. (2000), Sustained delivery and expression of DNA encapsulated in polymeric nanoparticles, *Gene Therapy* 7(22): 1896-1905.
- Daniher, D. I., & Zhu, J. (2008). Dry powder platform for pulmonary drug delivery. *Particuology*, 6(4), 225-238.
- Danish, F. Q. and E. L. Parrott. (1971). Effect of concentration and size of lubricant on flow rate of granules. *Journal of Pharmaceutical Sciences* 60(5): 752-754.



- Dave, R. N., Wu, C. Y., Chaudhuri, B., & Watano, S. (2000). Magnetically mediated flow enhancement for controlled powder discharge of cohesive powders. *Powder technology*, 112(1), 111-125.
- Dutta, A. and L. V. Dullea. (1990), Comparative evaluation of negatively and positively charged submicron particles as flow conditioners for a cohesive powder, *Advances in Fluidization Engineering*, November 5, 1989 - November 10, 1989, San Francisco, CA, USA, Publ by AIChE.
- Elbicki, J. M. and G. I. Tardos. (1998). Influence of fines on the flowability of alumina powders in test hoppers. *Powder Handling and Processing* 10(2): 147-149.
- Franks, J. R., & Pettit Jr, P. H. (1993). U.S. Patent No. 5,212,245. Washington, DC: U.S. Patent and Trademark Office.
- Fu, J. (2010). Study on Powder Coating Particles and Development of New Powder Coating Application Methods. Department of Chemical and Biochemical Engineering. London, The University of Western Ontario. Master: 2.
- Geldart, D. (1973). Types of gas fluidization. *Powder technology*, 7(5), 285-292.
- Gemmer, E. (1995). Process and Apparatus for the Preparation of Protective Coatings from Pulverulent Synthetic Thermoplastic Materials. Ger. patent. Germany. 933019.
- Gribble, P. (2003). Development Status of Powder Coatings for OEM Automotive Applications. *Finishing Today*.
- Hamaker H C. (1937). The London—van der Waals attraction between spherical particles. *physica*, 4(10): 1058-1072.
- Hans, M. L., & Lowman, A. M. (2002). Biodegradable nanoparticles for drug delivery and targeting. *Current Opinion in Solid State and Materials Science*, 6(4), 319-327.
- Hegemann, D., Brunner, H., & Oehr, C. (2003). Plasma treatment of polymers for surface and adhesion improvement. *Nuclear instruments and methods in physics research section B: Beam interactions with materials and atoms*, 208, 281-286.
- Hollenbach, A. M., Peleg, M., & Rufner, R. (1983). Interparticle surface affinity and the bulk properties of conditioned powders. *Powder Technology*, 35(1), 51-62.
- Hong, R. Y., Fu, H. P., Zhang, Y. J., Liu, L., Wang, J., Li, H. Z., & Zheng, Y. (2007). Surface - modified silica nanoparticles for reinforcement of PMMA. *Journal of Applied Polymer Science*, 105(4), 2176-2184.
- Huang, Q. (2009). Flow and fluidization properties of fine powder. Department of Chemical and Biochemical Engineering. London, The University of Western Ontario. Ph.D.: 192.
- Huang, Q., H. Zhang, et al. (2010). Flow properties of fine powders in powder coating. *Particuology* 8(1): 19-27.
- Irani, R., C. Callis, et al. (1960). Correction: FLOW Conditioning and Anticaking Agents. *Industrial & Engineering Chemistry* 52(5): 400-400.

- Ishida, M., Uchiyama, J., Isaji, K., Suzuki, Y., Ikematsu, Y., & Aoki, S. (2013). A novel approach to a fine particle coating using porous spherical silica as core particles. *Drug Development and Industrial Pharmacy*, (0), 1-11.
- J. Ruys, A. and Y.-W. Mai. (1999). The nanoparticle-coating process: a potential sol-gel route to homogeneous nanocomposites, *Materials Science and Engineering: A* 265(1-2): 202-207.
- Kablitz, C. D., Harder, K., & Urbanetz, N. A. (2006). Dry coating in a rotary fluid bed. *European journal of pharmaceutical sciences*, 27(2), 212-219.
- Kendall, K., & Stainton, C. (2001). Adhesion and aggregation of fine particles. *Powder technology*, 121(2), 223-229.
- Kittle, K. J., & Rushman, P. F. (1997). U.S. Patent No. 5,635,548. Washington, DC: U.S. Patent and Trademark Office.
- Kojima, T., & Elliott, J. A. (2013). Effect of silica nanoparticles on the bulk flow properties of fine cohesive powders. *Chemical Engineering Science*.
- Kong, J., Cassell, A. M., & Dai, H. (1998). Chemical vapor deposition of methane for single-walled carbon nanotubes. *Chemical Physics Letters*, 292(4), 567-574.
- Kono, H. O., C. C. Huang and M. Xi. (1989), Effect of flow conditioners on the tensile strength of cohesive powder structures, *Fluidization and Fluid Particle Systems: Fundamentals and Applications*, November 27, 1988 - December 2, 1988, Washington, DC, USA, Publ by AIChE.
- Kono, H. O., Huang, C. C., & Xi, M. (1990). Function and mechanism of flow conditioners under various loading pressure conditions in bulk powders. *Powder technology*, 63(1), 81-86.
- Krantz, M. (2009). Powder characterization and powder application in automotive coatings. Department of Chemical and Biochemical Engineering. London, The University of Western Ontario. Master.
- Licari, J. J. (2003). *Coating Materials for Electronic Applications: Polymers, Processing, Reliability, Testing*, Elsevier Science.
- Misev, T.A. (1991). *Powder Coatings: Chemistry and Technology*, John Wiley and Sons, New York
- Montz, K. W., Beddow, J. K., & Butler, P. B. (1989). Acoustic interactions with surface-adhered fine particles. *Applied Acoustics*, 28(1), 9-19.
- Mullarney M P, Beach L E, Davé R N, et al. (2011). Applying dry powder coatings to pharmaceutical powders using a comil for improving powder flow and bulk density. *Powder Technology*, 212(3): 397-402.
- Nagel, S., MacChesney, J., & Walker, K. (1982). An overview of the modified chemical vapor deposition (MCVD) process and performance. *Quantum Electronics, IEEE Journal of*, 18(4), 459-476.
- Qian, G. H., Bagyi, I., Burdick, I. W., Pfeffer, R., Shaw, H., & Stevens, J. G. (2001). Gas-solid fluidization in a centrifugal field. *AIChE journal*, 47(5), 1022-1034.

- Richart, D. (2001). Powder Coating Processes, in: Kirk-Othmer Encyclopedia of Chemical Technology. John Wiley & Sons, published online, vol. 7, pp 35-68
- Rong, M. Z., Zhang, M. Q., & Ruan, W. H. (2006). Surface modification of nanoscale fillers for improving properties of polymer nanocomposites: a review. *Materials science and technology*, 22(7), 787-796.
- Rumpf H. (1990). *Particle Technology*. London: Chapman and Hall.
- Sastry, S. V., Nyshadham, J. R., & Fix, J. A. (2000). Recent technological advances in oral drug delivery—a review. *Pharmaceutical science & technology today*, 3(4), 138-145.
- Sato, T. and R. Ruch (1980), *Stabilization of colloidal dispersions by polymer adsorption*, Dekker.
- Sauer, D., M. Cerea, et al. (2013). Dry powder coating of pharmaceuticals: A review. *International Journal of Pharmaceutics*.
- Schwedes, J. (2003). Review on testers for measuring flow properties of bulk solids. *Granular Matter*, 5(1), 1-43.
- Seville, J. P. K., C. D. Willett, et al. (2000). Interparticle forces in fluidization: a review. *Powder Technology* 113(3): 261-268.
- Taylor, M. K., Ginsburg, J., Hickey, A. J., & Gheyas, F. (2000). Composite method to quantify powder flow as a screening method in early tablet or capsule resin base development. *AAPS PharmSciTech*, 1(3), 20-30.
- Thomas, A., K. Saleh, et al. (2009). Characterisation of electrostatic properties of powder coatings in relation with their industrial application. *Powder Technology* 190(1–2): 230-235.
- Valverde, J. M., Castellanos, A., Ramos, A., & Watson, P. K. (2000). Avalanches in fine, cohesive powders. *Physical Review E*, 62(5), 6851.
- Visser, J. (1989). Van der Waals and other cohesive forces affecting powder fluidization. *Powder Technology*, 58(1), 1-10.
- Vollath, D., & Szabo, D. V. (1999). Coated nanoparticles: a new way to improved nanocomposites. *Journal of Nanoparticle Research*, 1(2), 235-242.
- Wang, Y., Dave, R. N., & Pfeffer, R. (2004). Polymer coating/encapsulation of nanoparticles using a supercritical anti-solvent process. *The Journal of supercritical fluids*, 28(1), 85-99.
- Weiss, K. D. (1997). Paint and coatings: A mature industry in transition. *Progress in Polymer Science*, 22(2), 203-245.
- Xia, L. (2013). Preparation and resin base of powder coating for application of enamelled wire. Department of Chemical and Biochemical Engineering. London, The University of Western Ontario. Master:16.
- Xie, H. Y. (1997). The role of interparticle forces in the fluidization of fine particles. *Powder Technology*, 94(2), 99-108.

- Yang J., Sliva A., Banerjee A., Dave R., Pfeffer R. (2005). Dry particle coating for improving the flowability of cohesive powders, *Powder Technology*, 158(1-3), 21-33
- Zhang, Y., Q. Zhang, Y. Li, N. Wang and J. Zhu. (2000), Coating of carbon nanotubes with tungsten by physical vapor deposition, *Solid State Communications* 115(1): 51-55.
- Zhu, J. X., and Zhang, H. (2005). Ultrafine powder coatings: an innovation. *Powder Coat*, 16, 39-47.
- Zhu, J. (2003). Fluidization of Fine Powders, Chapter 10 in *Advances in Granular Materials: Fundamentals and Applications*, 270-295.
- Zhu, J., and Zhang, H. (2004). Fluidization additives to fine powders. U. S. Patent. USA. 6833185."

## Appendices

### A1 Particle size

In chapter 3, the particle size of fine polyester and hybrid coating powders were tested, the tests were repeated three times following the same standard procedure and the average value was employed. The data and error analysis were listed in Table A.1.

**Table A.1 Particle size of polyester and hybrid coating powder samples**

<b>Sample</b>	<b><math>D_{50}</math></b>	<b><math>D_{10}</math></b>	<b><math>D_{90}</math></b>	<b>Average <math>D_{50}</math></b>	<b>Average <math>D_{10}</math></b>	<b>Average <math>D_{90}</math></b>	<b>Deviation of <math>D_{50}</math></b>	<b>Deviation of <math>D_{10}</math></b>	<b>Deviation of <math>D_{90}</math></b>
	22.32	8.56	41.78				-0.09%	-0.23%	0.00%
PE	22.40	8.62	41.81	22.34	8.58	41.78	0.27%	0.47%	0.07%
	22.31	8.56	41.74				-0.13%	-0.23%	-0.10%
	22.41	7.36	46.16				0.22%	-1.08%	1.10%
HB	22.40	7.55	45.32	22.35	7.44	45.66	0.18%	1.48%	-0.74%
	22.26	7.42	45.49				-0.45%	-0.27%	-0.37%

## A2 Semi-static flow property

### A3.1 Original Data

As the representative of semi-static flow property, Angle of Repose of all the powder samples was tested in chapter 3. For each sample, the testing process was repeated 3-5 times until three of them of which the differences were less than  $0.8^\circ$  were obtained and then the average value was used as the AOR for the certain sample. The data were listed in Table A.2 and Table A.3, respectively.

**Table A.2 Angle of repose of polyester powder samples**

<b>Powder sample</b>	<b>Trail 1</b>	<b>Trail 2</b>	<b>Trail 3</b>	<b>Average AOR(<math>^\circ</math>)</b>
PE-Control-0	49.26	49.10	49.40	49.25
PE-Control-0.15%	42.42	42.20	42.55	42.39
PE-Control-0.3%	42.15	41.67	42.28	42.03
PE-Control-0.5%	41.93	41.23	41.36	41.51
PE-Control-0.8%	42.55	42.69	42.60	42.61
PE-5%-0.15%	42.87	42.20	42.55	42.54
PE-5%-0.3%	41.77	41.70	41.63	41.70
PE-5%-0.5%	40.86	41.10	41.76	41.24
PE-5%-0.8%	42.67	42.27	42.03	42.32
PE-10%-0.15%	41.73	40.79	41.14	41.22
PE-10%-0.3%	40.56	40.29	39.63	40.16
PE-10%-0.5%	38.01	38.36	38.31	38.23
PE-10%-0.8%	41.78	41.60	41.26	41.55
PE-15%-0.15%	41.12	41.03	40.88	41.01
PE-15%-0.3%	40.91	40.99	40.80	40.90
PE-15%-0.5%	40.36	40.66	40.52	40.51
PE-15%-0.8%	39.94	40.25	40.72	40.30
PE-20%-0.15%	43.54	43.26	43.40	43.40
PE-20%-0.3%	41.69	41.58	41.87	41.71
PE-20%-0.5%	40.24	40.16	39.94	40.11
PE-20%-0.8%	40.15	40.23	40.59	40.32

**Table A.3 Angle of repose of hybrid powder samples**

<b>Powder sample</b>	<b>Trail 1</b>	<b>Trail 2</b>	<b>Trail 3</b>	<b>Average AOR(°)</b>
HB-Control-0	52.31	52.49	52.83	52.54
HB-Control-0.15%	46.33	46.72	46.35	46.47
HB-Control-0.3%	42.82	43.39	43.7	43.30
HB-Control-0.5%	38.99	39.02	38.7	38.90
HB-Control-0.8%	40.4	38.88	38.86	39.38
HB-5%-0.15%	44.78	44.43	44.28	44.50
HB-5%-0.3%	43.7	42.58	43.19	43.16
HB-5%-0.5%	41.49	41.59	41.77	41.62
HB-5%-0.8%	41.03	42.2	41.08	41.44
HB-10%-0.15%	44.52	45.37	45.07	44.99
HB-10%-0.3%	42.21	42.36	42.18	42.25
HB-10%-0.5%	37.79	37.68	37.89	37.79
HB-10%-0.8%	39.65	39.65	39.39	39.56
HB-15%-0.15%	46.49	46.51	46.57	46.52
HB-15%-0.3%	44.44	43.41	44.51	44.12
HB-15%-0.5%	39.63	39.18	40.19	39.67
HB-15%-0.8%	42.28	42.2	41.81	42.10
HB-20%-0.15%	45.33	45.48	45.24	45.35
HB-20%-0.3%	41.88	42.56	42.61	42.35
HB-20%-0.5%	39.11	40.88	39.31	39.77
HB-20%-0.8%	39.51	38.96	39.41	39.29

### A3.2 Error Analysis

Figure A.1 and Figure A.2 show the error bar of AOR results, based on Figure 4.10 and Figure 4.11.

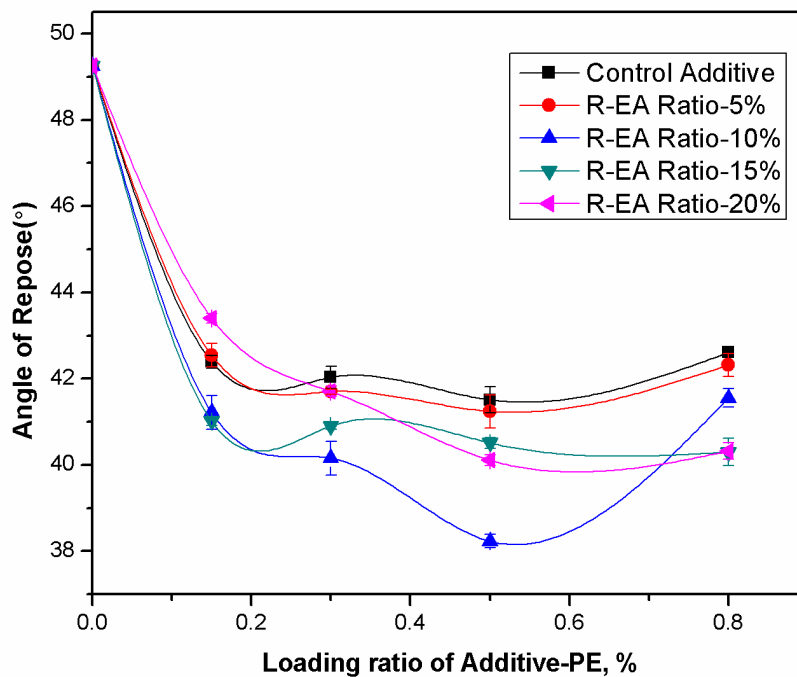


**Figure A.1 Error analysis of AOR for polyester samples  
(Additives were encapsulated with PE.  
Encapsulated additives were incorporated into PE powder)**

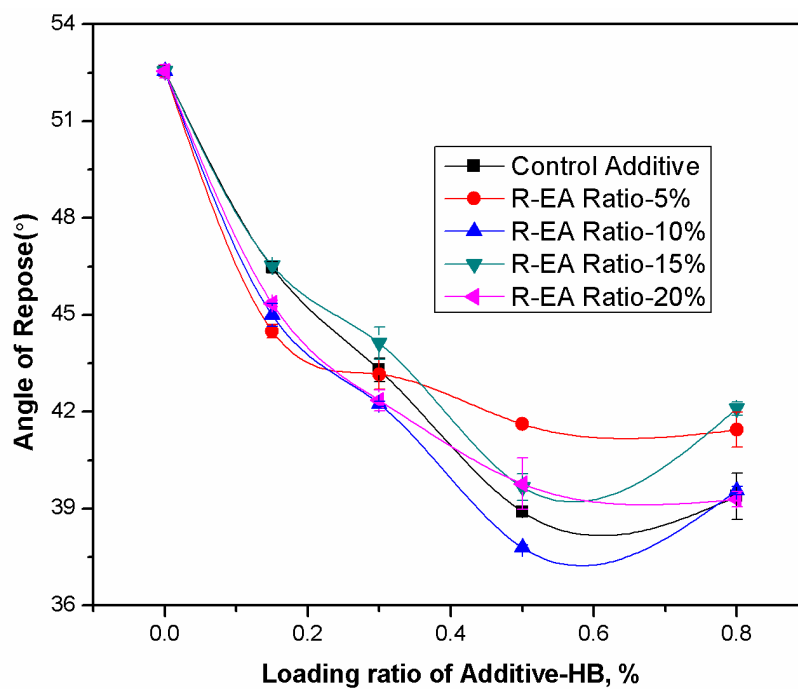


**Figure A.2 Error analysis of AOR for hybrid samples  
(Additives were encapsulated with HB.  
Encapsulated additives were incorporated into HB powder)**



## A3 Dynamic flow property

### A3.1 Original Data

In chapter 4, AVA of all the powder samples was tested. For AVA measurement of each sample, two hundred powder avalanches were repeated and average value was presented. It was noticed that some of the results were obvious unreasonable, for instance, there might be an  $11.45^\circ$  while the other hundred were all around  $50^\circ$ . All these irrational results were ignored, based on the same tolerance criterion for all the samples. The data were listed in Table A.4 and Table A.5 for polyester and hybrid powder samples respectively.

**Table A.4 Avalanche angle of polyester powder samples**

<b>Powder sample</b>	<b>Average AVA(<math>^\circ</math>)</b>
PE-Control-0.15%	61.33
PE-Control-0.3%	54.04
PE-Control-0.5%	55.72
PE-Control-0.8%	57.02
PE-5%-0.15%	56.00
PE-5%-0.3%	52.96
PE-5%-0.5%	54.90
PE-5%-0.8%	56.47
PE-10%-0.15%	54.70
PE-10%-0.3%	51.92
PE-10%-0.5%	54.26
PE-10%-0.8%	55.67
PE-15%-0.15%	55.37
PE-15%-0.3%	52.29
PE-15%-0.5%	53.67
PE-15%-0.8%	55.59
PE-20%-0.15%	57.96
PE-20%-0.3%	55.57
PE-20%-0.5%	54.46
PE-20%-0.8%	56.33

**Table A.5 Avalanche angle of hybrid powder samples**

<b>Powder sample</b>	<b>Average AVA(°)</b>
HB-Control-0.15%	59.15
HB-Control-0.3%	57.38
HB-Control-0.5%	57.51
HB-Control-0.8%	58.23
HB-5%-0.15%	58.16
HB-5%-0.3%	56.53
HB-5%-0.5%	57.11
HB-5%-0.8%	58.38
HB-10%-0.15%	57.81
HB-10%-0.3%	56.86
HB-10%-0.5%	57.55
HB-10%-0.8%	58.55
HB-15%-0.15%	57.76
HB-15%-0.3%	57.05
HB-15%-0.5%	57.78
HB-15%-0.8%	58.41
HB-20%-0.15%	58.20
HB-20%-0.3%	56.95
HB-20%-0.5%	57.89
HB-20%-0.8%	58.14

### A3.2 Error Analysis

Figure A.3 and A.4 shows the error bar of AVA results, based on Figure 4.12 and Figure 4.13.

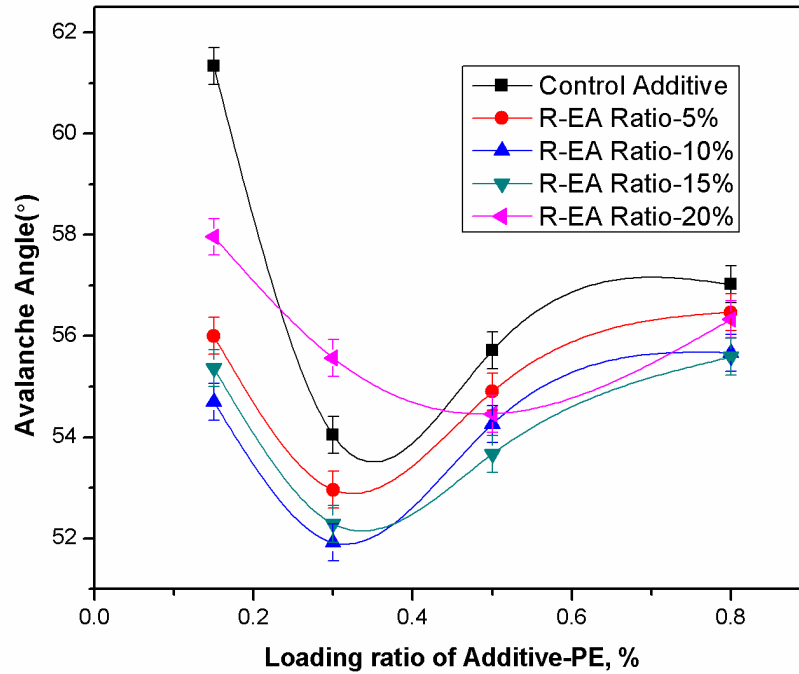


**Figure A.3 Error analysis of AVA for polyester samples (Additives were encapsulated with PE. Encapsulated additives were incorporated into PE powder)**

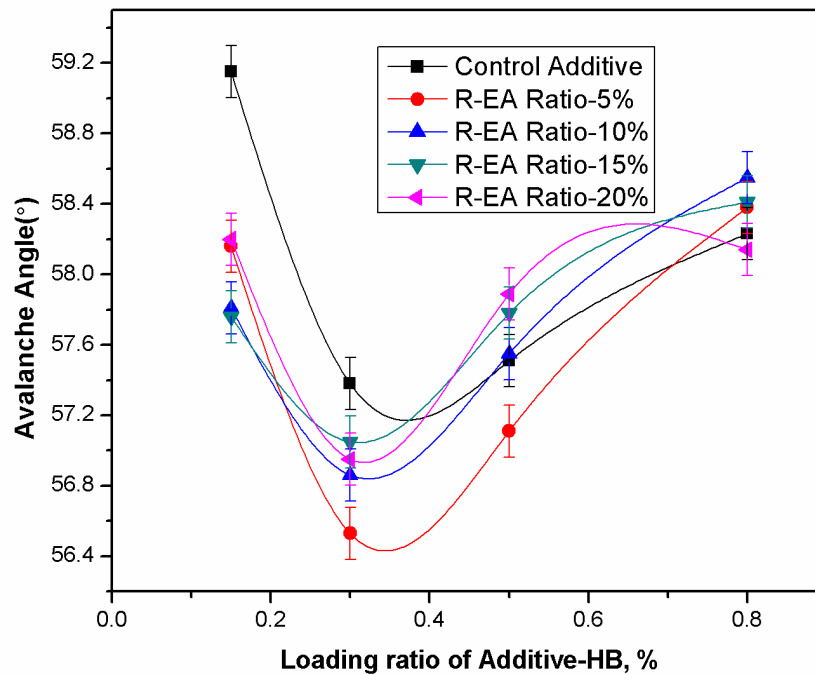


**Figure A.4 Error analysis of AVA for hybrid samples (Additives were encapsulated with HB. Encapsulated additives were incorporated into HB powder).**

## A4 Film qualities

### A4.1 Thickness

After spraying and curing, the thickness of each panel was tested in chapter 5. For each powder sample, three panels were sprayed and cured for repeatability. For each panel, nine different zones were selected to measure the film thickness and the average value was used as the thickness of the certain panel. All data of thickness of polyester samples and hybrid panel samples were listed in Table A.6 and Table A.7.

**Table A.6 Thickness of polyester coated panel samples**

Panel sample	NO	1	2	3	4	5	6	7	8	9	Average Thickness (micron)	Deviation	Average Thickness (micron)	Deviation
PE-Control-0.15%	#1	47	46	48	49	50	48	52	49	49	48.88	1.633	49.30	1.886
	#2	50	48	50	49	47	46	50	49	48	48.38	1.343		
	#3	52	54	48	50	49	50	52	50	52	50.63	1.750		
PE-Control-0.3%	#1	48	52	50	52	54	52	52	50	49	51.38	1.764	50.92	1.755
	#2	50	50	54	52	52	50	52	48	47	50.63	2.061		
	#3	50	50	50	52	52	52	52	50	48	50.75	1.333		
PE-Control-0.5%	#1	47	48	47	50	50	52	49	52	50	49.75	1.771	48.46	1.908
	#2	49	47	47	48	48	46	49	48	47	47.50	0.943		
	#3	54	50	49	50	49	47	47	47	46	48.13	2.299		
PE-Control-0.8%	#1	46	48	46	50	49	49	52	50	52	49.50	2.079	51.46	2.753
	#2	50	49	48	54	50	49	56	54	50	51.25	2.643		
	#3	49	54	53	54	54	56	54	52	52	53.63	1.853		
PE-5%-0.15%	#1	54	49	48	50	49	48	48	46	46	48.00	2.261	50.17	3.817
	#2	46	44	44	54	52	52	56	58	58	52.25	5.315		

Panel sample	NO	1	2	3	4	5	6	7	8	9	Average Thickness (micron)	Deviation	Average Thickness (micron)	Deviation
PE-5%-0.3%	#3	50	47	47	54	52	49	54	50	49	50.25	2.485	50.13	2.595
	#1	52	52	52	54	54	54	52	52	50	52.50	1.257		
	#2	50	47	48	50	49	48	50	48	48	48.50	1.054		
	#3	43	47	48	46	49	50	52	52	51	49.38	2.828		
PE-5%-0.5%	#1	50	52	52	50	52	50	48	47	48	49.88	1.792	49.17	1.626
	#2	50	48	49	50	48	48	50	49	48	48.75	0.875		
	#3	47	47	46	50	49	48	52	49	50	48.88	1.764		
PE-5%-0.8%	#1	50	47	48	52	52	49	49	48	48	49.13	1.685	49.63	1.897
	#2	52	49	49	50	48	46	49	52	54	49.63	2.283		
	#3	50	48	52	52	50	49	52	50	48	50.13	1.523		
PE-10%-0.15%	#1	48	48	50	50	48	50	48	47	49	48.75	1.054	48.25	1.988
	#2	52	47	52	49	47	49	46	44	44	47.25	2.820		
	#3	52	48	49	50	49	50	49	47	48	48.75	1.370		
PE-10%-0.3%	#1	50	48	49	50	47	48	49	49	48	48.50	0.943	47.58	1.286
	#2	48	46	49	48	47	46	47	47	48	47.25	0.943		
	#3	50	47	47	47	45	47	48	46	49	47.00	1.414		
PE-10%-0.5%	#1	48	49	50	54	52	52	52	50	49	51.00	1.826	50.71	1.641
	#2	50	49	50	54	49	50	52	52	50	50.75	1.563		
	#3	49	48	52	52	50	49	52	49	51	50.38	1.474		
PE-10%-0.8%	#1	52	50	48	52	54	49	48	46	46	49.13	2.629	48.63	2.149
	#2	48	49	46	49	48	45	49	45	47	47.25	1.563		
	#3	50	48	50	50	48	49	50	49	52	49.50	1.165		
PE-15%-0.15%	#1	49	45	50	52	48	47	50	48	47	48.38	1.950	49.29	2.250
	#2	50	48	48	52	49	49	50	49	47	49.00	1.370		
	#3	54	50	48	56	50	52	50	50	48	50.50	2.514		
PE-15%-0.3%	#1	47	45	46	52	48	48	54	52	49	49.25	2.867	48.83	2.397

Panel sample	NO	1	2	3	4	5	6	7	8	9	Average Thickness (micron)	Deviation	Average Thickness (micron)	Deviation
	#2	50	47	47	52	48	47	50	47	46	48.00	1.872		
	#3	47	46	47	52	48	48	52	52	49	49.25	2.261		
	#1	49	46	46	52	49	47	48	47	47	47.75	1.792		
PE-15%-0.5%	#2	54	52	52	50	49	49	52	50	49	50.38	1.685	50.04	2.372
	#3	48	52	50	52	50	52	54	52	54	52.00	1.832		
	#1	52	48	46	54	49	47	52	47	47	48.75	2.685		
PE-15%-0.8%	#2	52	49	49	52	54	54	54	52	52	52.00	1.826	50.00	2.643
	#3	49	47	48	54	50	52	48	48	47	49.25	2.250		
	#1	52	50	50	54	52	52	52	50	50	51.25	1.333		
PE-20%-0.15%	#2	48	46	45	52	49	47	50	48	47	48.00	2.000	49.13	2.596
	#3	44	44	46	50	52	49	48	48	48	48.13	2.494		
	#1	50	52	50	54	52	52	50	47	48	50.63	2.061		
PE-20%-0.3%	#2	49	48	50	49	49	50	46	44	46	47.75	1.969	49.29	2.274
	#3	49	47	48	52	52	49	52	49	47	49.50	1.950		
	#1	49	48	47	52	52	50	50	47	47	49.13	1.912		
PE-20%-0.5%	#2	48	46	50	52	50	49	48	45	46	48.25	2.149	47.96	2.193
	#3	46	45	48	47	46	45	50	46	45	46.50	1.571		
	#1	50	52	54	50	52	50	54	54	50	52.00	1.750		
PE-20%-0.8%	#2	47	48	46	52	46	52	54	49	50	49.63	2.708	50.88	2.363
	#3	46	50	50	50	52	52	52	50	52	51.00	1.832		

**Table A.7 Thickness of hybrid coated panel samples**

<b>Panel sample</b>	<b>NO</b>	<b>1</b>	<b>2</b>	<b>3</b>	<b>4</b>	<b>5</b>	<b>6</b>	<b>7</b>	<b>8</b>	<b>9</b>	<b>Average Thickness (micron)</b>	<b>Deviation</b>	<b>Average Thickness (micron)</b>	<b>Deviation</b>
HB-Control- 0.15%	#1	49	50	54	52	54	52	49	47	54	51.50	2.439	50.04	2.317
	#2	47	45	48	50	50	48	50	48	47	48.25	1.595		
	#3	52	49	51	50	52	52	52	49	48	50.38	1.499		
HB-Control- 0.3%	#1	48	52	52	56	58	56	54	51	53	54.00	2.867	51.13	2.973
	#2	48	46	48	54	52	50	52	48	47	49.63	2.543		
	#3	48	50	48	52	49	49	52	49	49	49.75	1.423		
HB-Control- 0.5%	#1	50	48	52	56	52	50	54	48	48	51.00	2.685	51.14	2.347
	#2	48	49	49	52	52	52	54	54	54	52.43	2.217		
	#3	50	50	49	52	48	47	52	52	49	50.00	1.728		
HB-Control- 0.8%	#1	44	47	46	49	50	50	52	50	50	49.25	2.357	50.29	2.333
	#2	48	49	47	54	50	49	52	52	50	50.38	2.079		
	#3	50	49	52	52	54	54	50	49	50	51.25	1.853		
HB-5%-0.15%	#1	47	48	50	50	48	48	46	45	44	47.38	1.944	49.67	2.872
	#2	49	49	49	49	49	48	49	48	48	48.63	0.471		
	#3	50	54	52	56	56	54	52	50	50	53.00	2.309		
HB-5%-0.3%	#1	49	49	49	49	52	50	48	48	48	49.13	1.197	49.25	2.263
	#2	50	47	46	52	50	49	50	47	46	48.38	2.006		
	#3	52	52	50	56	50	52	47	49	46	50.25	2.833		
HB-5%-0.5%	#1	54	54	54	54	54	56	50	48	48	52.25	2.793	50.09	2.872
	#2	50	50	49	52	47	49	47	48	47	48.63	1.618		
	#3	50	49	52	49	50	54	45	46	50	49.38	2.587		
HB-5%-0.8%	#1	47	48	52	52	52	52	50	52	52	51.25	1.872	49.83	2.722
	#2	46	49	46	52	50	50	48	46	47	48.50	2.043		
	#3	56	52	52	50	52	52	49	47	44	49.75	3.270		

Panel sample	NO	1	2	3	4	5	6	7	8	9	Average Thickness (micron)	Deviation	Average Thickness (micron)	Deviation
HB-10%-0.15%	#1	49	49	50	50	49	52	47	46	47	48.75	1.750	51.17	2.349
	#2	50	50	52	52	54	54	52	50	50	51.75	1.571		
	#3	49	52	50	54	54	54	54	52	54	53.00	1.832		
HB-10%-0.3%	#1	46	48	46	52	52	50	54	52	50	50.50	2.667	50.71	2.452
	#2	54	50	52	54	52	49	54	52	49	51.50	1.931		
	#3	50	50	49	54	54	50	49	47	48	50.13	2.283		
HB-10%-0.5%	#1	54	54	52	52	52	52	48	48	47	50.63	2.494	50.25	2.424
	#2	50	48	50	52	49	50	49	48	48	49.25	1.247		
	#3	52	54	52	56	52	50	48	47	48	50.88	2.828		
HB-10%-0.8%	#1	49	49	49	54	52	50	54	49	47	50.50	2.309	51.42	2.728
	#2	46	50	50	52	54	50	50	48	52	50.75	2.200		
	#3	49	50	50	54	52	50	58	56	54	53.00	2.948		
HB-15%-0.15%	#1	49	52	52	52	52	54	47	49	49	50.88	2.108	50.8	2.278
	#2	52	52	54	50	52	54	52	49	48	51.38	1.950		
	#3	52	52	52	50	52	54	46	48	47	50.13	2.582		
HB-15%-0.3%	#1	54	52	54	52	47	48	46	45	47	48.88	3.337	49.38	2.447
	#2	54	50	52	52	50	52	50	48	50	50.50	1.663		
	#3	49	47	46	50	49	49	50	49	50	48.75	1.315		
HB-15%-0.5%	#1	48	48	47	49	49	52	46	50	50	48.88	1.685	50.34	2.758
	#2	46	47	46	52	49	47	54	54	50	49.88	3.059		
	#3	52	52	56	52	52	54	48	52	52	52.25	1.988		
HB-15%-0.8%	#1	58	54	53	52	52	54	56	54	54	53.63	1.792	53.17	2.782
	#2	50	50	58	54	54	56	58	54	48	54.00	3.370		
	#3	48	50	50	54	52	54	54	52	49	51.88	2.166		
HB-20%-0.15%	#1	47	47	45	49	49	50	52	50	52	49.25	2.211	50.17	2.159
	#2	50	50	52	52	52	54	50	50	52	51.50	1.333		



<b>Panel sample</b>	<b>NO</b>	<b>1</b>	<b>2</b>	<b>3</b>	<b>4</b>	<b>5</b>	<b>6</b>	<b>7</b>	<b>8</b>	<b>9</b>	<b>Average Thickness (micron)</b>	<b>Deviation</b>	<b>Average Thickness (micron)</b>	<b>Deviation</b>
HB-20%-0.3%	#3	47	47	49	50	52	52	47	49	52	49.75	2.061	51.92	3.281
	#1	46	50	48	54	54	52	48	48	50	50.50	2.667		
	#2	50	50	52	58	60	54	56	56	52	54.75	3.326		
	#3	48	48	49	52	52	52	50	49	52	50.50	1.685		
HB-20%-0.5%	#1	43	46	46	50	49	52	48	50	52	49.13	2.833	51	3.357
	#2	45	48	48	54	52	54	56	56	56	50.88	3.900		
	#3	48	52	49	48	52	52	50	54	50	53.00	1.950		
HB-20%-0.8%	#1	47	46	52	49	49	52	48	49	49	49.25	1.886	51.25	3.367
	#2	48	52	47	58	60	52	54	54	56	54.13	4.031		
	#3	52	50	54	50	52	52	47	49	49	50.38	2.006		

## A4.2 Film Gloss

In chapter 5, gloss of powder panels were measured. For each panel, five different spots were measured with the same test condition and an average value was employed. The Data were listed in the following Table A.8 and Table A.9.

**Table A.8 Film gloss of polyester coated panel samples**

Panel sample	NO.	Measure spot					Average gloss of each panel	Average gloss
		1	2	3	4	5		
PE-Control-0.15%	#1	93.0	92.1	92.6	93.5	93.4	92.92	93.02
	#2	93.7	91.8	92.7	93.7	93.3	93.04	
	#3	93.5	92.0	93.0	93.6	93.4	93.10	
PE-Control-0.3%	#1	91.0	91.4	91.6	91.7	91.9	91.52	91.74
	#2	91.4	91.8	91.5	92.0	92.2	91.78	
	#3	91.8	91.9	91.9	91.8	92.2	91.92	
PE-Control-0.5%	#1	89.4	89.1	89.1	89.6	89.4	89.32	89.32
	#2	89.8	89.6	89.7	89.4	89.6	89.62	
	#3	89.0	88.6	88.9	89.3	89.3	89.02	
PE-Control-0.8%	#1	87.2	87.3	87.3	87.2	87.6	87.32	87.03
	#2	86.7	86.9	86.6	86.9	87.1	86.84	
	#3	86.9	86.8	86.6	87.2	87.1	86.92	
PE-5%-0.15%	#1	93.7	94.2	94.1	93.8	93.8	93.92	93.85
	#2	93.8	94.0	93.9	94.0	93.9	93.92	
	#3	93.7	93.6	93.6	94.0	93.6	93.70	
PE-5%-0.3%	#1	91.5	91.9	92.1	92.0	92.0	91.90	91.98
	#2	92.1	92.2	91.8	92.5	92.2	92.16	
	#3	91.5	92.0	91.7	92.0	92.2	91.88	
PE-5%-0.5%	#1	89.8	89.5	89.5	89.4	89.3	89.50	89.62
	#2	89.6	89.5	89.7	89.7	89.7	89.64	
	#3	89.7	89.7	89.7	89.7	89.8	89.72	
PE-5%-0.8%	#1	87.4	87.2	86.9	86.8	87.0	87.06	87.15
	#2	87.6	87.2	87.2	87.5	87.5	87.40	
	#3	87.0	87.1	86.9	87.1	86.9	87.00	
PE-10%-0.15%	#1	93.6	94.3	93.9	94.0	94.4	94.04	94.14
	#2	94.4	94.4	94.3	94.2	94.3	94.32	
	#3	94.0	94.2	94.0	94.2	93.9	94.06	
PE-10%-0.3%	#1	91.9	91.9	92.3	92.4	92.1	92.12	92.26
	#2	92.2	92.4	92.6	92.4	92.4	92.40	

Panel sample	NO.	Measure spot					Average gloss of each panel	Average gloss
		1	2	3	4	5		
PE-10%-0.5%	#3	92.1	92.2	92.4	92.4	92.2	92.26	90.38
	#1	89.8	90.2	90.3	90.4	90.5	90.24	
	#2	90.3	90.7	90.2	90.4	90.5	90.42	
	#3	90.3	90.3	90.5	90.6	90.7	90.48	
PE-10%-0.8%	#1	87.9	87.8	87.9	88.2	88.1	87.98	87.92
	#2	87.8	88.1	88.0	88.1	87.9	87.98	
	#3	87.5	87.7	87.9	88.0	87.9	87.80	
PE-15%-0.15%	#1	94.2	94.4	94.2	94.0	94.1	94.18	94.06
	#2	94.1	93.8	94.0	94.5	94.1	94.10	
	#3	93.3	93.9	93.8	94.1	94.4	93.90	
PE-15%-0.3%	#1	91.6	92.4	92.1	92.3	92.4	92.16	92.33
	#2	92.4	92.1	92.7	92.4	92.3	92.38	
	#3	92.6	92.4	92.4	92.4	92.4	92.44	
PE-15%-0.5%	#1	90.4	90.4	90.2	90.6	90.3	90.38	90.42
	#2	90.3	90.6	90.5	90.4	90.6	90.48	
	#3	90.0	90.5	90.4	90.5	90.6	90.40	
PE-15%-0.8%	#1	87.8	87.9	88.0	87.9	88.5	88.02	88.19
	#2	88.0	87.9	88.2	88.2	88.1	88.08	
	#3	88.4	88.2	88.8	88.7	88.2	88.46	
PE-20%-0.15%	#1	93.7	93.6	94.2	94.1	94.2	93.96	94.30
	#2	94.2	94.5	94.3	94.3	94.7	94.40	
	#3	94.5	94.4	94.5	94.4	94.9	94.54	
PE-20%-0.3%	#1	93.0	93.0	92.8	92.7	92.8	92.86	92.82
	#2	92.7	92.6	93.1	92.7	92.5	92.72	
	#3	92.8	93.0	93.0	92.9	92.7	92.88	
PE-20%-0.5%	#1	90.6	90.7	90.7	90.9	90.6	90.70	90.93
	#2	91.1	91.3	91.0	90.9	91.0	91.06	
	#3	91.0	91.1	91.1	90.8	91.1	91.02	
PE-20%-0.8%	#1	89.3	89.2	89.3	89.0	89.4	89.24	88.95
	#2	89.1	88.8	88.7	89.1	88.4	88.82	
	#3	88.7	88.5	88.8	89.1	88.8	88.78	

**Table A.9 Film gloss of hybrid coated panel samples**

Panel sample	NO.	Measure spot					Average gloss of each panel	Average gloss
		1	2	3	4	5		
HB-Control-0.15%	#1	75.8	75.8	76.0	75.9	76.0	75.9	76.18
	#2	76.0	76.3	76.7	76.4	76.6	76.4	
	#3	75.8	76.3	76.3	76.3	76.5	76.24	
HB-Control-0.3%	#1	74.1	74.2	74.3	74.7	75.0	74.46	74.86
	#2	75.2	75.3	75.4	75.7	75.6	75.44	
	#3	74.4	74.5	74.7	75.0	74.8	74.68	
HB-Control-0.5%	#1	71.0	71.0	71.4	71.7	71.9	71.4	71.41
	#2	70.7	70.7	71.1	71.2	70.9	70.92	
	#3	71.6	72.0	72.0	72.0	72.0	71.92	
HB-Control-0.8%	#1	68.1	68.4	69.0	69.0	69.0	68.7	69.31
	#2	69.2	69.3	69.5	70.2	70.0	69.64	
	#3	69.2	69.5	69.7	69.7	69.9	69.6	
HB-5%-0.15%	#1	75.8	75.9	76.1	76.4	76.4	76.12	76.17
	#2	76.1	76.1	76.5	76.5	76.3	76.3	
	#3	76.0	76.0	76.3	76.3	75.9	76.1	
HB-5%-0.3%	#1	74.5	74.4	74.1	74.7	74.8	74.5	74.93
	#2	74.9	75.1	75.5	75.7	75.7	75.38	
	#3	74.5	74.9	74.7	75.2	75.3	74.92	
HB-5%-0.5%	#1	71.0	70.9	71.1	71.5	71.4	71.18	71.61
	#2	71.1	71.3	71.2	71.8	72.2	71.52	
	#3	71.7	71.7	72.1	72.6	72.6	72.14	
HB-5%-0.8%	#1	70.1	70.3	70.7	71.0	71.7	70.76	70.39
	#2	69.5	69.8	70.1	70.9	70.5	70.16	
	#3	69.9	70.3	70.0	70.8	70.2	70.24	
HB-10%-0.15%	#1	75.8	76.7	76.8	76.7	76.5	76.5	76.73
	#2	76.0	76.4	76.5	76.7	76.9	76.5	
	#3	76.9	77.3	77.4	77.3	77.1	77.2	
HB-10%-0.3%	#1	74.6	74.3	74.6	74.7	74.9	74.62	75.11
	#2	75.5	75.4	75.6	75.9	75.9	75.66	
	#3	74.9	74.6	75.0	75.2	75.6	75.06	
HB-10%-0.5%	#1	72.2	71.8	72.6	73.0	72.9	72.5	72.31
	#2	72.0	72.2	73.0	72.9	72.9	72.6	
	#3	71.4	71.7	71.7	72.0	72.4	71.84	
HB-10%-0.8%	#1	68.3	68.3	68.9	69.0	68.8	68.66	69.47
	#2	69.4	69.4	69.4	69.9	69.8	69.58	
	#3	69.5	70.2	70.4	70.3	70.4	70.16	

Panel sample	NO.	Measure spot					Average gloss of each panel	Average gloss
		1	2	3	4	5		
HB-15%-0.15%	#1	76.1	76.0	76.0	75.9	76.2	76.04	76.33
	#2	76.4	76.7	76.6	76.4	76.9	76.6	
	#3	76.0	76.2	76.3	76.5	76.7	76.34	
HB-15%-0.3%	#1	74.7	74.3	74.9	74.6	75.2	74.74	75.35
	#2	75.9	75.7	75.6	75.7	76.2	75.82	
	#3	75.1	75.3	75.4	75.7	75.9	75.48	
HB-15%-0.5%	#1	72.4	73.1	73.0	73.2	73.6	73.06	73.06
	#2	72.8	73.3	73.3	73.9	73.6	73.38	
	#3	72.2	72.8	72.7	72.7	73.3	72.74	
HB-15%-0.8%	#1	70.1	70.4	70.8	70.7	70.8	70.56	70.04
	#2	69.5	69.2	69.3	69.6	69.5	69.42	
	#3	69.8	70.3	70.0	70.4	70.2	70.14	
HB-20%-0.15%	#1	76.2	75.9	76.0	75.9	76.1	76.02	76.24
	#2	76.6	76.2	76.3	76.3	76.6	76.4	
	#3	76.1	76.4	76.5	76.3	76.2	76.3	
HB-20%-0.3%	#1	74.5	74.8	74.5	74.3	75.1	74.64	75.29
	#2	75.5	75.9	75.7	75.8	76.1	75.8	
	#3	74.9	75.1	75.6	75.6	75.9	75.42	
HB-20%-0.5%	#1	73.1	73.3	73.2	73.6	74.1	73.46	73.35
	#2	72.8	73.5	73.6	73.6	73.7	73.44	
	#3	72.4	73.6	72.7	73.4	73.6	73.14	
HB-20%-0.8%	#1	70.0	69.9	69.8	70.4	70.7	70.16	70.63
	#2	71.0	70.5	70.7	71.4	71.0	70.92	
	#3	70.2	70.7	70.4	71.5	71.3	70.82	

## Error analysis

Figure A.5 and A.6 shows the error bar of gloss results, based on Figure 5.10 and Figure 5.11.

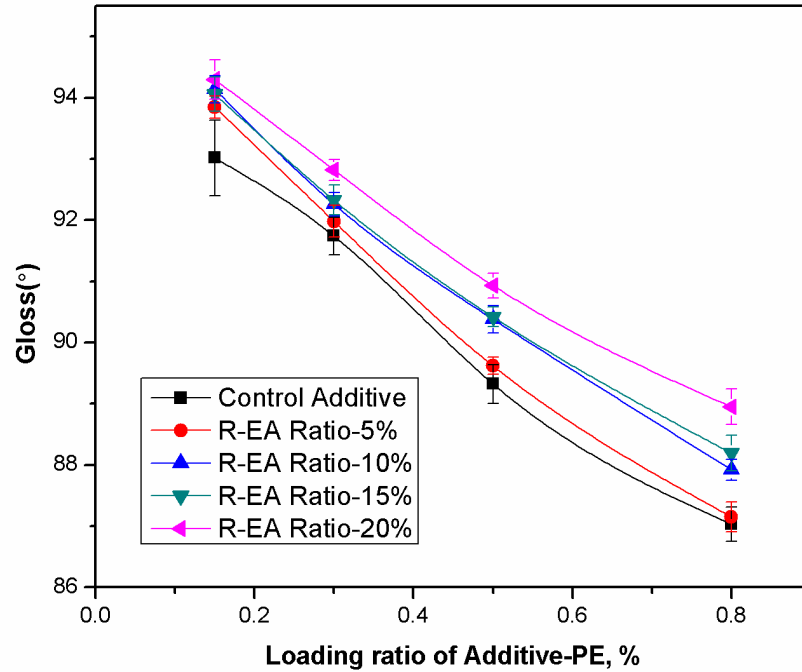


**Figure A.5 Error analysis of gloss for polyester samples  
(Additives were encapsulated with PE.  
Encapsulated additives were incorporated into PE powder)**

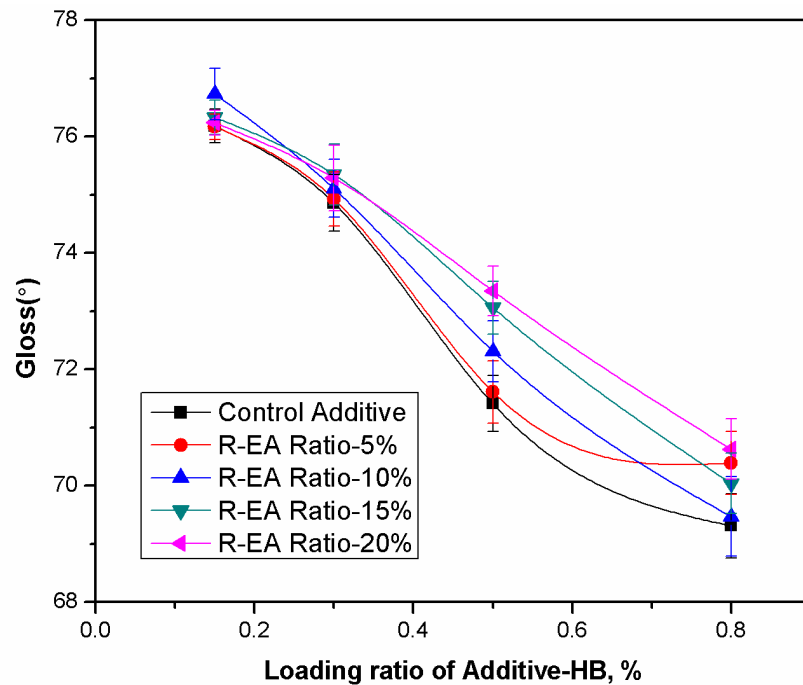


**Figure A.6 Error analysis of gloss for hybrid samples  
(Additives were encapsulated with HB.  
Encapsulated additives were incorporated into HB powder)**

### A4.3 Roughness

In chapter 5, roughness of powder panels were measured. For each panel, three scanning were conducted with the same test condition and an average value was employed. The Data were listed in the following Table A.10.

**Table A.10 Roughness of panel samples**

<b>Panel Sample</b>		<b>Scan 1</b>	<b>Scan 2</b>	<b>Scan 3</b>	<b>Average</b>	<b>Average Roughness</b>	<b>Deviation</b>
PE-Control-0.3%	#1	0.040	0.047	0.048	0.045	0.049	0.009
	#2	0.047	0.043	0.067	0.052		
Pe-Control-0.5%	#1	0.097	0.070	0.074	0.080	0.080	0.012
	#2	0.066	0.075	0.096	0.079		
PE-10%-0.3%	#1	0.063	0.033	0.057	0.051	0.047	0.010
	#2	0.046	0.040	0.041	0.042		
PE-10%-0.5%	#1	0.060	0.052	0.052	0.055	0.066	0.015
	#2	0.078	0.094	0.061	0.078		
PE-20%-0.3%	#1	0.041	0.038	0.030	0.036	0.043	0.009
	#2	0.040	0.053	0.056	0.050		
PE-20%-0.5%	#1	0.040	0.037	0.062	0.046	0.050	0.012
	#2	0.069	0.048	0.045	0.054		
HB-Control-0.3%	#1	0.081	0.084	0.074	0.080	0.080	0.004
	#2	0.085	0.077	0.077	0.080		
HB-Control-0.5%	#1	0.101	0.107	0.166	0.125	0.131	0.026
	#2	0.131	0.117	0.166	0.138		
HB-10%-0.3%	#1	0.097	0.081	0.082	0.087	0.090	0.011
	#2	0.090	0.109	0.079	0.093		
HB-10%-0.5%	#1	0.089	0.091	0.097	0.092	0.094	0.003
	#2	0.091	0.095	0.098	0.095		
HB-20%-0.3%	#1	0.075	0.096	0.080	0.084	0.083	0.008
	#2	0.075	0.079	0.092	0.082		
HB-20%-0.5%	#1	0.100	0.090	0.089	0.093	0.092	0.005
	#2	0.090	0.087	0.096	0.091		

## A4.4 Number of Seeds

In chapter 5, number of seeds on the surface of powder panels was measured. For each panel, the number of seeds was counted by three times with the same standard and an average value was employed. The Data were listed in the following Table A.11 and Table A.12.

**Table A.11 Number of seeds of polyester coated panel samples**

<b>Panel sample</b>	<b>NO</b>	<b>1</b>	<b>2</b>	<b>3</b>	<b>Average number</b>	<b>Average number</b>
PE-Control-0.15%	#1	13	14	14	13.67	14.11
	#2	15	13	14	14.00	
	#3	13	16	15	14.67	
PE-Control-0.3%	#1	19	20	17	18.67	18.22
	#2	16	20	18	18.00	
	#3	17	18	19	18.00	
PE-Control-0.5%	#1	20	22	22	21.33	21.00
	#2	17	20	22	19.67	
	#3	21	23	22	22.00	
PE-Control-0.8%	#1	22	24	25	23.67	24.33
	#2	24	22	23	23.00	
	#3	26	28	25	26.33	
PE-5%-0.15%	#1	13	13	12	12.67	12.44
	#2	10	12	14	12.00	
	#3	13	12	13	12.67	
PE-5%-0.3%	#1	19	17	18	18.00	18.11
	#2	16	19	19	18.00	
	#3	17	18	20	18.33	
PE-5%-0.5%	#1	21	17	21	19.67	19.44
	#2	17	18	20	18.33	
	#3	19	21	21	20.33	
PE-5%-0.8%	#1	23	22	19	21.33	20.89
	#2	22	18	23	21.00	
	#3	20	20	21	20.33	
PE-10%-0.15%	#1	10	15	13	12.67	12.56
	#2	10	15	14	13.00	
	#3	11	12	13	12.00	
PE-10%-0.3%	#1	13	16	18	15.67	14.67
	#2	12	13	15	13.33	



Panel sample	NO	1	2	3	Average number	Average number
PE-10%-0.5%	#3	12	16	17	15.00	16.22
	#1	15	17	18	16.67	
	#2	16	15	16	15.67	
	#3	15	15	19	16.33	
PE-10%-0.8%	#1	21	20	19	20.00	20.67
	#2	19	23	20	20.67	
	#3	24	21	19	21.33	
PE-15%-0.15%	#1	15	18	20	17.67	16.56
	#2	13	16	17	15.33	
	#3	15	18	17	16.67	
PE-15%-0.3%	#1	18	16	20	18.00	17.67
	#2	17	18	16	17.00	
	#3	16	19	19	18.00	
PE-15%-0.5%	#1	18	22	24	21.33	21.00
	#2	19	23	21	21.00	
	#3	18	21	23	20.67	
PE-15%-0.8%	#1	21	20	22	21.00	23.78
	#2	25	30	27	27.33	
	#3	20	23	26	23.00	
PE-20%-0.15%	#1	16	19	20	18.33	19.33
	#2	19	18	21	19.33	
	#3	23	18	20	20.33	
PE-20%-0.3%	#1	23	21	24	22.67	22.78
	#2	23	22	23	22.67	
	#3	20	24	25	23.00	
PE-20%-0.5%	#1	23	27	25	25.00	25.00
	#2	24	24	25	24.33	
	#3	26	27	24	25.67	
PE-20%-0.8%	#1	27	27	27	27.00	27.11
	#2	25	28	26	26.33	
	#3	29	27	28	28.00	

**Table A.12 Number of seeds of hybrid coated panel samples**

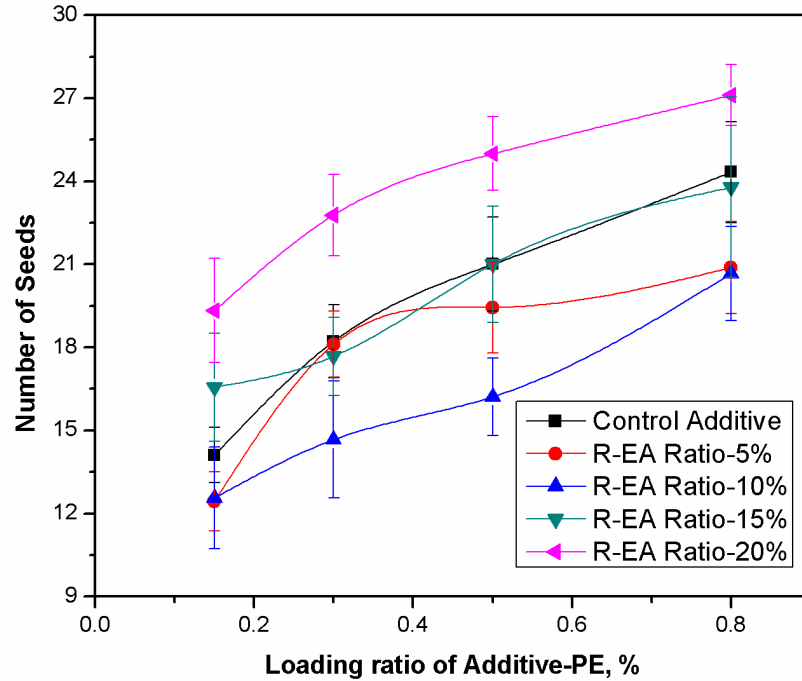
Panel sample	NO	1	2	3	Average number	Average number
PE-Control-0.15%	#1	23	26	24	24.33	24.11

	#2	21	24	22	22.33	
	#3	25	26	26	25.67	
	#1	25	26	27	26.00	
PE-Control-0.3%	#2	26	24	26	25.33	26.89
	#3	32	28	28	29.33	
	#1	29	31	29	29.67	
PE-Control-0.5%	#2	33	35	31	33.00	31.33
	#3	31	32	31	31.33	
	#1	34	32	37	34.33	
PE-Control-0.8%	#2	32	31	30	31.00	31.33
	#3	30	29	27	28.67	
	#1	22	23	19	21.33	
PE-5%-0.15%	#2	20	24	20	21.33	21.78
	#3	24	23	21	22.67	
	#1	23	25	21	23.00	
PE-5%-0.3%	#2	25	26	23	24.67	22.89
	#3	19	21	23	21.00	
	#1	26	26	23	25.00	
PE-5%-0.5%	#2	27	28	27	27.33	27.11
	#3	28	29	30	29.00	
	#1	29	31	29	29.67	
PE-5%-0.8%	#2	29	27	27	27.67	29.67
	#3	28	35	32	31.67	
	#1	16	16	17	16.33	
PE-10%-0.15%	#2	20	19	24	21.00	19.22
	#3	17	21	23	20.33	
	#1	23	23	25	23.67	
PE-10%-0.3%	#2	20	22	22	21.33	22.22
	#3	20	23	22	21.67	
	#1	27	25	28	26.67	
PE-10%-0.5%	#2	22	18	23	21.00	24.67
	#3	25	26	28	26.33	
	#1	30	31	35	32.00	
PE-10%-0.8%	#2	29	25	27	27.00	28.78
	#3	25	28	29	27.33	
	#1	22	21	18	20.33	
PE-15%-0.15%	#2	23	25	22	23.33	22.33
	#3	20	24	26	23.33	
	#1	27	31	29	29.00	
PE-15%-0.3%	#2	25	24	26	25.00	27.56

	#3	30	29	27	28.67	
	#1	29	34	32	31.67	
PE-15%-0.5%	#2	29	26	31	28.67	30.22
	#3	30	32	29	30.33	
	#1	35	33	31	33.00	
PE-15%-0.8%	#2	32	29	31	30.67	33.11
	#3	34	37	36	35.67	
	#1	20	24	23	22.33	
PE-20%-0.15%	#2	25	26	27	26.00	24.22
	#3	23	25	25	24.33	
	#1	26	29	28	27.67	
PE-20%-0.3%	#2	29	30	32	30.33	29.11
	#3	28	31	29	29.33	
	#1	29	27	29	28.33	
PE-20%-0.5%	#2	30	35	32	32.33	30.22
	#3	21	37	32	30.00	
	#1	36	35	35	35.33	
PE-20%-0.8%	#2	36	38	38	37.33	35.44
	#3	34	35	32	33.67	

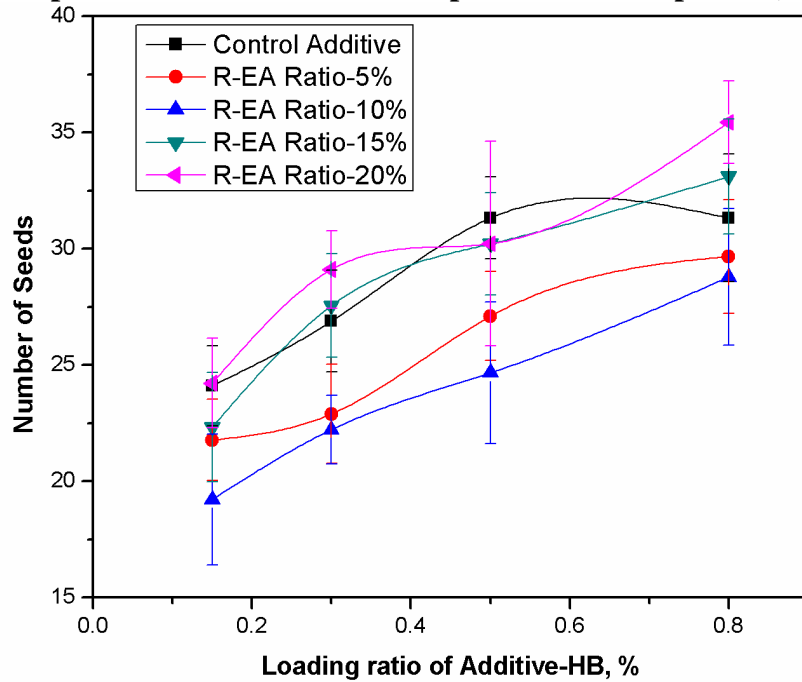
## Error analysis

Figure A.7 and Figure A.8 show the error bar of results of number of seeds, based on Figure 5.14 and Figure 5.15.



**Figure A.7 Error analysis for number of seeds for polyester samples  
(Additives were encapsulated with PE.**

**Encapsulated additives were incorporated into PE powder)**



**Figure A.8 Error analysis for number of seeds for hybrid samples  
(Additives were encapsulated with HB.**

**Encapsulated additives were incorporated into HB powder)**

## Curriculum Vitae

**Name:** Dangchen Xue

**Post-secondary  
Education and  
Degrees:** The University of Western Ontario  
London, Ontario, Canada  
Master of Engineering Science(Chemical and Biochemcial)  
August 2013

China University of Petroleum, Beijing  
Beijing, The People Republic of China  
June 2011

**Related Work  
Experience** Teaching Assistant  
The University of Western Ontario  
2013

Research Assistant  
The University of Western Ontario  
2012-2013